DIGITALCOMMONS
@WAYNESTATE

Wayne State University

Wayne State University Dissertations

January 2018

Identifying The Role Of The Type-Ii Transmembrane Serine Protease Tmprss13 In Breast Cancer

Andrew Stevan Murray
Wayne State University, amurray@med.wayne.edu

Follow this and additional works at: https://digitalcommons.wayne.edu/oa_dissertations

Part of the Cell Biology Commons

Recommended Citation

Murray, Andrew Stevan, "Identifying The Role Of The Type-Ii Transmembrane Serine Protease Tmprss13 In Breast Cancer" (2018). *Wayne State University Dissertations*. 1950.
https://digitalcommons.wayne.edu/oa_dissertations/1950

This Open Access Dissertation is brought to you for free and open access by DigitalCommons@WayneState. It has been accepted for inclusion in Wayne State University Dissertations by an authorized administrator of DigitalCommons@WayneState.

IDENTIFYING THE ROLE OF THE TYPE-II TRANSMEMBRANE SERINE PROTEASE TMPRSS13 IN BREAST CANCER

by

ANDREW STEVAN MURRAY

DISSERTATION

Submitted to the Graduate School

of Wayne State University,

Detroit, Michigan

in partial fulfillment of the requirements

for the degree of

DOCTOR OF PHILOSOPHY

2018

MAJOR: CANCER BIOLOGY

Approved By:

_____

Advisor Date

_____

_____

_____

_____

DEDICATION

I would like to dedicate my dissertation to my family. To my parents, Kevin and Beth Murray, I am very grateful for your love and encouragement. The support you have provided throughout my life has given me the opportunity to pursue this and I am eternally thankful. To my siblings, Elissa, Meredith, and Cameron, I am thankful for all the great times we have shared during my time in graduate school and I look forward of more to come.

ACKNOWLEDGEMENTS

Foremost, I would like to acknowledge my mentor, Dr. Karin List. Your mentorship has been the foundation to my success as a graduate student. Your encouragement and confidence in my abilities allowed me to grow as a student and excel as a researcher. Through our experiences, laughs, and (your) headaches that we have shared together, I consider myself fortunate to not only consider you as my mentor, but as a true friend as well. Thank you for all the memories and stories, and it was a pleasure to have had the opportunity to learn from you.

I would also like to thank my committee members, Dr. Julie Boerner, Dr. Izabela Podgorski, and Dr. Sokol Todi. The guidance and expertise you have provided has allowed this project to grow into an exciting body of work, and allowed me to grow as a student.

I would also like to thank Dr. Larry Matherly and the Cancer Biology Graduate Program here at Wayne State University. The accomplishments of the graduate students from this program would not be possible without the support and leadership you have provided for myself and the other graduate students.

I would also like to acknowledge all the friends I have gained as a graduate student. It was always enjoyable sharing our experiences during our times outside in Woodbridge, or during our lunchbreaks. I am truly grateful for the friendships I have made and thank you for the encouragements we have shared.

TABLE OF CONTENTS

DEDICATION ii

ACKNOWLEDGEMENTS iii

LIST OF FIGURES vii

Chapter 1: Introduction 1

1.1 Proteases as targets in breast cancer 1

1.2 Major classes of human proteases 2

1.2.1 Metalloproteases 2

1.2.2 Cysteine proteases 3

1.2.3 Serine proteases 4

1.3 Membrane-anchored serine proteases 5

1.4 Characteristic features of Type-II transmembrane serine proteases 7

1.4.1 Inhibition of TTSP proteolytic activity by endogenous inhibitors 9

1.5 TTSP's in normal development 11

1.5.1 Matriptase 11

1.5.2 Hepsin 12

1.5.3 TMPRSS6 13

1.5.4 TMPRSS13 13

1.6.0 TTSP's in cancer progression 14

1.6 Matriptase 14

1.6.2 Hepsin 16

1.6.3 TMPRSS2 18

1.6.4 TMPRSS4 20

Chapter 2: The Role of TMPRSS13 in Breast Cancer: Background and Specific Aims 22

2.1 Identification of novel TTSP's in breast cancer 22

2.2 Specific Aims: 23

Chapter 3: Biochemical Characterization of TMPRSS13 25

3.1 Materials and Methods 25

3.1.1 Cloning of full-length TMPRSS13 plasmid constructs 25

3.1.2 Transient transfections and Western blots 26

3.1.3 Cloning and expression of the TMPRSS13 active serine protease domain in Pichia pastoris 28

3.1.4 Chromogenic Proteinase Assays 29

3.1.5 Deglycosylation of TMPRSS13 29

3.1.6 Dephosphorylation of TMPRSS13 in lysates 29

3.1.7 Knockdown of TMPRSS13 expression in cancer cells 30

3.1.8 α2-Macroglobulin capture assay 30

3.1.9 Immunoprecipitation 31

3.1.10 Immunocytochemistry 31

3.1.11 Biotin labeling of cell surface proteins 32

3.1.12 USP2 deubiquitination assay 32

3.1.13 Glycosylation, intrinsic disorder, and phosphorylation predictions 33

3.2 Biochemical characterization of TMPRSS13 – Introduction 33

3.3 Biochemical characterization of TMPRSS13 – Results 35

3.3.1 TMPRSS13 is expressed as a 70 kDa glycosylated active protease in mammalian cells 35

3.3.2 Catalytic inactivation of TMPRSS13 promotes TMPRSS13 cell surface localization . 41

3.3.3 TMPRSS13 is capable of auto-activation 45

3.3.4 TMPRSS13 is phosphorylated 47

3.3.5 Endogenous TMPRSS13 is phosphorylated and glycosylated 53

3.3.6 HAI-1 and HAI-2 mediate TMPRSS13 cell-surface localization and phosphorylation 56

3.3 Biochemical Characterization Discussion 64

Chapter 4: TMPRSS13 in Breast Cancer 68

4.1 Materials and methods 68

4.1.1 Animals 68

4.1.2 Western blotting 69

4.1.3 Cell culture of human breast cancer cell lines 69

4.1.4 X-gal staining of mouse tissue.....70

4.1.5 Immunohistochemistry analysis of mouse tissue 70

4.1.6 Breast cancer tissue array.....71

4.1.7 Proliferation assays in human breast cancer cell lines 71

4.1.8 Invasion assays 71

4.1.9 Cell viability assays 72

4.2 TMPRSS13 in breast cancer - Introduction.....72

4.3 TMPRSS13 in breast cancer - Results 74

4.3.1 Increased expression of TMPRSS13 in breast cancer 74

4.3.2 Increased TMPRSS13 expression in the MMTV-PymT model of breast cancer 74

4.3.3 TMPRSS13 deficiency delays tumor development and decreases tumor burden, growth rate, and metastasis *in vivo* 76

4.3.4 TMPRSS13 deficiency decreases tumor cell proliferation and increases apoptotic cell death *in vivo*.....78

4.3.7 Loss of TMPRSS13 enhances chemosensitivity in triple negative breast cancer cell lines 83

4.4 Discussion 87

Chapter 5: Future Directions 89

APPENDIX: SUPPLEMENTARY FIGURE 93

REFERENCES 94

ABSTRACT.....117

AUTOBIOGRAPHICAL STATEMENT 119

LIST OF FIGURES

Figure 1: The membrane anchored serine proteases 8

Figure 2: TMPRSS13 is a 70-kDa active glycoprotein in human cells. 36

Figure 3: Detection of TMPRSS13 under different expression concentrations and sample collection methods 37

Figure 4: Proteolytic activity of TMPRSS13 serine protease domain 40

Figure 5: Catalytic inactivation of TMPRSS13 promotes its cell surface localization and produces a higher molecular weight TMPRSS13 species 43

Figure 6: TMPRSS13 is proteolytic activity promotes its own activation 46

Figure 7: TMPRSS13 is a phosphorylated TTSP family member 48

Figure 8: TMPRSS13 is not ubiquitinated.....50

Figure 9: Endogenous TMPRSS13 is phosphorylated.....54

Figure 10: HAI-1 and HAI-2 mediate TMPRSS13 phosphorylation.....58

Figure 11: HAI-1 and HAI-2 mediate TMPRSS13 cell-surface localization 62

Figure 12: Localization of phosphorylated TMPRSS13 on the cell surface.....63

Figure 13: TMPRSS13 expression in breast cancer 75

Figure 14: TMPRSS13 is expressed in cancer cells of murine mammary carcinomas.....77

Figure 15: Delayed tumor development, smaller tumors, decreased growth rate and metastasis in TMPRSS13$^{-/-}$ mice.....79

Figure 16: Decreased proliferation and increased apoptosis in TMPRSS13$^{-/-}$ mice 81

Figure 17: TMPRSS13 silencing decreases human TNBC cell proliferation and induces apoptosis 82

Figure 18: TMPRSS13 silencing decreases human TNBC cell proliferation and induces apoptosis 84

Figure 19: Increased chemosensitivity upon TMPRSS13 silencing in TNBC cell lines 86

Figure 20: Oxidative stress induced phosphorylation of TMPRSS13.....90

Supplementary Figure 21: Endogenous TMPRSS13 species size and glycosylation status.....93

CHAPTER 1: INTRODUCTION

1.1 Proteases as targets in breast cancer

According to the American Cancer Society statistics, breast cancer is the second leading cause of cancer related deaths in women and it is estimated that 41,000 women will die from breast cancer in 2017. Various types of breast cancers are defined by the cellular origin of the malignancy, with the most common form of breast cancer being invasive ductal carcinoma (IDC). IDC comprises approximately 80% of all breast cancers and arises from malignancy of the breast ductal epithelium. For therapeutic reasons, IDC is divided into subtypes based on the expression of cellular markers. These subtypes include estrogen/progesterone receptor positive (ER/PR+), and HER2+ breast cancers. If breast tumors lack these markers then they are classified as triple-negative breast cancers (TNBC), which comprises ~10-20% of breast cancers in the United States (1).

Due to the lack of expression of hormonal markers and HER2, TNBC lack targeted therapeutic options. Therefore, identification and validation of novel therapeutic targets in triple-negative breast cancer is needed. Dysregulated proteolysis is a hallmark of cancer, and contributes to various events in cancer progression including angiogenesis, inflammation, invasion, and cell survival (2). Pericellular and secreted proteases have garnered recent attention due not only to their ability to degrade extracellular components to allow for invasion into the surrounding stroma, but also for their ability to mediate signaling pathways through processing of cytokines, growth factors, and adhesion molecules (3). During cancer progression various environmental stimuli (e.g. hypoxia and acidification), and paracrine signaling between tumor cells and stromal cells, induce the expression of proteases that promote tumor development (2). Thus, identifying novel tumor promoting proteases is pivotal to our understanding of the tumor/tumor-microenvironment interaction, and may translate into candidate proteases for targeted therapy.

1.2 Major classes of human proteases

Proteolysis is a post-translational modification of proteins that is indispensable for normal development and is carried out by a class of protein enzymes known as proteases. Proteases are classified into subgroups based on their mechanism of catalysis and include: serine, threonine, cysteine, aspartic, glutamic, and metallo- proteases. In total, the human degradome (the entire set of known human proteases) consists of 569 proteases, with 34% being metalloproteases, 31% serine, 26% cysteine, 5% threonine, and 4% aspartic proteases. (4) Given the essential function of proteases, the regulation of both their expression and activity is critical during normal physiological processes and perturbations in their expression and activity is observed in many diseases, including cancer, making them attractive candidates in drug discovery. (2)

1.2.1 Metalloproteases

The most well characterized metalloproteases in humans are members of the Metzincins clan of metalloproteases, which include the matrix-metalloproteases (MMPs), the 'a disintegrin and metalloprotease' [ADAMs], and meprin families (5,6). All metalloproteases are characterized by the necessity for zinc ions to hydrolyze peptide bonds, thus the prefix of "metallo"-protease. The MMPs, ADAMs, and meprin families of metalloproteases are synthesized as zymogens, which functions as a control mechanism to prevent unintended proteolysis (5). In humans there are a total of 24 MMPs, 22 ADAMs, and 2 meprin proteins encoded within the human genome, giving rise to diverse functional roles (6,7).

In terms of drug discovery, MMP inhibitors were one of the first class of proteolytic inhibitors to be tested in cancer patients. However, these protease inhibitors failed in clinical trial settings as a result of severe side effects and little to no anti-tumor efficacy (8-10). A main reason for the failure in clinical trials was due to the broad-spectrum inhibitor profile of these drugs towards MMPs. The drugs used included marimastat, prinomastat, and hydroxamates batimastat which have subsequently been shown to have a broad, rather than specific, inhibitory

profile against MMP family members (8). Also contributing to the disappointing outcome of the clinical trials was the lack of knowledge of the physiological roles and target substrates for this family of proteases. Since the clinical trials, many studies have identified important roles of these proteases in normal physiological cellular processes (8). The lessons learned from these studies highlight the need to identify important biological features of proteases during drug development, and the necessity for highly selective targeting of protease inhibitors to achieve optimal anti-cancer effects while ensuring few and manageable side effects.

1.2.2 Cysteine proteases

The catalytic triad of cysteine proteases consists of Cysteine-Histidine-Asparagine amino acid residues. The cysteine amino acid residue is responsible for the nucleophilic attack on the reactive peptide bond of the target substrate. There are several well-known families of cysteine proteases including cathepsins, caspases, and calpain protease families (11,12). The family of caspase cysteine proteases were termed ‘C’-‘aspases’ with the C representing cysteine of the cysteine protease family, and ‘aspase’ representing cleavage specificity after aspartic amino acid residues of target substrates (13,14). Since their discovery, several caspases have been found to play pivotal roles in mediating cell death through apoptosis (14). These proapoptotic cysteine proteases are further classified as either initiator or executioner caspases. Upon induction of apoptotic stimuli through either intrinsic or extrinsic pathways, initiator caspases (caspases -8, -9, -10) are activated through an allosteric mechanism where two inactive monomers form active dimer complexes. These activated initiator caspases then activate effector caspases (caspase -3, -6, -7) directly through proteolytic cleavage, which mediate the ‘execution’ phase of apoptosis resulting in cell death (15,16).

Cathepsins are another class of proteases which are composed of 11 different types of cysteine proteases (16). Cathepsins are found primarily in lysosomal compartments and function in protein turnover. In addition to protein turnover, several cathepsins have been found to play other important roles in cellular processes, such as bone reabsorption, generation of

peptides for MHC II molecules, and apoptosis (17,18). In cancer, the aberrant extracellular localization of several cathepsin family members have been shown to cleave various extracellular matrix proteins, including laminin and type IV collagen (18). Calpains are another well studied class of cysteine proteases with several of these proteases requiring calcium for their activation (19). Currently there are 14 known calpain family members which have been implicated in roles including cell motility and apoptosis (19).

1.2.3 Serine proteases

Serine proteases represent one of the most abundant and diverse groups of proteases, involved in functions relating to blood coagulation, digestion, development, fibrinolysis, immunity, and apoptosis (20). Serine proteases mediate catalysis through a neutrophilic attack by a serine residue towards carbonyl moiety of the substrates peptide bond. The other amino acids typically involved in catalysis of serine proteases include histidine and aspartic residues, which form a charge-relay system to mediate hydrolysis of peptide bonds. One of the most well-studied families of serine protease are the S1A family of the PA clan of serine proteases, comprised of trypsin, chymotrypsin, and thrombin protease subfamilies.

One of the most well characterized serine protease pathways is the coagulation cascade (i.e. bleeding arrest). To prevent excessive blood loss upon endothelial vessel injury, the liver produces fibrinogen which upon conversion to fibrin stabilizes platelet plugs as an initial barrier for the damaged vessel wall. A critical regulatory mechanism to prevent aberrant fibrin strand formation, is that fibrin is first synthesized as inactive fibrinogen that is present in its soluble form at high concentration in the blood at 2-5 mG/mL (21), but is incapable of producing fibrin strands before activation by proteolytic cleavage. Upon endothelial injury, fibrin is converted from fibrinogen by the protease thrombin, and thrombin is converted from prothrombin through the coagulation cascade (22). Several bleeding disorders are caused by mutations in individual components of the serine protease coagulation cascade. The most common disorders are Hemophilia; Hemophilia A is due to deficiency of factor VIII, and hemophilia B is due to

deficiency of factor IX (23). Hemophilia can be efficiently treated by replacement therapy with recombinant coagulation factors.

Another well studied serine proteolytic system, known as the fibrinolytic system, prevents excessive clot formation. Upon tissue occlusion during clot formation, the serine protease tissue-plasminogen activator (tPA) is released from the endothelium. tPA then converts plasminogen into its active form known as plasmin. Plasmin is then responsible for the breakdown of fibrin blood clots into fibrin degradation products (22). A rare congenital disease, known as human plasminogen deficiency, occurs in patients who have a mutation in the plasminogen gene. This results in loss of the ability to break down fibrin during clot formation and often leads to inflammation in the conjunctiva of the eye due to fibrin build-up. Plasminogen deficient mice also display the same defect, with lost ability to degrade fibrin, leading to thrombosis. However the mice develop normally and are able to reproduce, highlighting the specific role of plasminogen in the fibrinolytic system (24).

1.3 Membrane-anchored serine proteases

Many well studied proteases are either secreted, for example plasminogen, or reside intracellularly, for example cathepsins and caspases. However, at the turn of the millennium as a result of the human genome sequencing project, a new group of serine proteases emerged that reside on the cell surface and are termed either Type-I, Type-II, or GPI-anchored serine proteases (3). The largest membrane anchored serine protease family is the Type-II transmembrane serine proteases (TTSP), and are attached to the cell membrane through a single amino- terminal hydrophobic region that signals for membrane localization. Two other membrane anchored serine proteases, testisin and prostasin, localize to the cell surface through a glycosyl-phosphatidylinositol linkage (GPI-anchored). Tryptase-γ1, also known as transmembrane tryptase, is the only Type-I transmembrane serine protease that contains a carboxy- terminal hydrophobic region that signals for membrane localization (25).

Tryptase-γ1 is highly expressed in the mast cells of both humans and mice (26-28). Mature mast cells often reside close to the host-environment interface and thus play an important role in the first line of defense to environmental insult and pathogens. Once mature mast cells are activated, degranulation occurs resulting in the release of bioactive granule compounds that incite an inflammatory response (29). Thus, given the high expression of tryptase-γ1 in mast cells suggests a role for it in host defense against pathogens and insults. Tryptase-γ null mice display no outwardly phenotype, however under experimentally induced chronic obstructive pulmonary disease (COPD), tryptase-γ1 null mice displayed reduced pulmonary macrophages, decreased histopathology scores, and decreased fibrosis in their small airways (30). Additionally, in experimentally induced colitis experiments via dextran sodium sulfate exposure, tryptase-γ null mice had a more positive outcome compared to WT mice, with reduced histopathology scores and increased weight retention (30).

The GPI-anchored transmembrane serine proteases prostasin and testisin have been shown to play important roles in normal physiological development through characterization of knockout mouse models. Global knockout of prostasin results in embryonic lethality due to impaired placental labyrinth maturation, indicating an essential role of prostasin during embryonic development (31). Additionally, genetically engineered mice that have specific knockout of prostasin in the skin die within 60 hours after birth due to a severely impaired epidermal barrier leading to rapid dehydration, indicating an additional essential function for prostasin in epidermal barrier development (32). Testisin displays high expression in the testis in both humans and mice, and testisin knockout mice display no overt outward phenotype (33,34). However, testisin knockout mice to have impaired spermatozoa development, with decreased viable sperm counts, reduced motility, and decreased fertilization abilities, indicating that testisin plays an important role in sperm maturation (34).

The type-II transmembrane serine protease (TTSP) family is the largest group of membrane-anchored serine proteases and consists of 17 structurally unique multi-domain

serine proteases (26). This family of proteases is sub-classified into four groups based off the phylogenetic analysis of the serine protease (SP) domain, and the protein domain structure within the stem region. These subfamilies include the Matriptase, Hepsin/TMPRSS, HAT/DESC, and Corin subfamilies (Fig. 1). Several members of the TTSP family have been intensely studied and it has been demonstrated that some of these membrane-anchored serine proteases regulate fundamental cellular and developmental processes, including tissue morphogenesis, epithelial barrier function, ion and water transport, and cellular iron export (35) (discussed in more detail in section 1.5).

1.4 Characteristic features of Type-II transmembrane serine proteases

TTSP's are synthesized as "single-chain" inactive zymogens that require proteolytic cleavage at conserved activation sites to generate "two-chain" active proteases. Upon activation, the serine protease domain remains tethered to the stem-region through a di-sulfide bond, thus remaining surface-associated. This feature of TTSPs functions as a mechanism to control spatial and temporal proteolytic activity when appropriate. The physiologically relevant proteases responsible for proteolytic activation of TTSP family members is not known for many TTSPs, however several TTSP family members have been shown to be capable of auto-activation (36). The mechanism by which auto-activation occurs is unknown, however it likely involves a homo-dimerization or oligomerization. (36)

Other post-translational modifications of TTSP family members include glycosylation and phosphorylation. N-linked glycosylation of several TTSP family members has been shown to play a critical role in their activation and localization. For example, N-linked glycosylation is critical for both activation and ectodomain shedding of corin and matriptase-2. (37,38). Additionally, glycosylation of matriptase is essential for matriptase auto-activation (39). The intracellular domains of TTSPs vary in length from 20 to 160 amino acids, with Hepsin containing the shortest, and TMPRSS13 containing the longest. (25) Several TTSP family members contain putative consensus sequences for phosphorylation sites within the

Figure 1: The membrane anchored serine proteases

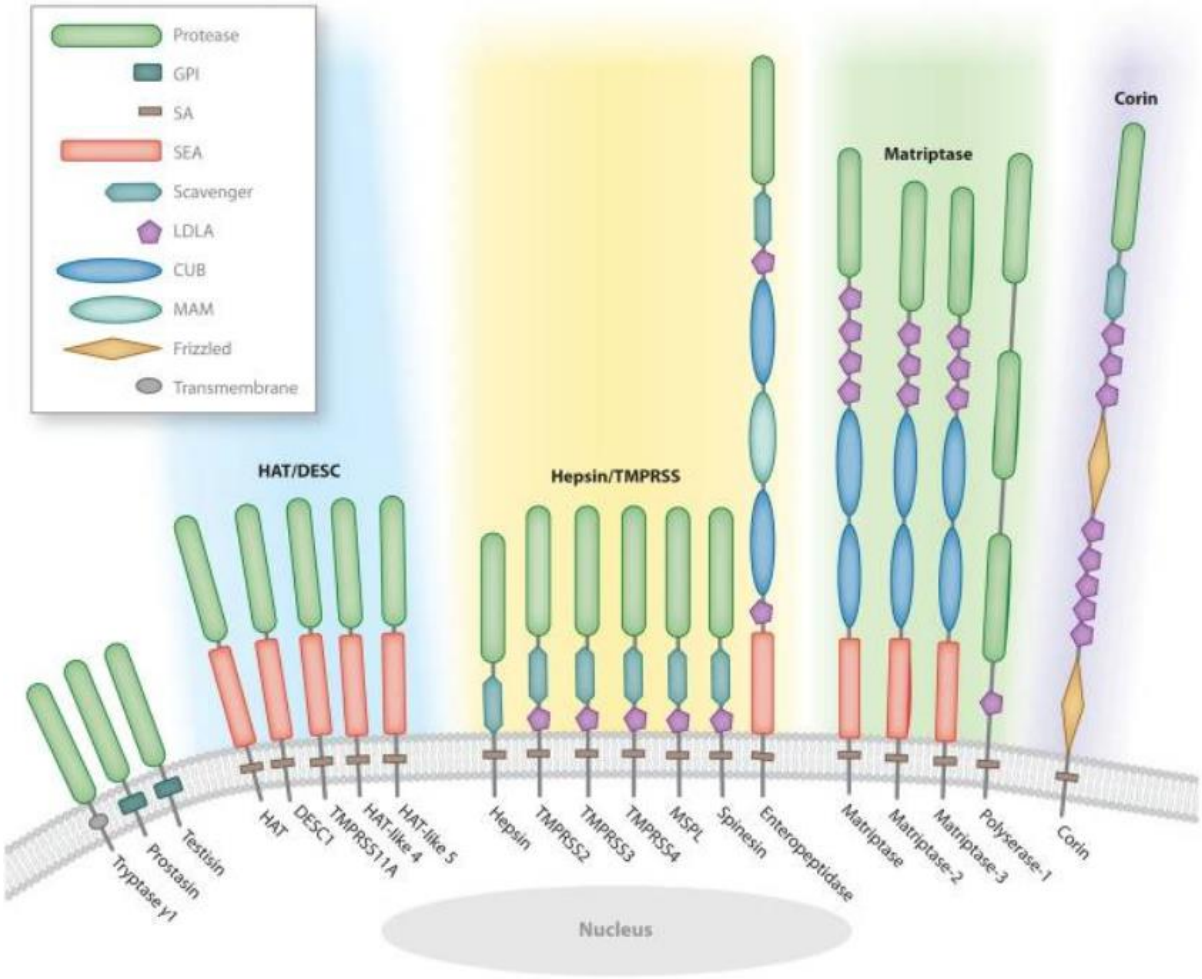

Figure 1. Membrane anchored serine proteases. The 20 known membrane anchored serine proteases. Tryptase-γ is the only known type-I transmembrane serine protease, and contains a carboxy-terminal hydrophobic region and an N-terminal serine protease domain (green oval). The two GPI-anchored serine proteases prostasin and testisin attach to the membrane through a glycophosphatidylinositol (GPI) anchor. The stem regions of the type-II transmembrane serine protease (TTSP) family members are composed of ow-density lipoprotein receptor class A (LDLA); sea urchin sperm protein, enteropeptidase, and agrin (SEA); Cls/Clr, urchin embryonic growth factor, and bone morphogenic protein-1 (CUB); meprin, A5 antigen, and receptor protein phosphatase μ (MAM); frizzled; and group A scavenger receptor. The four TTSP subfamilies are known as the HAT/DESC, hepsin/TMPRSS, Matriptase, and corin subfamilies.

intracellular domains, and TMPRSS13 was the first and currently only TTSP family member identified to be modified by phosphorylation (discussed in detail in section 3.3) (40).

Unlike the Type-I and GPI-anchored membrane serine proteases, where the catalytic domain lies adjacent to the cell surface, TTSP family members also contain several protein domain structures within the stem region, with the SP domain localizing at the C-terminus (extracellular side of the cell membrane) (See Fig. 1). These protein domain structures within the stem region play important roles in binding interactions, activation, and inhibition (26). The most common protein domain of TTSP family members is the low density lipoprotein receptor class A domain (LDLRA). Additional domains include: Group A scavenger receptor (SR) domains, frizzled domains, Cls/Clr, urchin embryonic growth factor and bone morphogenic protein 1 (CUB) domains, sea urchin sperm protein, enterokinase, agrin (SEA) domains, and meprin, A5 antigen, and receptor protein phosphatase μ (MAM) domains. Recently, it has been suggested that SEA domain cleavage of matriptase is required for efficient transport to the cell surface by inhibitor mediated stabilization by the endogenous TTSP inhibitor hepatocyte growth factor activator inhibitor-2 (HAI-2), highlighting the unique regulatory role of these protein domain structures in TTSP function (41).

1.4.1 Inhibition of TTSP proteolytic activity by endogenous inhibitors

As mentioned previously, TTSPs are synthesized as inactive zymogens that require proteolytic cleavage to generate an active “two-chain” protease. To prevent unabated proteolysis upon activation, TTSP family members are inhibited by the endogenous serine protease inhibitors, HAI-1 and HAI-2 (42). HAI-1, -2 are kunitz domain type serine protease inhibitors that both contain two kunitz domains (KD1 and KD2), however the KD1 domain of HAI-1 is responsible for the proteolytic inhibition of matriptase (43), and thus may be the primary kunitz domain to elicit inhibitory activity towards other TTSP family members. HAI-1 and HAI-2 are a competitive type of inhibitor that form a tight non-covalent complex with the SP domain. These two inhibitors play essential roles in normal development, since genetic ablation of either

HAI-1 or HAI-2 results in embryonic lethality due to defects in placental labyrinth development in both HAI-1 and HAI-2 null mice, as well as neural tube closure in HAI-2-null mice (44-46). The embryonic lethality upon loss of HAI-1 or HAI-2 is rescued upon concomitant genetic loss of matriptase (46,47). These findings underscore the importance of precise regulation of matriptase proteolytic activity during embryonic development.

A mutation in HAI-2 has been discovered in patients who suffer from a congenital disease known as congenital sodium diarrhea (CSD). Patients who have this mutation suffer from dehydration and diarrhea due to increased sodium levels in the intestinal tract (48). Although the exact mechanism by which electrolyte and nutrient imbalance occurs is unknown, it has been proposed that loss of inhibitory activity of HAI-2 towards matriptase results in increased amounts of prostasin activation, which in turn activates the Epithelium sodium channel (ENaC), causing aberrant sodium transport in these patients (49,50). An alternative hypothesis has also recently been proposed, where loss of proteolytic inhibition of matriptase in HAI-2 mutant patients results in increased matriptase mediated cleavage of EpCAM. This then causes dysregulated tight-junction stabilization and formation, resulting in impaired paracellular transport of ions (51). Interestingly, a recent study examining the effects of this mutation *in vitro* on TTSP family members observed a complete loss of proteolytic inhibition towards TMPRSS13, as well as partial loss of inhibitory activity towards matriptase (52).

It has been demonstrated that dysregulated expression level ratios of TTSP's and the HAI-1, -2 inhibitors contributes in cancer progression, with decreased expression of inhibitors relative to TTSP family members (53). List *et al*. demonstrated that transgenic expression of matriptase in the epidermis results in the development of squamous cell carcinoma, however double transgenic mice expressing matriptase with the inhibitor HAI-1 significantly reduced tumor development in these mice (54). Therefore, this indicates that the matriptase:HAI-1 expression ratio may play a role in the development of cancer, and that inhibition of matriptase proteolytic activity effectively abrogates matriptase mediated tumor development.

In addition to functioning as important inhibitors towards TTSP proteolytic activity, HAI-1, and -2 have garnered recent attention in their ability to stabilize and promote proper activation, localization, and expression of TTSP's. Therefore it is demonstrated that the HAI-1 and HAI-2 inhibitors interact with the inactive zymogen forms of TTSP family members, including matriptase (39,41,43), hepsin (55), and TMPRSS13 (40), to facilitate their activation. HAI-1, -2 mediated transport of TMPRSS13 is discussed in more detail in chapter 3.

1.5 TTSP's in normal development

Research of TTSP family members has revealed significant insight towards the physiological roles of many TTSP family members. However, the *in vivo* substrates for many TTSP family members remain unknown, thus limiting the knowledge of the precise mechanisms by which TTSP's promote normal development. Nevertheless, numerous knock-out mouse studies have revealed that many of these family members play important roles in maintaining a normal phenotype *in vivo* and for a subset of TTSPs the physiological substrates have been identified and validated in mouse models and/or in humans harboring TTSP mutations. The section below covers a select number of TTSP family members that have been implicated to play important roles in normal human development through characterization of genetically engineered mouse models.

1.5.1 Matriptase

Matriptase is one of the most well-studied TTSP family members to date, and is critically involved in proper skin epidermal differentiation and development. Matriptase has a broad expression profile in the epithelium of tissue, and is found at highest expression in the skin, gastrointestinal tract, hair follicles, and kidney in adult tissue. Matriptase null mice suffer from severe post-natal dehydration resulting in mortality due to defects in the epidermal skin barrier, exemplifying the importance of matriptase in epidermal barrier development (56). Physiological substrates for matriptase include the GPI-anchored serine protease, prostasin, which was discovered by characterizing prostasin-null mice, which exhibit an identical phenotype to

matriptase-null mice (32,57). Furthermore, it was demonstrated that the epidermis from newborn matriptase null mice contained no detectable active two-chain prostasin in contrast to control littermate mice where active prostasin was readily detected (57). Therefore, a matriptase-prostasin proteolytic cascade has been hypothesized to be essential for proper epidermal barrier development.

Mutations of matriptase have also been discovered in patients who suffer from a congenital disease known as Autosomal Recessive Ichthyosis with Hypotrichosis (ARIH). Patients who harbor matriptase mutations display abnormal epidermal differentiation and hair abnormalities (58,59) and at the molecular level, these patients also have impaired profilligrin processing, a key step in epidermal differentiation. Interestingly, these phenotypes are mimicked in matriptase hypomorphic mice that have reduced matriptase proteolytic activity.

1.5.2 Hepsin

Hepsin is a member of the Hepsin/TMPRSS subfamily of TTSP family members and was originally cloned from human liver cDNA libraries in 1988. Since its discovery it has been implicated in roles including cochlear development and hepatic structural homeostasis. The first study characterizing hepsin-null mice unexpectedly observed defects in normal hearing, resulting from defective cochlear development (60). The mechanism by which hepsin regulates proper cochlear development is unclear, however hepsin-null mice do display low levels of the thyroid hormone thyroxine, which has previously been shown to be critical in cochlear development. Therefore, it is suggested that the hearing defect in hepsin-null mice may be due to defects in thyroid hormone metabolism. (60)

An *in vivo* substrate for hepsin has been identified in liver tissue. Hsu *et al*. characterized the liver architecture of hepsin null mice and observed defects in hepatocyte architecture and decreased activation of c-Met signaling in the liver (61). This phenotype was rescued when hepsin null mice were treated with active recombinant HGF, thus suggesting the defects observed were caused by insufficient hepsin-mediated pro-HGF processing. To test whether the

livers of hepsin-null mice have defects in pro-HGF processing, lysates from livers of WT or hepsin null mice were treated with pro-HGF to assess the ability of HGF processing *in vitro*. Liver lysates from hepsin-null mice displayed impaired pro-HGF processing compared to WT-hepsin liver lysates (61). Therefore, hepsin plays an important role in maintaining proper liver architecture through pro-HGF processing.

1.5.3 TMPRSS6

TMPRSS6, also known as matriptase-2, plays a vital role in iron homeostasis by regulating hepcidin expression. The hepatic hormone hepcidin is a negative regulator of iron export into the plasma since it is responsible for down-regulation of the iron exporter, ferroportin. TMPRSS6 null mice display a marked up-regulation of hepcidin and a corresponding decrease in expression of ferroportin, thus resulting in iron deficiency anemia (62). Patients with frame-shift and missense mutations in the TMPRSS6 gene show a similar phenotype to TMPRSS6 null mice, resulting in iron deficiency anemia (63). TMPRSS6 has been shown to regulate hepcidin expression by degradation of hemojuvelin, which is a co-factor of bone morphogenic protein that regulates hepcidin expression (64).

1.5.4 TMPRSS13

TMPRSS13 deficient mice were first characterized by Madsen *et al*. in 2014 and revealed that TMPRSS13 has a broad expression profile, with the strongest expression occurring in the skin, tongue, lip, hard palate, cornea, and bladder (65). Madsen *et al.* also observed that TMPRSS13 deficiency results in impaired epidermal skin barrier development as measured by an increased rate of trans-epidermal fluid loss in TMPRSS13 deficient mice, and a compacted stratum corneum. Interestingly however, the impaired epidermal barrier did not seem to be caused by abnormal tight-junction formation. In contrast to matriptase null mice that succumb to the severely compromised epidermal barrier function within 24-48 after birth (List et al.), TMPRSS13 deficient mice display a much less severe phenotype and no lethality is seen. At weaning age the mice are indistinguishable from control mice and no difference in overall

adult health and life span is observed. (65). Currently the *in vivo* substrates for TMPRSS13 are unknown, however TMPRSS13 can activate the oncogenic signaling molecule pro-HGF under *in vitro* conditions (66).

1.6.0 TTSP's in cancer progression

This research (section 1.6.0 thru 1.6.4) was originally published in the journal Biological Chemistry. Murray AS, Varela FA, List K. Type II transmembrane serine proteases as potential targets for cancer therapy. DOI: 10.1515/hsz-2016-0131.

Beyond the role that TTSPs play in normal physiological processes, TTSPs have also been studied extensively in disease, including cancer, where their expression is often dysregulated. Promotional or causal roles of several TTSPs have been demonstrated *in vivo* using genetic engineering or administration of protease inhibitors to manipulate protease levels and activity. As evidence continues to accumulate about their functional roles in cancer development and progression, TTSPs represent exciting future therapeutic targets. This section will focus on select TTSPs that to date have been most extensively studied in cancer.

1.6 Matriptase

This protease is one of the most extensively studied TTSPs with more than 300 published articles characterizing expression profiles, gene-regulation, structural biology, regulation by endogenous inhibitors, identification of critical substrates, determination of physiological and pathophysiological functions, and development of synthetic inhibitors and imaging tools. Matriptase is upregulated in breast, cervical, colorectal prostate, endometrial, esophageal squamous cell carcinoma, gastric, head and neck, and pancreatic carcinoma; and in tumors of the lung, liver, and kidney among others (67-70). Increased matriptase expression correlates with advanced clinicopathological stages in many of these cancers, and *de novo* expression is found in ovarian and cervical carcinoma where expression levels also correlate with histopathological grade (71-73).

Matriptase activity is mainly regulated by the transmembrane serine protease inhibitors, HAI-1 and HAI-2 *in vivo* (44,46,74,75). In expression studies, an imbalance between matriptase, HAI-1 and HAI-2 exists in several cancer types including ovarian and colorectal cancer where the matriptase/ HAI-1 ratio is increased and in prostate and endometrial carcinoma where matriptase/HAI-2 ratios are increased (76-80).

The role of matriptase *in vivo* has also been studied in detail in breast cancer. In an oncogene-induced mouse mammary carcinoma model, hypomorphic matriptase mice with reduced levels of matriptase displayed a significant delay in tumor formation and blunted tumor growth (81). The reduced tumor growth was associated with a profound decrease in cancer cell proliferation. Mechanistic studies demonstrated that the proliferation deficiency was caused by the impairment of carcinoma cells, in cell lines and *in vivo*, to initiate the activation of the c-Met signaling pathway in response to fibroblast-secreted pro-hepatocyte growth factor (pro-HGF). In primary mammary carcinoma cells and human breast cancer cell lines, addition of HAI-1 and HAI-2 inhibited pro-HGF mediated c-Met signaling and cell proliferation (81). Importantly, inhibition of matriptase catalytic activity using a selective small-molecule inhibitor efficiently abrogates the activation of c-Met, Gab1 and AKT, in response to pro-HGF, which functionally leads to attenuated cancer cell proliferation and invasion. The selective inhibitor of matriptase, IN-1 used in the study contains a ketobenzothiazole serine trap and was designed based on the auto-catalytic domain (RQAR) of matriptase (82). It still remains to be tested whether IN-1 is suitable as an anti-tumor drug *in vivo*. Other inhibitors have been developed including MCoTI-II (based on cyclic microproteins of the squash Momordica cochinchinensis trypsin-inhibitor family) which inhibits the proteolytic activation of pro-HGF by matriptase but not by hepsin, in both purified and cell-based system (83).

In prostate cancer, several matriptase inhibitors have been tested in xenograft models. In an ectopic subcutaneous model, a small molecule inhibitor of matriptase, CVS-3983, significantly suppressed the growth of human prostate cancer cell lines in nude mice (84). The

authors propose that the effect was mainly caused by the abrogation of invasion since tumors remained localized to the site of injection in treated mice and failed to invade the subscapular area as compared to tumors in vehicle treated mice. Similarly, using matriptase inhibitors based on bis-basic secondary amides of sulfonylated 3-amidinophenylalanine in an orthotopic xenograft mouse model of prostate cancer resulted in reduced tumor growth, and tumor dissemination (85). Together, these findings demonstrate that matriptase is critically involved in cancer progression and lay the groundwork for future studies developing and testing small-molecule matriptase inhibitors and their potential as novel targeted therapeutic drugs in cancer.

1.6.2 Hepsin

Hepsin/TMPRSS1 was the first serine protease characterized to contain a transmembrane domain, and was named based on its original identification in hepatocytes (86). Hepsin is also expressed in kidney, pancreas, stomach, prostate and thyroid (87,88). Studies of knockout mouse models of hepsin have demonstrated that this protease plays an important role in cochlear development, is involved in regulating levels of the thyroid secreted hormone, thyroxine, and is responsible for pro-HGF activation in the liver (60) (89) (61).

Many cancers display increased expression levels of hepsin including cancer of the prostate, breast (90), ovary (91), kidney (92), and endometrium (93). Several studies have revealed that hepsin is critically involved in prostate cancer progression. Klezovitch and colleagues used transgenic mice to show that the overexpression of hepsin, under the control of the probasin (PB) promotor, leads to a disorganized basement membrane and promotes prostate cancer metastasis to the liver, bone and lungs when crossed to the LPB-Tag prostate cancer model (94).

The Wnt/β-Catenin signaling pathway has been shown to play an important role in prostate cancer progression. Dysregulation of this pathway by prostate-specific deletion of the adenomatous polyposis coli (Apc) gene results in high-grade prostatic intraepithelial neoplasia (PIN) lesions with rare occurrences of microinvasive characteristics in mice (95,96). Crossing

PB-Hepsin mice to the prostate-specific Apc-deletion model (APCPBKO) to generate PB-Hepsin/APCPBKO mice results in progression from high-grade PIN lesions to large invasive adenocarcinomas (95). Prostate tumors from PB-Hepsin/APCPBKO mice are hyperproliferative, and contained significant numbers of apoptotic cells (95).

In an orthotopic xenograft model of prostate cancer, LnCaP cells were stably transfected to overexpress hepsin (LnCaP-34) and injected into the anterior lobe of the prostate. Increased final tumor weights were observed in mice injected with LnCaP-34 cells compared to LnCaP cells expressing endogenous levels of hepsin (LnCaP-17 cells) (97). Additionally, metastatic lesions to the periaortic lymph nodes were observed in mice injected with LnCaP-34 cells and not found in mice injected with LnCaP-17 cells (97). To determine whether inhibition of hepsin decreases the tumor growth in vivo, mice injected with LnCaP-34 cells were treated with a PEGylated form of Kunitz domain-1, a potent hepsin active site inhibitor derived from HAI-1. Treatment of established orthotopic LnCaP-34 xenografts tumors with PEGylated Kunitz domain-1 significantly decreased contralateral prostate invasion and lymph node metastasis (97).

In addition to prostate cancer, hepsin has been shown to have increased expression in breast cancer (90). To determine whether hepsin promotes tumor progression in breast cancer, Tervonen et al. performed grafting studies using primary mouse mammary epithelial cells from transgenic mice harboring a Whey acidic protein (Wap) promoter-controlled c-Myc transgene. The primary cells, that also expressed doxycyclin-inducible hepsin, were transplanted into cleared fat pads of syngeneic wild-type virgin hosts. Chronic doxycyclin-induced expression of hepsin resulted in decreased tumor latency in these mice, thus indicating a promotional role for hepsin in breast cancer progression (98). Interestingly, hepsin acutely downregulated its cognate inhibitor, HAI-1, in human MCF10A immortalized mammary epithelial cells, thereby further increasing the hepsin/HAI-1 ratio. Furthermore, hepsin induced cellular changes in

MCF10A cells commonly associated with invasive phenotypes and endowed cells with a strong capacity to proteolytically activate pro-HGF, leading to activation of the c-Met receptor.

1.6.3 TMPRSS2

TMPRSS2 and TMPRSS4 are two other members of the TMPRSS/Hepsin subfamily of TTSPs and remain relatively uncharacterized. Like many other TTSPs, expression of TMPRSS2 is localized to several types of epithelial tissues, including in the colon, small intestine, lung, kidney, pancreas, and most notably in the prostate (99), where expression is highest. Both the physiological function and substrates of TMPRSS2 have yet to be identified; therefore, much of what is known about TMPRSS2 originates from its association with cancer. TMPRSS2 has long been associated with prostate cancer following the identification of the oncogenic gene fusion product with erythroblast transformation specific (ETS) transcription factors, such as ETS-related gene (ERG) (100,101). Despite this, the role of the native TMPRSS2 protein and its proteolytic activity in cancer is vastly understudied. In normal prostate epithelia, TMPRSS2 expression is localized to the cell membrane, however, mislocalization to the cytoplasm in prostate cancer has been observed (102). In addition, both primary and metastatic prostate tumors from patients display increases in TMPRSS2 levels, with increasing expression correlating with elevated Gleason score, suggesting that TMPRSS2 may play a pro-oncogenic and pro-metastatic role (102). Knockdown studies in human LNCaP prostate cancer cells demonstrated that reduction of TMPRSS2 expression in cancer cells decreased cellular invasion, tumor size, and incidence of metastases following xenografting in mice (103). Interestingly, loss of TMPRSS2 expression does not impact cellular proliferation of LnCaP cells in culture (103). However, a role of the tumor micro-environment is not taken into consideration in mono-culture, therefore, a role for TMPRSS2 for cancer cell proliferation cannot conclusively be excluded. It is worth noting that in a similar study, shRNA-mediated silencing of TMPRSS2 in LNCaP-derived, bone metastatic castration-resistant (LNCaP C4-2B) cells led to a significant reduction in cell proliferation and cell invasion compared with scrambled shRNA controls (104).

In a study employing mice with a targeted deletion of the Tmprss2 gene, it was demonstrated that the protease regulates cancer cell invasion and metastasis to distant organs in the TRansgenic Adenocarcinoma Mouse Prostate (TRAMP) model of prostate carcinogenesis (104). TRAMP tumors in Tmprss2−/− mice were significantly larger than those in control mice, however, the incidence of metastasis to distant solid organs was substantially lower in the TRAMP tumors arising in the Tmprss2−/− background. It was demonstrated that TMPRSS2 activated signaling incompetent pro-HGF to active HGF in vitro and it is hypothesized that TMPRSS2-activated HGF consistently promotes invasion and metastasis, but differentially enhances or suppresses proliferation. Importantly, a TMPRSS2 chemical inhibitor (bromhexine hydrochloride) suppressed distant metastasis to lung and liver sites in TRAMP mice (104).

These links to prostate malignancy makes TMPRSS2 a promising target for drug therapies. Of notable interest is that no phenotype affecting normal development or physiological function has been observed in TMPRSS2 deficient mice. This suggests that targeted ablation of TMPRSS2 in cancer may have minimal side effects (105). Upstream, TMPRSS2 expression in prostate has been shown to be driven by androgen receptor signaling; one notable consequence of this is the pro-oncogenic TMPRSS2-ERG fusion protein. This link between androgen receptor signaling and TMPRSS2 has further pushed interest in androgen receptor inhibitors as possible targets for inhibiting prostate cancer growth and metastasis. The pro-oncogenic potential of TMPRSS2 has, as mentioned above, been linked to its activity, specifically pertaining to its role in activating the HGF/cMET pathway (104). More recently, work has uncovered matriptase as a possible substrate for TMPRSS2. A recent study found that levels of active matriptase are increased in prostate cancer without increases in matriptase transcript levels (103). Furthermore, orthotopic grafts of LNCaP cells over-expressing TMPRSS2 exhibited increased levels of active matriptase, as well as increased metastases, when compared to grafts expressing a control vector or catalytically dead TMPRSS2 (103). Proteolytic homeostasis is important for maintaining normal tissue function, and increases in

TMPRSS2 expression may shift the balance between matriptase activity and cognate inhibitors. Additionally, beyond the HGF pathway, TMPRSS2 has been shown to activate protease-activated receptor 2 (PAR-2) in LNCaP cells (106), inciting another pathway which may be involved in promoting metastasis (107). In addition to the TMPRSS2 inhibitor bromhexine hydrochloride mentioned above, other synthetic inhibitors based on substrate analogs have been developed and demonstrated to inhibit TMPRSS2 activity, as measured by cleavage of influenza hemagglutinin (HA) (108). TMPRSS2 in airway epithelia is important for influenza infection, and inhibition of TMPRSS2 with small molecule antagonists can prevent influenza infection (109). However, these small molecule inhibitors also have strong affinities for other proteases, such as matriptase, making the precise therapeutic mechanism by which these molecules function unclear.

1.6.4 TMPRSS4

The physiological role of TMPRSS4 is currently not known, however, a mutation in this gene has been associated with autosomal recessive cerebral atrophy (ARCA) (110). TMPRSS4 has been demonstrated to be upregulated in pancreatic, colorectal, thyroid, lung, and several other cancers (111-114). Because of this broad expression profile in cancer, TMPRSS4 has been a focal point of anti-cancer research in recent years. TMPRSS4 has been shown to promote proliferative processes in lung and thyroid cancer cells, while shRNA targeting of TMPRSS4 transcripts causes reductions in proliferation (115-117). Work using cultured lung cancer cells demonstrated that TMPRSS4 promotes a mesenchymal and invasive phenotype, suggesting a role for epithelial to mesenchymal transition (EMT) (117). Interestingly, increases in markers for cancer stem cells (CSCs) such as aldehyde dehydrogenase (ALDH) and octamer-binding transcription factor 4 (OCT-4) are strongly positively correlated with TMPRSS4 expression (118). Several reports have suggested that TMPRSS4 associates with poor prognosis and survival in a variety of different cancers (117,119-122), which may be a result of an increase in the CSCs population, although the factors leading to TMPRSS4 upregulation are

still not identified. One recent finding suggests that increased TMPRSS4 in cancer may result from gene-silencing of tissue factor pathway inhibitor 2 (TFPI-2), a consequence of improper methylation (116). However, the mechanism which connects TFPI-2 and TMPRSS4 expression remains unknown.

While the physiological substrates for TMPRSS4 are not yet fully elucidated, targeting the activity of this protease may have benefits in the treatment of several types of cancer. With several studies reporting reduced invasive and proliferative potential in lung and thyroid cells following silencing of TMRSS4 expression (114,115), inhibitors of TMPRSS4 may provide an edge in cancer treatment. Also, overexpression of TMPRSS4 in cell culture causes cancer cells to be more resistant to several chemotherapeutics (118). A few small molecule inhibitors derived from 2-hydroxydairylamide have been developed with inhibitory effects on the proteolytic activity of TMPRSS4, with the consequence of impacting cancer cell invasiveness in colorectal SW480 cancer cells (123). Given that TMPRSS4 impacts signaling pathways such as cyclic AMP response element-binding protein (CREB)-cyclin D1 (115), inhibition of TMPRSS4 could impact many downstream processes important for a variety pro-oncogenic processes.

In conclusion, several TTSPs are candidate targets for cancer therapy and further investigations are needed to identify whether other novel TTSP family members promote tumor progression, thus validating them as potential therapeutic targets.

CHAPTER 2: THE ROLE OF TMPRSS13 IN BREAST CANCER: BACKGROUND AND SPECIFIC AIMS

2.1 Identification of novel TTSP's in breast cancer

To identify novel TTSP family members that promote breast cancer progression, we performed a systematic *in silico* screening of TTSPs in human and murine breast cancers using the Oncomine™ microarray database. *In silico* analysis revealed a significant increase in the overall TMPRSS13 transcript levels in human invasive ductal carcinoma (IDC) patient samples compared to normal breast tissue (Fig. 13A). This finding was validated experimentally by Western blot (WB) and immunohistochemistry (IHC) analyses, where higher expression of TMPRSS13 was observed in human invasive ductal carcinoma patient samples and human breast cancer cell lines compared to non-malignant breast tissue and cell lines, respectively (Fig. 13).

TMPRSS13 is a relatively uncharacterized TTSP family member and little is known about its basic biochemical features. TMPRSS13, also known as mosaic serine protease large-form (MSPL), belongs to the hepsin/transmembrane protease, serine (TMPRSS) subfamily. TMPRSS13 contains an N-terminal intracellular domain, a transmembrane domain, a stem region, and a C-terminal serine protease domain (5,6). The protease was originally cloned from a human lung cDNA library and transcripts were detected in lung, placenta, pancreas, and prostate (5). Subsequent studies revealed a broad TMPRSS13 protein expression profile in epithelial tissue including epidermis, oral cavity, esophagus, bladder, stomach, small intestine, thymus, kidney, and cornea (7). A physiological role for TMPRSS13 in epidermal barrier development has been demonstrated in TMPRSS13-deficient mice, which display improper formation of the cornified layer of the epidermis (7). Furthermore, TMPRSS13 has been implicated in viral infection, since it proteolytically cleaves the viral hemagglutinin (HA) protein, thereby enabling membrane fusion of highly pathogenic avian influenza viruses and coronaviruses (8-10).

Deficiency in knowledge of important biochemical features of TMPRSS13, including activation and localization patterns, prompted an investigation to elucidate critical features of TMPRSS13 to better understand its potential biochemical mechanisms of action. Additionally, studies to identify whether increased expression of TMPRSS13 in breast cancer plays a causal or promotional role were performed to identify whether TMPRSS13 represents a potential new therapeutic target in breast cancer. **Hypothesis:** TMPRSS13 expression is increased as normal cells undergo neoplastic transformation, and is critically involved in breast cancer progression and metastasis.

2.2 Specific Aims:

AIM 1) Biochemical characterization of proteolytic features of TMPRSS13

The activation, localization, regulation by inhibitors, and post-translational modifications of TTSP family members play an important role in determining the physiological function of these proteases in both normal physiological conditions and disease. These important features are currently unknown for TMPRSS13 and were examined to better understand the functional role of TMPRSS13 in breast cancer.

AIM 2) Expression profiling and functional analysis of TMPRSS13 in breast cancer progression.

Expression of TMPRSS13 in breast cancer: The expression profile of TMPRSS13 was assessed by *in silico* analysis followed by IHC and Western blotting to determine whether TMPRSS13 there is differential expression of TMPRSS13 in breast cancer. Expression of murine TMPRSS13 in the mammary cancer genetic model, MMTV-PymT, was also be assessed,

Functional analysis upon loss of TMPRSS13 expression in breast cancer

In vivo: The TMPRSS13 loss-of-function (null) genetic mouse models will be intercrossed with the MMTV-PymT transgenic breast cancer model to determine effects on tumor onset, primary tumor growth, and metastasis to the lungs.

AIM 3) The role of TMPRSS13 in pro-oncogenic cellular processes.

*TMPRSS13-dependent proliferation, apoptosis, invasion, and chemosensitivity***:** Due to the lack of targeted therapeutic options, we will determine whether TMPRSS13 functions in a protective role to enhance tumor cell survival. The effects of RNAi-mediated silencing of TMPRSS13 will be examined to determine whether loss of TMPRSS13 affects breast cancer cell proliferation, cell death, and invasive capability. We will determine if TMPRSSS13 loss enhances chemosensitivity in triple-negative breast cancer cells.

CHAPTER 3: BIOCHEMICAL CHARACTERIZATION OF TMPRSS13

This research (Chapter 3) was originally published in the Journal of Biological Chemistry. Murray AS, Varela FA, Hyland TE, Schoenbeck AJ, White JM, Tanabe LM, Todi SV, List K. Phosphorylation of the type II transmembrane serine protease, TMPRSS13 in Hepatocyte Growth Factor Activator Inhibitor-1 and 2-mediated cell surface localization. J. Biol. Chem. 2017; 292:14867-14884. © the American Society for Biochemistry and Molecular Biology.

3.1 Materials and Methods

3.1.1 Cloning of full-length TMPRSS13 plasmid constructs

The human TMPRSS13 plasmid construct was obtained from GeneCopia with Accession: BC114928.1 (Rockville, MD). The full-length human TMPRSS13 was PCR amplified using a high-fidelity Platinum®Taq polymerase (Invitrogen, Life Technologies, Grand Island, NY) with the following primers: 5'-GCCACCATGGAGAGGGACAGCCACGGG-3' and 5'-GGATTTTCTGAATCGCACCTCGCTCTC-3'. The resulting PCR fragment was cloned into the pcDNA 3.1/V5-His TOPO® TA (Invitrogen, Life Technologies, Grand Island, NY) in frame with a C-terminal His-tag and V5 epitope using standard TA cloning techniques. Point mutations for S506A-TMPRSS13 and R320Q-TMPRSS13 were generated using a QuikChange II Site-Directed Mutagenesis Kit (Agilent Technologies, Santa Clara, CA) following the manufacturers protocol. Primers used for S506A mutagenesis were: 5' – AAGAGGCCCCCCGGCGTCTCCCTGGCAG – 3' and 5' – CTGCCAGGGAGACGCCGGGGGGCCTCTT – 3'. Primers used for R320Q mutagenesis were: 5' – CCATGACCGGGCAGATCGTGGGAGG – 3' and 5' – CCTCCCACGATCTGCCCGGTCATGG – 3'. Primers used for K151R mutagenesis were: 5' - CGCCAGGTGAACCTGGGCAGGCTC G – 3' and 5' - CGAGCCTGCCCAGGTTCACCTGGCG – 3'. Primers used for K159R mutagenesis were 5' - GGTAGCTGCCTCTGGCCCTCCCGCC – 3' and 5' - GGCGGGAGGGCCAGAGGCAGCTACC – 3'

Untagged TMPRSS13 constructs were generated by PCR amplification of WT, S506A, and R320Q expression vectors using the Platinum®Taq polymerase. The primers used for PCR amplification were 5' – AACCGGATCCATGGAGAGGGACAGCCACGGGAAT – 3' and 5' – AACCCTCGAGTTAGGATTTTCTGAATCGCAC – 3' which resulted in the PCR amplified product encoding the native stop codon. PCR amplified products and empty vector pcDNA 3.1/V5-His TOPO® TA were digested using the BamHI and XhoI restriction enzymes and ligated using the T4 DNA Ligase (New England Biolabs, Ipswich, MA) following the manufacturers protocol. N-terminal HA-tagged constructs were generated by PCR amplification of untagged WT- and S506A-TMPRSS13 from of the pcDNA3.1 V5/His TOPO® expression vectors. The plasmid containing the N-terminal HA tag was a kind gift from Dr. Todi and is encoded in the pcDNA3.1-HA vector. PCR amplified products and the pcDNA3.1-HA plasmid were digested using BamHI and XhoI restriction enzymes. Digested products were ligated with the T4 DNA Ligase (New England Biolabs, Ipswich, MA) following the manufacturers protocol. Transformation of all vectors was performed in TOP-10 competent cells (Invitrogen, Life Technologies, Grand Island, NY) and positive clones were isolated and amplified using standard techniques.

3.1.2 Transient transfections and Western blots

Transfection of HEK293T (ATCC, Manassas, VA) was performed using Lipofectamine® LTX according to the manufacturer's instructions (Invitrogen, Life Technologies, Grand Island, NY). HEK293T cells were cultured in Dulbecco's modified Eagle's media (DMEM) (Gibco, Life Technologies, Grand Island, NY) supplemented with 10% fetal bovine serum (Atlanta Biologicals, Lawrenceville, GA). Transfection was performed with 1 µg plasmid DNA for single transfections or 2 µg total plasmid DNA for co-transfections. Vectors included in transfections were pcDNA3.1-TMPRSS13 vectors, empty vector pcDNA3.1, pcDNA3.1-HAI-1, pcDNA3.1-HAI-2, or pEYFP-N1-HAI-2. The HAI vectors were kindly provided by Dr. Stine Friis, University of Copenhagen. To analyze samples by Western blotting using the polyclonal anti-TMPRSS13

antibody (α-extra-TMPRSS13)(PA5-30935 – Thermo Fisher Scientific, Life Technologies, Grand Island, NY), twenty-four hours post transfection cells were washed 3x with PBS and serum free DMEM was added for six hours when analyzing cell lysates and conditioned media from cells expressing untagged TMPRSS13 constructs. Cells were then washed again 3x with PBS after six hours and 1 ml of serum free media was added. Twenty-four hours after addition of serum free media, conditioned media and lysates were collected. Cells were lysed using RIPA buffer: 50 mM, Tris, 150 mM, NaCl, 0.1% SDS, 0.5% deoxycholic-acid, 1% NP-40, pH 7.4 supplemented with protease inhibitor cocktail (Sigma-Aldrich, St. Louis, MO) and cleared by centrifugation at 12,000 x g at 4°C. Protein concentrations were determined using a Pierce BCA Protein Assay Kit (Thermo Scientific, Waltham, MA). For stringent lysis condition, SDS lysis buffer (50 mM Tris-HCl pH 6.8, .25% Bromophenol Blue, 5% glycerol 1.5% SDS, and 100 mM DTT) was boiled for 10 mins. Cells were washed 1x with PBS and then boiling stringent lysis buffer was added to cells. Cells were scraped and collected and boiled for 10 minutes. After boiling, cell lysates were centrifuged at 16,000 x g for 10 minutes at room temperature. Samples were then boiled again for 5 minutes and 15 µl of each sample was loaded onto 10% SDS gels. Protein samples were separated by SDS-PAGE using 10% Mini-PROTEAN® TGX Precast gels (Bio-Rad Laboratories Hercules, CA) under reducing conditions and analyzed by Western blotting. Primary antibodies used in Western blotting were polyclonal rabbit anti-TMPRSS13 raised against a recombinant protein fragment corresponding to a region within amino acids 195 and 562 of Human TMPRSS13 (anti-extra-TMPRSS13) (PA5-30935 – Thermo Fisher Scientific, Life Technologies, Grand Island, NY), rabbit anti TMPRSS13 intracellular domain antibody (anti-intra-TMPRSS13) raised against an epitope within the first (N-terminal) 60 amino acids (ab59862 – Abcam, Cambridge, MA), V5 mouse monoclonal antibody (R96025 - Thermo Fisher Scientific, Life Technologies, Grand Island, NY), HA rabbit polyclonal antibody (NB600-363 - Novus Biologicals, Littleton CO), rabbit anti Phospho-(Ser/Thr) Phe antibody (#9631 - Cell Signaling Technology, Danvers, MA) goat anti-HAI-1 (AF1048 - R&D Systems Inc., Minneapolis,

MN), or goat anti-HAI-2 (AF1106 - R&D Systems Inc., Minneapolis, MN). Secondary antibodies included goat anti-rabbit, goat anti-mouse (Millipore, Billerica, MA), and rabbit anti-goat (Dako, Carpinteria, CA) HRP-conjugated antibodies.

3.1.3 Cloning and expression of the TMPRSS13 active serine protease domain in Pichia pastoris

The human TMPRSS13 active serine protease domain was produced in yeast using a Pichia Expression Kit (Invitrogen, Life Technologies, Grand Island, NY). Human TMPRSS13 serine protease domain was amplified and cloned into the pPIC9 vector at the XhoI and NotI sites, using the primers 5'-TCTCTCGAGAAAAGAATCGTGGGAGGGGCGCTGGCCTCG -3' and 5'-ATTCGCGGCCGCTTAGGATTTTCTGAATCGCAC -3'. Cloning resulted in TMPRSS13 serine protease domain sequence (Ile-Val-Gly) being inserted immediately following a Leu-Glu-Lys-Arg KEX2 cleavage site encoded by the vector. The Leu-Glu-Lys-Arg-Ile-Val-Gly is cleaved between Arg and Ile by the yeast protease KEX2 which is a transmembrane protease located in the Golgi, rendering a secreted activated TMPRSS13 serine protease domain. The *Pichia pastoris* secreted active TMPRSS13 SP-domain contains the same domain IVG N-terminus as the mammalian active SP-domain. Transformation was performed in TOP-10 competent cells (Invitrogen, Life Technologies, Grand Island, NY) and pPIC9-TMPRSS13 positive clones were isolated and amplified using standard techniques. For transformation of *Pichia pastoris*, 20 µg of pPIC9-human-TMPRSS13 or pPIC9 empty vector was digested with SalI, and purified by phenol-chloroform extraction. Electroporation of linearized plasmid into the GS115 yeast strain (Invitrogen, Life Technologies, Grand Island, NY) was performed at 1.5 kV using 0.2 cm cuvettes (BioRad, Hercules, CA) in a BTX-Transporator Plus (Harvard Apparatus, Holliston, MA). The expression of recombinant proteases in the conditioned media from individual yeast clones was analyzed by SDS-PAGE and Western blotting using anti-extra-TMPRSS13 (PA5-30935 – Thermo Fisher Scientific, Life Technologies, Grand Island, NY)

3.1.4 Chromogenic Proteinase Assays

The assays were performed in 96-well plates in a total reaction volume of 100 µl using 50 mM Tris-HCl pH 8.0, 150 mM NaCl, 0.01% Tween-20, 0.01% BSA for dilution of all samples. 5 nM of active recombinant TMPRSS13, matriptase, or empty vector control media was incubated at 37 °C for 60 min with 100 µM of the synthetic peptide L-1720 Suc-Ala-Ala-Pro-Arg-pNA (Bachem, Bubendorf, Switzerland) in the absence or the presence (inhibitor and substrate added concomitantly) of recombinant soluble HAI-1 (60 nM) (R&D, Minneapolis, MN), HAI-2 (40 nM) (R&D, Minneapolis, MN), aprotinin (2 µM), leupeptin (20 µM), or benzamidine (2 mM) (Thermo Scientific, Waltham, MA). Changes in absorbance at 405 nm were monitored using a Magellan NanoQuant Infinite M200 Pro plate reader (Tecan US, Inc., Morrisville, NC). For measurement of chromogenic activity in cell extracts, samples were prepared and analyzed according to (124).

3.1.5 Deglycosylation of TMPRSS13

Proteins in lysates or conditioned media prepared as indicated above were deglycosylated using the PNGase F deglycosylation kit according to the manufacturer's instructions (New England Biolabs, Ipswich, MA).

3.1.6 Dephosphorylation of TMPRSS13 in lysates

For CIP treatment, 5 µg of protein lysates was added to 1x CutSmart® Buffer (New England Biolabs, Ipswich, MA) for a total volume of 50 µl and treated with, or without, Alkaline Phosphatase, Calf Intestinal (CIP) (New England Biolabs, Ipswich, MA). Lysates were incubated at 37ºC for 60 minutes. After 60 minutes, Laemmli Sample Buffer with 5% 2-Mercaptoethanol was added to the reaction and samples were boiled prior to Western blot analysis. For dephosphorylation of MCF-7 lysates, 40 µg of protein was incubated in 1X NE Buffer for Protein Metallo Phosphatases, 1mM $MnCl_2$, and ddH_2O for a total reaction volume of 50 µl, then 800 units of Lambda Protein Phosphatase (New England Biolabs, Ipswich, MA) or vehicle was added to the sample. Reactions were incubated for 30 minutes at 30ºC. After 30 minutes,

Laemmli Sample Buffer with 5% 2-Mercaptoethanol was added to the reaction and samples were boiled prior to SDS-PAGE and Western blot analysis.

3.1.7 Knockdown of TMPRSS13 expression in cancer cells

MCF-7, BT20, and HCC1937 breast carcinoma cells and DLD1 colorectal adenocarcinoma cell line were purchased from ATCC (Manassas, VA). MCF-7 cells were cultured in Dulbecco's modified Eagle's media (DMEM) (Gibco, Life Technologies, Grand Island, NY) supplemented with 10% fetal bovine serum (Atlanta Biologicals, Lawrenceville, GA). BT-20 cells were grown in Eagles + NEAA media (Eagle's MEM with 2mM L-glutamine and Earle's BSS adjusted to contain 1.5 g/l sodium bicarbonate, 0.1 mM non-essential amino acids, 1 mM sodium pyruvate, and 10% FBS), HCC 1937 cells were grown in RPMI + L-GLUT media (RPMI-1640 media with 2 mM L-glutamine adjusted to contain 1.5 g/l sodium bicarbonate, 4.5 g/l glucose, 10 mM HEPES, 1 mM sodium pyruvate, and 10% FBS), DLD1 cells were grown in RPMI + L-GLUT media adjusted to contain 10% FBS. Transient knockdown of TMPRSS13 expression was performed using Lipofectamine® RNAiMAX according to the manufacturer's instructions (Invitrogen, Life Technologies, Grand Island, NY). Stealth siRNA™ constructs were obtained from Invitrogen life technologies (HSS130533 [corresponding to 33 in figure 5C], and HSS130531 [corresponding to 31 in figure 5C). To detect endogenous TMPRSS13 species by Western blotting, the polyclonal rabbit anti TMPRSS13 intracellular domain antibody was used (ab59862 – Abcam, Cambridge, MA)

3.1.8 α2-Macroglobulin capture assay

30 µl of conditioned media from cells expressing WT-TMPRSS13 were added to 30 µl buffer (50 mM Tris-HCl pH 7.5, 150 mM NaCl, and 2.5 mM $CaCl_2$) and treated with or without 30 nM α2-Macroglobulin (Calbiochem, San Diego, CA). Samples were incubated at room temperature for 1 hour. Additionally, α2-macrogloublin was incubated with buffer alone as control. Samples were treated with Laemmli buffer with 5% 2-Mercaptoethanol and boiled for 5 minutes prior to Western blot analysis.

3.1.9 Immunoprecipitation

48 hours post transfection, HEK293T cells expressing either empty vector (EV), TMPRSS13, and/or HAI constructs were lysed with RIPA lysis buffer with protease inhibitor cocktail. One µl of primary mouse anti-V5 (Invitrogen, Life Technologies, Grand Island, NY) was added to 150 µg of protein lysates and lysis buffer was added for a total reaction volume of 250 µl. Lysates were then rotated at 4ºC for 60 minutes. For HA immunoprecipitation, HEK293T cells expressing HA-S506A-TMPRSS13 were lysed with RIPA lysis buffer with protease inhibitor cocktail and equal amounts of lysates were separated and immunoprecipitated with either 1.0 µg of α-HA or α- Rabbit mAb IgG (DA1E – Cell Signaling Technology, Danvers, MA) antibodies for 2 hours at 4ºC. For anti-intra-TMPRSS13 immunoprecipitation, whole lysates of DLD1 cells were prepared with RIPA lysis buffer with protease inhibitor cocktail and 1.0 µg of anti-intra TMPRSS13 or α- Rabbit mAb IgG was added to equal volume of lysates and rotated at 4ºC overnight. After all immunoprecipitations, 30 µl of EZview™ Red Protein A affinity gel (Sigma-Aldrich, St. Louis, MO) were added to the reaction per manufacturers protocol. Samples were then rotated at 4ºC for an additional 60 minutes at which point beads were pelleted at 4ºC and washed 5x with cold PBS pH 7.5. After the final wash, 60 µl of 2x Laemmli buffer with 5% 2-Mercaptoethanol was added and samples were analyzed by SDS-PAGE and Western blotting.

3.1.10 Immunocytochemistry

Cell-surface imaging was performed using HEK293T cells transfected with human full-length TMPRSS13-V5 vectors. Cells were seeded on coverslips coated with rat type-2 collagen (BD Biosciences, Franklin Lakes, NJ) and allowed to adhere and grow overnight. Cells were transiently transfected and 36 hours post transfection, media was removed and cells were fixed in Z-Fix (ANATECH LTD, Battle Creek, MI) for 15 min at room temperature. In permeabilized samples, cells were treated with 0.05% Triton-X in PBS. Cells were then blocked with 5% BSA in PBS for 1 hour prior to staining. TMPRSS13-V5 was detected using a monoclonal anti-V5 antibody (Invitrogen, Life Technologies, Grand Island, NY) or an isotype control antibody

(Sigma, St. Louis, MO). HAI-1 was detected using the M19 antibody (125) kindly provided by Drs. Chen-Yong Lin and Michael Johnson, Georgetown University. Secondary AlexaFlour-488-conjugated goat-anti-mouse and AlexaFlour-647-conjugated antibodies (Invitrogen, Life Technologies, Grand Island, NY) were used to detect TMPRSS1-V5 and/or HAI-1. HAI-2 was detected using a HAI-2-EYFP fusion protein (kindly provided by Dr. Stine Friis, University of Copenhagen) (124). Cells were washed with PBS and mounted with Prolong gold with DAPI (Invitrogen, Carlsbad, CA). Confocal images were acquired on the Zeiss LSM 780 scope at the Microscopy Imaging and Cytometry Resources Core at Wayne State University School of Medicine.

3.1.11 Biotin labeling of cell surface proteins

HEK293T cells expressing empty vector, TMPRSS13, and/or HAI constructs were washed 3x with PBS 48 hours post transfection. Cells were then gently detached and re-suspended in 1.0 ml of PBS, and EZ-Link Sulfo-NHS-SS-Biotin (Thermo Scientific, Waltham, MA) was added for a final concentration of 800 µM. Cells were biotin-labeled for 30 minutes at room temperature. After biotin labeling, cells were pelleted and washed 3x with PBS containing 50 mM Tris, pH 8.0. Cells were then lysed in RIPA buffer supplemented with protease inhibitor cocktail (Sigma-Aldrich, St. Louis, MO) and protein concentrations were quantitated. 150 µg protein were added to 40 µl streptavidin-agarose (Sigma-Aldrich, St. Louis, MO) in a final reaction volume of 200 µl and rotated at 4ºC for 60 minutes. Beads were pelleted by centrifugation at 8,800 x g and supernatant containing non-biotinylated proteins was collected (wash). Beads were washed 5x with cold PBS and subsequently treated with 60 µl of Laemmli Sample Buffer with 5% 2-Mercaptoethanol and boiled for 5 minutes prior to SDS-PAGE.

3.1.12 USP2 deubiquitination assay

HEK293T cells transfected with S506A-TMPRSS13-V5 were lysed 48 hours post transfection in 450 µl RIPA buffer: 150 mM NaCl, 50 mM Tris/HCl, pH 7.4, 0.1% SDS, 1% NP-40, supplemented with protease inhibitor cocktail (Sigma-Aldrich, St. Louis, MO). Lysates were

aliquoted into separate 1.5 ml microcentrifuge tubes and USP2 catalytic domain (BostonBiochem, Cambridge, MA) (final concentration of 2 µM) or vehicle was added. At 10, 30, 120, and 240 minutes after incubation, aliquots of the reaction were removed and treated with Laemmli buffer supplemented with 5% 2-Mercaptoethanol and boiled for 5 minutes prior to SDS-PAGE and Western blot analysis. Samples were run in parallel and TMPRSS13 was detected using mouse anti-V5 (Invitrogen, Life Technologies, Grand Island, NY) and ubiquitin was detected using rabbit anti-ubiquitin (Dako, Carpinteria, CA)

3.1.13 Glycosylation, intrinsic disorder, and phosphorylation predictions

NetNGlyc 1.0 Server was used for glycosylation prediction (http://www.cbs.dtu.dk/services/NetNGlyc/). To predict the disorder disposition we utilized the PONDR-FIT analysis tool (http://disorder.compbio.iupui.edu/pondr-fit.php). The full-length FASTA sequence for each corresponding protein was analyzed and the intracellular domains were plotted on a single graph. Kinase Predictions. Three separate kinase prediction tools were used to identify potential kinases responsible for TMPRSS13 phosphorylation. NetPhospho3.1 (http://www.cbs.dtu.dk/services/NetPhos/), GPS 3.0 (http://gps.biocuckoo.org/online.php) and PhosphoNet (http://www.phosphonet.ca/). For NetPhospho3.1 and GPS 3.0, the FASTA sequences of the intracellular domains were analyzed.

3.2 Biochemical characterization of TMPRSS13 – Introduction

TMPRSS13 belongs to the type-II transmembrane serine protease (TTSP) family that was discovered at the turn of the millennium (3,35,36,126). In humans, the family consists of 17 proteases divided into four subfamilies, based on phylogenetic analyses of their serine protease domains and the domain structure of their extracellular stem regions (3,35,36,126). TMPRSS13, also known as mosaic serine protease large-form (MSPL), belongs to the hepsin/transmembrane protease, serine (TMPRSS) subfamily. TMPRSS13 contains an N-terminal intracellular domain, a transmembrane domain, a stem region, and a C-terminal serine protease domain (127,128). The protease was originally cloned from a human lung cDNA library

and transcripts were detected in lung, placenta, pancreas, and prostate (127). Subsequent studies revealed a broad TMPRSS13 protein expression profile in epithelial tissue including epidermis, oral cavity, esophagus, bladder, stomach, small intestine, thymus, kidney, and cornea (65). A physiological role for TMPRSS13 in epidermal barrier development has been demonstrated in TMPRSS13-deficient mice, which display improper formation of the cornified layer of the epidermis (65). Furthermore, TMPRSS13 has been implicated in viral infection, since it proteolytically cleaves the viral hemagglutinin (HA) protein, thereby enabling membrane fusion of highly pathogenic avian influenza viruses and coronaviruses (129-131).

A defining characteristic of TTSPs is that they are synthesized as single-chain zymogens that require proteolytic cleavage to generate the two-chain active proteases. Upon activation, catalytic activity of several TTSPs, including matriptase, matriptase-2, hepsin, human airway trypsin-like protease (HAT), and HAT-like 5, are inhibited by the endogenous, transmembrane, Kunitz-type serine protease inhibitors, hepatocyte growth factor activator inhibitor (HAI-1) -1 and -2 (55,132-134). A distinctive feature of TMPRSS13 is that it possesses the largest intracellular domain of all the TTSP family members, consisting of 160 amino acids. Upon analysis of the intracellular domain sequence, we identified regions rich in proline, serine, and threonine residues that are predicted to be intrinsically disordered regions (IDRs), which are natively unfolded and do not adopt typical tertiary structures (135). IDRs are frequently subjected to post-translational modifications, such as phosphorylation, that increase the functional state in which a protein can exist in the cell (136). Here we describe a comprehensive study on the biochemical and cell-biological properties of TMPRSS13 and report for the first time that TMPRSS13 is a phosphorylated TTSP. Importantly, our results show that HAI-1 and HAI-2 enhance TMPRSS13 phosphorylation and facilitate cell surface localization.

3.3 Biochemical characterization of TMPRSS13 – Results

3.3.1 TMPRSS13 is expressed as a 70 kDa glycosylated active protease in mammalian cells

Like other TTSPs, TMPRSS13 contains a C-terminal catalytic serine protease (SP) domain, an N-terminal intracellular domain, a transmembrane signal anchor, and a stem region. The stem region in TMPRSS13 is composed of a group A scavenger cysteine-rich receptor (SRCR) domain, preceded by a single, low-density lipoprotein receptor class A domain (LDLA) (Fig. 1A, panel I). The catalytic domain of human TMPRSS13 contains the essential serine protease catalytic triad residues, H^{361}, D^{409}, S^{506}, and the substrate binding pocket residues, D^{500}, S^{525} and G^{527}(129). TTSP's are universally synthesized as inactive zymogens that are activated by cleavage at a conserved activation site motif, predicted to be R^{320}IVGG in TMPRSS13 (indicated with an arrow in Fig. 2A, panel I) (127,129). Upon activation, the catalytic domain remains tethered via a disulfide bond to the stem region of the protease. Therefore, the active SP-domain can be visualized by SDS-PAGE and Western blotting under reducing conditions. In a previous study, using recombinant TMPRSS13 in which the putative activation cleavage sequence was replaced with the enterokinase recognition sequence (DDDDK), activation with enterokinase under cell-free conditions was achieved and TMPRSS13 displayed proteolytic activity towards synthetic peptide substrates (66). However, this earlier work did not examine whether this phenomenon applies in a cellular environment. To determine whether TMPRSS13, containing its native activation sequence, is expressed as an active protease in mammalian cells, we expressed full-length human TMPRSS13 in HEK293T cells and analyzed whole cell lysates by Western blotting (Fig. 2B) using an anti-TMPRSS13 polyclonal antibody raised against the extracellular part of the TMPRSS13 antibody (α-extra-TMPRSS13, indicated in 2A, panel I). The predicted molecular weights of the 586 amino acid full-length protease and the 266 amino acid SP-domain are 61 kDa and 27 kDa, respectively. Two major proteins of approximately 70 kDa and 32 kDa were detected in lysates (Fig. 2B). These species migrated

Figure 2: TMPRSS13 is a 70-kDa active glycoprotein in human cells.

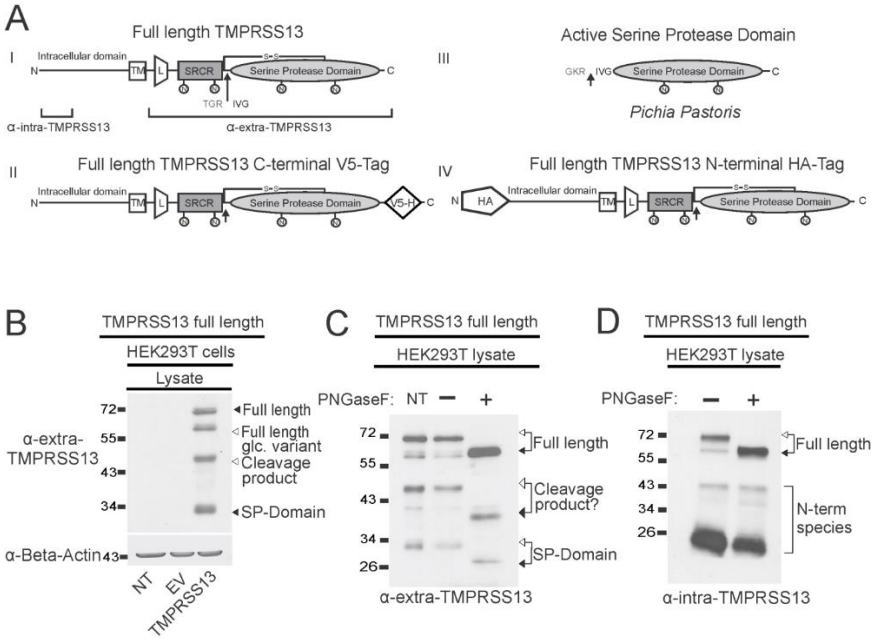

Figure 2. (A) Schematic representation of the four different recombinant TMPRSS13 proteins generated for this study. (I) Full-length human TMPRSS13 (WT-TMPRSS13); TM=Transmembrane domain, L=lipoprotein receptor class A domain, SRCR= group A scavenger cysteine-rich receptor, N=predicted *N*-glycosylation sites, the activation cleavage site is indicated with an arrow, and S-S represents the disulfide bridge linking the stem region to the serine protease (SP) domain. The epitopes for the two anti-TMPRSS13 antibodies used are indicated. A polyclonal antibody raised against a recombinant protein fragment corresponding to a region within amino acids 195 and 562 of Human TMPRSS13, (α-extra-TMPRSS13), that recognizes the extracellular part of the protease. An additional polyclonal antibody, (α-TMPRSS13-intra), was raised against a peptide within residues 1-60 which recognizes the N-terminal intracellular domain. (II) C-terminally tagged full-length human TMPRSS13 (WT-TMPRSS13-V5); V5-H=V5-His epitope. (III) Active soluble TMPRSS13 serine protease domain protein generated in Pichia Pastoris. (IV) N-terminally HA-tagged full-length human TMPRSS13 (HA-WT-TMPRSS13); HA=Human influenza hemagglutinin tag. (B) Whole cell protein lysates from HEK293T cells, expressing non-tagged full-length human TMPRSS13 were separated by SDS-PAGE under reducing conditions. TMPRSS13 was detected by Western blotting using the rabbit α-extra-TMPRSS13 antibody against the extracellular part of TMPRSS13. Non-transfected cells (NT) and cells transfected with empty vector (EV) were included as controls. The full-length TMPRSS13 and SP-domain are indicated with black arrowheads and full-length glycosylation and cleavage variants are indicated with open arrowheads. (C-D) Proteins were separated by SDS-PAGE and analyzed by Western blotting using α-extra-TMPRSS13 (C) and α-intra-TMPRSS13 (**D**), respectively. Lanes with protein extracts treated with PNGaseF prior to SDS-PAGE are indicated with "+", and control extracts treated and incubated in parallel without PNGaseF with "-", NT=No treatment. The white *arrowheads connected to black arrowheads* indicate the reduction in apparent molecular weight of the glycosylated forms of TMPRSS13.

Figure 3: Detection of TMPRSS13 under different expression concentrations and sample collection methods

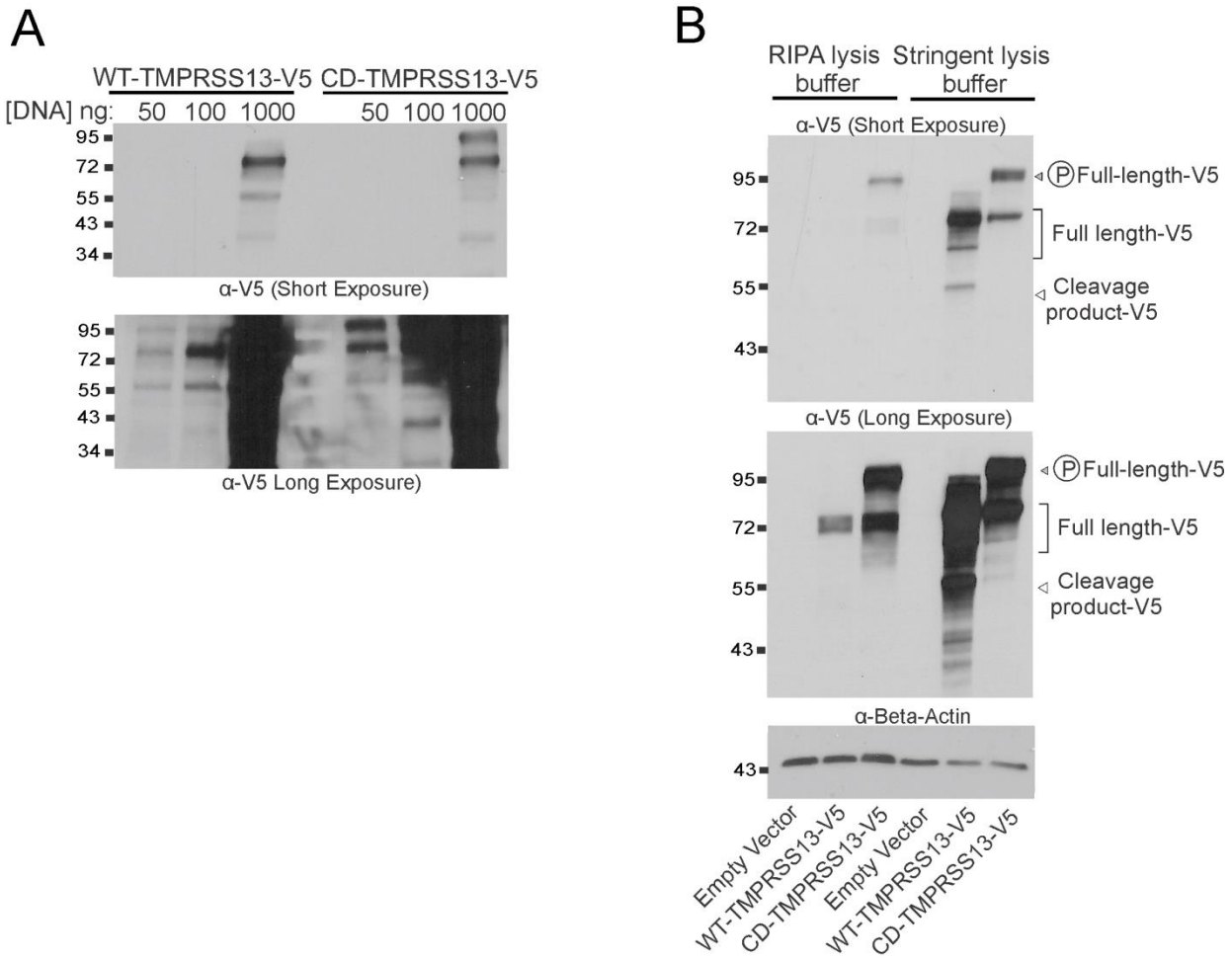

Figure 3. (**A**) HEK293T cells transfected were transfected with WT, - or S506A-TMPRSS13-V5 at the plasmid concentrations indicated resulting in different expression levels of recombinant TMPRSS13. Lysates were made in stringent lysis buffer (1.5% SDS and 100 mM DTT) that had been pre-boiled for 10 minutes prior to addition to cells. Lysates were separated by SDS-PAGE under reducing conditions followed by Western blot analysis using an α-V5 antibody. (**B**) Whole lysates from HEK293T cells transfected with WT, - or S506A-TMPRSS13-V5 were prepared using RIPA buffer with protease inhibitor cocktail at 4°C, or stringent SDS buffer, and analyzed as described in (A).

at higher molecular weights than predicted for the full-length and SP-domain, suggesting that TMPRSS13 could be post-translationally modified. Analysis of the amino acid sequence of human TMPRSS13 using the NetNGlyc 1.0 Server revealed four potential N-glycosylation sites, two of which are located in the serine protease domain (Fig. 2A). In addition to the 70 kDa and 32 kDa species, two forms of approximately 60 kDa and 50 kDa were recognized by the α-extra-TMPRSS13 antibody in whole cell lysates (Fig. 2B). To minimize the risk of cleavage events occurring as a result of cell lysate preparation, or due to high levels of recombinant TMPRSS13 expression, we analyzed cell lysates with low expression levels and lysates prepared using highly stringent conditions (boiling in 1.5% SDS with 100 mM DTT; Fig. 4A and B). We did not observe any discernible differences in protein band pattering by Western blotting between TMPRSS13 low- and high-expressing cells (Fig. 3A). Furthermore, no noticeable differences were observed when cell lysis was performed in RIPA buffer versus stringent SDS buffer (Fig. 3B).

To examine whether TMPRSS13 is post-translationally modified by glycosylation in mammalian cells, protein extracts from transfected HEK293T cells were subjected to enzymatic deglycosylation by PNGaseF prior to Western blot analysis and probed with α-extra-TMPRSS13 (Fig. 2C). Upon deglycosylation and probing with α-extra-TMPRSS13, we observed a reduction in the molecular weight of the proposed full-length 70 kDa form, to a form closer to the predicted lower molecular weight (~60 kDa); this band coincides with the 60 kDa species seen before deglycosylation. These results indicate that the full-length form of TMPRSS13 exists as two different glycosylation variants (Fig. 2C). The presumed SP-domain shifted to the predicted molecular weight upon deglycosylation, indicating that one or both of the potential *N*-linked glycosylation sites in the SP-domain are utilized (Fig. 2C). The 50 kDa band migrated at approximately 40 kDa and may represent an ectodomain cleavage product generated upon cleavage in the LDLA domain of the stem region. Several TTSPs have been shown to be cleaved in the stem region including corin, where two fragments result from corin autocleavage

in the frizzled 1 domain and LDLA 5 domain, respectively (137). The cleavage event generating the 50 kDa TMPRSS13 species appears to be dependent on TMPRSS13 proteolytic activity since the fragment is not detected in cells transfected with a catalytically inactive from of TMPRSS13 and may result from autocleavage (Fig. 3B). Deglycosylated lysates were also analyzed using an antibody raised against a peptide localized within the first 60 (N-terminal) amino acids (α-intra-TMPRSS13) as indicated in the schematic representation of TMPRSS13 in Figure 2A. Similarly to α-extra-TMPRSS13, we observed the 70 kDa form drop to 60 kDa upon deglycosylation (Fig. 2D). In addition, other N-terminal processed forms of approximately 43 kDa and 22 kDa are observed. The latter may result from cleavage within the LDLA domain, i.e. represent the N-terminal half of the C-terminal 50 kDa half detected with α-extra-TMPRSS13 in Fig. 2C.

In addition to whole cell lysates, conditioned media (CM) samples collected from the same cells were analyzed. One band corresponding to the predicted SP-domain was detected in cells transfected with full-length TMPRSS13 (Fig. 4A) suggesting that TMPRSS13 is shed mainly in its active form. To validate that the SP-domain is in fact a catalytically active serine protease, we performed an α_2-macroglobulin (α_2M) capture assay (Fig. 4B). Incubation of α_2M with CM from cells expressing full-length TMPRSS13 resulted in the formation of a TMPRSS13 high molecular weight complex, consisting of TMPRSS13 SP-domain covalently linked to α_2M subunits, indicating that expression of TMPRSS13 in mammalian cells produces a catalytically active serine protease (Fig. 4B).

To further confirm the enzymatic activity of the TMPRSS13 SP-domain, the *Pichia pastoris* expression system which utilizes the intracellular yeast protease KEX2 was employed. The KEX2 transmembrane serine protease belongs to the subtilisin-like, pro-protein convertase family with specificity for cleavage after paired basic amino acids and is localized in the late Golgi compartment. By cloning the TMPRSS13 SP-domain into the PIC9 vector with the TMPRSS13 active serine protease domain sequence (^{321}IVG) immediately following the LGKR

Figure 4: Proteolytic activity of TMPRSS13 serine protease domain

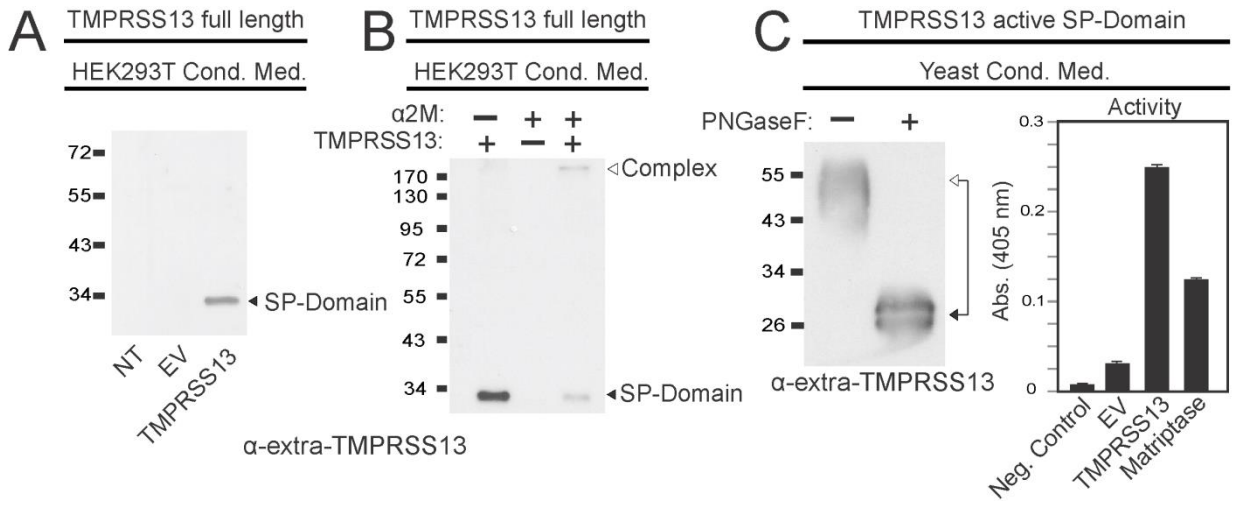

Figure 4. **(A)** Conditioned media from untreated cells (NT), or cells transfected EV or non-tagged full-length human TMPRSS13 were analyzed by Western blotting. Only the SP-domain is detected. **(B)** To determine whether the TMPRSS13 SP-domain is secreted into conditioned medium as an active protease, an α_2-M capture experiment was performed and samples were separated by SDS-PAGE under reducing conditions, and detected by Western blotting using α-extra-TMPRSS13. The positions of the non-complexed TMPRSS13 SP-domain (black arrowhead) and the SP-domain/α_2-M complex (open arrowhead) are indicated. **(C)** Detection of the SP-domain in conditioned media from *Pichia pastoris* expressing cleaved, active TMPRSS13 with (+) and without (-) PNGaseF treatment by reducing SDS-PAGE and Western blotting (left panel). The white *arrowheads connected to black arrowheads* indicate the reduction in molecular mass of the glycosylated form of the SP-domain. Bar graph, right panel; Conditioned media samples from *Pichia pastoris* clones transfected with either the expression vector without protease insert (EV),TMPRSS13 SP-domain, or matriptase SP-domain *were* incubated at 37 °C for 60 min with the synthetic chromogenic peptide Suc-Ala-Ala-Pro-Arg-pNA (100 µm) and the absorbance at 405 nm was recorded. Negative control (Neg. control) lane contains buffer and peptide with no media added.

KEX2 cleavage site encoded by the vector, a novel fusion cleavage site was generated (Fig. 2, panel III, see arrow indicating cleavage site). The new LGKR|IVG sequence is cleaved between R and I by KEX2, generating a secreted active TMPRSS13 SP-domain with the same IVG N-terminus as mammalian active SP-domain (Fig. 2, panels I and III). The presence of TMPRSS13 serine protease in conditioned media from *Pichia pastoris* clones transfected with the PIC9-TMPRSS13 vector was confirmed by Western blotting using the polyclonal α-extra-TMPRSS13 antibody (Fig. 4C, left panel). Deglycosylation of the untagged, cleaved, active form of the TMPRSS13 SP-domain, secreted by transfected *Pichia pastoris,* results in a form with an apparent molecular weight of ∼29 kDa (Fig. 4C, left panel). This indicates that both human and yeast-expressed active serine protease domain migrate at the same approximate molecular weight upon deglycosylation. The catalytic activity of TMPRSS13 SP-domain was confirmed using the serine protease chromogenic peptidolytic substrate Suc-Ala-Ala-Pro-Arg-pNA (Fig. 4C, right panel). Conditioned media from cells transfected with empty PIC9 vector was included as a negative control to ensure the absence of interfering secreted yeast proteases, and the well-characterized TTSP, matriptase, which was produced in parallel in *Pichia pastoris,* was included as positive control. Collectively, these data demonstrate that TMPRSS13 is a glycosylated protease with peptidolytic activity.

3.3.2 Catalytic inactivation of TMPRSS13 promotes TMPRSS13 cell surface localization

Analysis of the TMPRSS13 protein sequence using the TMHMM Server v. 2.0 reveals the presence of a single transmembrane domain, predicting that the TMPRSS13 protein, similar to previously characterized members of the TTSP family, will localize on the cell surface (3,36,126,129). To investigate the cellular localization of TMPRSS13, HEK293T cells transiently expressing the wild type (WT) full-length protease with a C-terminal V5-tag (WT-TMPRSS13-V5) (Fig 1A, panel II) were analyzed by fluorescent immunocytochemistry. To detect the localization of WT-TMPRSS13-V5, an anti-V5 antibody was used on non-permeabilized cells in combination with a FITC-conjugated secondary antibody to visualize cell surface TMPRSS13.

Interestingly, little to no WT-TMPRSS13-V5 was detected under non-permeabilized conditions (Fig.5A, top left panel). In contrast, intense green fluorescent signal confined to the cytoplasm in permeabilized cells was observed, indicating that the majority of WT-TMPRSS13-V5 is retained within the cells (Fig. 5A, bottom left panel). When primary antibodies were substituted with non-immune IgG, no detectable staining was observed (Fig. 5A right panels). Since untagged, WT-TMPRSS13 appeared to be present in its active form in lysates and CM as demonstrated by Western blotting above (Figs. 2B and 3A), we speculated that the active protease fails to properly localize to the cell surface due to the deleterious effects of unopposed proteolytic activity. To test this possibility, we utilized a catalytically inactive form of TMPRSS13 (S506A-TMPRSS13-V5) where the serine in the catalytic triad is mutated to an alanine (Fig. 5B). In addition, we also generated a “zymogen-locked” form (R320Q-TMPRSS13-V5) in which the conserved activation site is mutated to prohibit activation cleavage. Upon transfection, both S506A- and R320Q- TMPRSS13-V5 clearly localized to the cell surface in both permeablilized and non-permeabilized cells (Fig. 5B and 5C). This observation is in agreement with the expected distribution of the predicted membrane anchored topology of TMPRSS13, indicating that catalytically incompetent TMPRSS13 primarily localizes to the cell surface.

Lysates of transfected cells were then examined by Western blotting to analyze the state of WT-TMPRSS13-V5 compared to the two mutant versions. To ensure that WT-TMPRSS13-V5 exists in its intact full-length form with both the N- and C-terminus present, we probed with α-intra-TMPRSS13 and α- -V5 (Fig. 5D). The two full-length glycosylation variant forms (~65 and ~75 kDa, which include the ~5 kDa V5-tag) were detected in WT-TMPRSS13, as well as in S506A- and R320Q- TMPRSS13-V5 with both antibodies. Thus, the C-terminal V5 tag appears intact and the N-terminus is most likely intact since the α-intra-TMPRSS13 antibody was raised against an N-terminal peptide. Surprisingly, in lysates from cells expressing S506A- or R320Q-TMPRSS13-V5 (Fig. 5D) an additional, prominent and higher molecular weight (HMW) TMPRSS13 form of ~95 kDa was observed. This HMW species was resistant to extraction in

Figure 5: Catalytic inactivation of TMPRSS13 promotes its cell surface localization and produces a higher molecular weight TMPRSS13 species

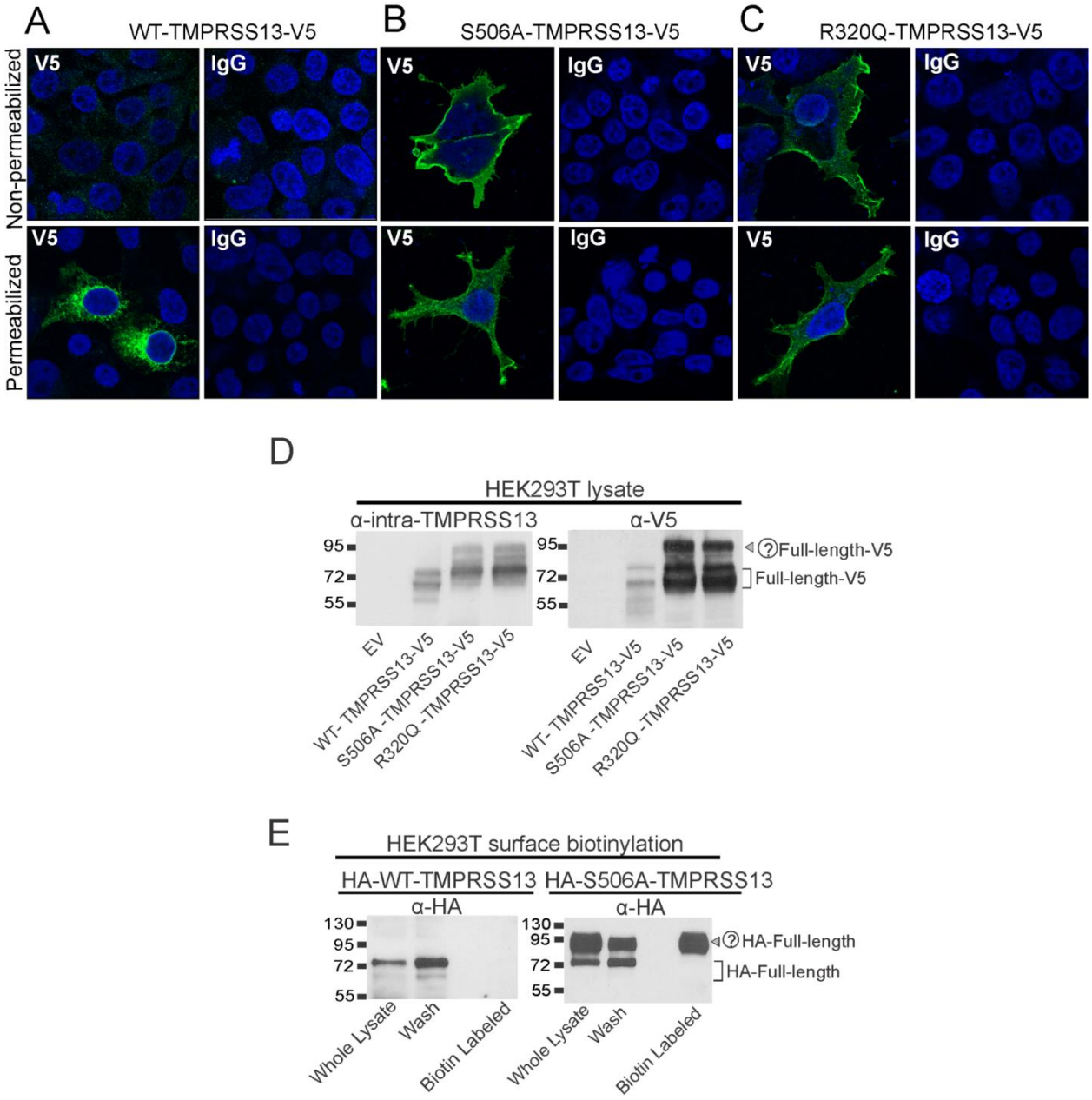

Figure 5. HEK293T cells were transiently transfected with full-length human WT-TMPRSS13-V5 **(A),** S506A-TMPRSS13-V5 **(B)**, or R320Q-TMPRSS13-V5 **(C)** expression plasmids**.** Non-permeabilized cells (upper panels) or permeabilized cells (lower panels) were incubated with an anti-V5 antibody, followed by incubation with FITC-labeled secondary antibodies and DAPI staining to visualize nuclei. The cells were visualized by confocal fluorescence microscopy at 351– 364 nm excitation wavelength (DAPI) or 488 nm (FITC). Merged images obtained at the

two excitation wavelengths are shown. Non-immune IgG was included instead of anti-V5 as negative controls. (**D**) Protein lysates from HEK293T cells expressing empty vector (EV), WT-TMPRSS13-V5, S506A-TMPRSS13-V5, or R320Q-TMPRSS13-V5 were analyzed by Western blotting using the α-intra-TMPRSS13 antibody recognizing the N-terminus, or α-V5 recognizing the C-terminus. The higher molecular weight (HMW) species is indicated with grey arrowhead. **(E)** Cell surface proteins of HEK293T cells expressing either HA-WT-TMPRSS13, or HA-S506A-TMPRSS13 were biotin labeled at room temperature for 30 minutes. Biotin labeled cell surface proteins were separated from non-labeled proteins by incubation with streptavidin agarose for 60 minutes at 4ºC. The streptavidin agarose beads were then pelleted and the supernatant containing proteins not precipitated by streptavidin agarose was collected (wash lane). Biotin labeled proteins were eluted from the beads by addition of Laemmli sample buffer with 5% 2-Mercaptoethanol. Samples were separated by SDS-PAGE and analyzed by Western blot using an α-HA antibody.

RIPA buffer followed by boiling in Laemmli sample buffer with 5% 2-Mercaptoethanol (Fig. 5D) and to extraction under stringent conditions (1.5% SDS with 100 mM DTT) (Fig. 3B), suggesting the possibility of covalent post-translational modifications, in addition to glycosylation, in two different catalytically incompetent forms of TMPRSS13. To further validate these findings, we analyzed lysates from cells expressing TMPRSS13 with an N-terminal HA-tag (depicted in Fig. 1, Panel IV, HA-WT-TMPRSS13) in combination with cell-surface biotinylation analysis using a membrane-impermeable biotinylation reagent (Fig. 5E). Cell surface biotinylated proteins were pulled down using streptavidin agarose. In accordance with the observations above, the full-length HA-WT-TMPRSS13 species (~65 and~75 kDa) were detected with an α-HA antibody in whole lysates confirming that the ~65 and ~75 kDa species both contain an intact N-terminus. The HMW form of TMPRSS13 was also detected with the α-HA antibody in lysates expressing the HA-tagged S506A mutant (Fig. 5E, right panel) thereby confirming that the ~65, ~75 kDa and ~95 kDa are all full-length proteins that contain both the N- and C-termini. The biotinylation assay confirmed that WT-TMPRSS13 is not present in detectable amounts in the cell surface fraction (Fig. 5E, left panel) while S506A -TMPRSS13 is readily detected on the cell surface (Fig. 5E, right panel), mainly it its HMW form. Detailed characterization of the HMW form is described below in the section “TMPRSS13 is phosphorylated”.

3.3.3 TMPRSS13 is capable of auto-activation

We consistently observed decreased detection of the cleaved active SP-domain in S506A-TMPRSS13 expressing cells in comparison to the levels of the active species seen in cells transfected with WT-TMPRSS13 (Fig. 6A). Quantitative ratio comparisons of the active (SP-domain) versus inactive full-length forms of TMPRSS13 confirmed that the majority of TMPRSS13 in S506A-TMPRSS13 expressing cells is in its inactive full-length forms (Fig. 6B). These data indicate that TMPRSS13 proteolytic activity is important for its own activation and that TMPRSS13, like several other TTSPs, is likely capable of auto-activation. To further explore the possibility of auto-activation, intact cells transfected with S506A-TMPRSS13-V5

Figure 6: TMPRSS13 is proteolytic activity promotes its own activation

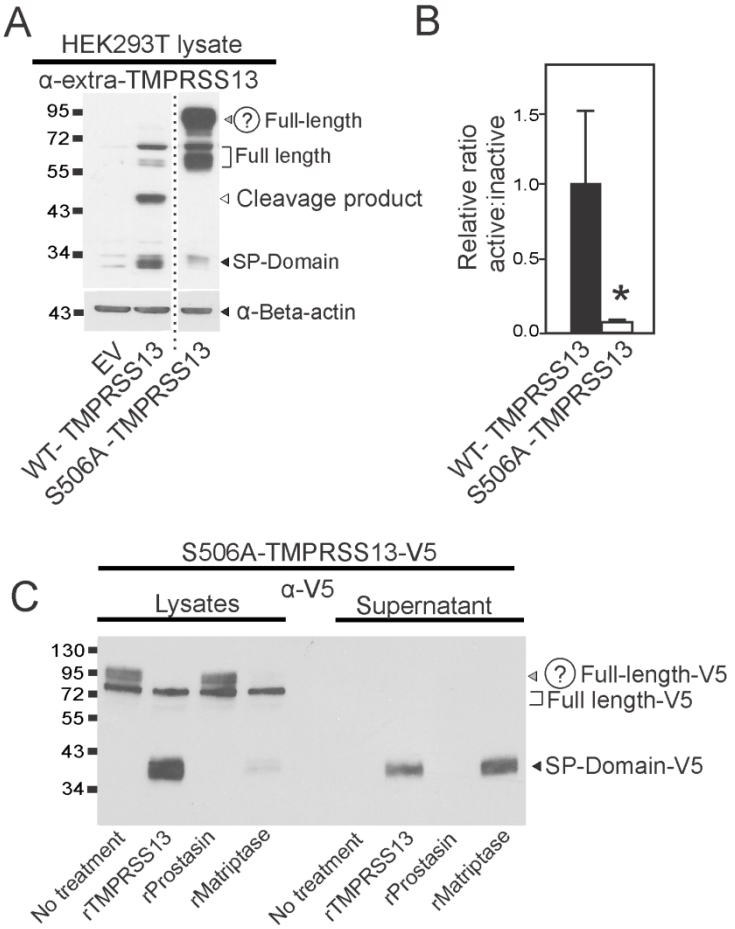

Figure 6. (**A**) Protein lysates from HEK293T cells expressing empty vector (EV), WT-TMPRSS13, or S506A-TMPRSS13 were analyzed by reducing SDS-PAGE and Western using the α-extra-TMPRSS13 antibody. (**B**) Graph depicting the relative ratios of staining intensity after Western development of active TMPRSS13 (SP-domain) compared to the inactive (full-length) species from three separate experiments. $P < 0.05$, student's t test (**C**) Cells expressing S506A-TMPRSS13-V5 were mechanically lifted from the plates by gentle pipetting in PBS, pelleted by centrifugation at 1,000 x g and re-suspended in PBS pH 7.4 (57). Cells were then incubated with 100 nM active recombinant matriptase, prostasin, or TMPRSS13 or left untreated (no treatment lane), and incubated at 37ºC for 30 minutes. After incubation, cells were pelleted by centrifugation at 1,000 x g and supernatant was collected. Cells were then washed 5 times with PBS. After the last wash cells were lysed with RIPA lysis buffer with protease inhibitor cocktail and analyzed by Western blotting under reducing conditions.

were treated with soluble recombinant SP-domain of TMPRSS13, prostasin, or matriptase (Fig. 6C). After protease treatment, cells were pelleted by centrifugation and the supernatant was collected to detect TMPRSS13 released by shedding. Treatment of cells with exogenous, active TMPRSS13 SP-domain led to robust activation as evidenced by detection of the SP-domain in lysates and supernatant. The TMPRSS13 SP-domain is the result of cleavage and activation of full-length, S506A-TMPRSS13-V5 and not detection of the exogenous *Pichia Pistoris* active SP-domain since the recombinant *Pichia Pistoris* active SP-domain lacks the V5 epitope. The active, recombinant SP-domain from prostasin, a non-TTSP, GPI-anchored cell surface serine protease, had no effect whereas a low level of TMPRSS13 SP-domain was detected upon treatment with the TTSP, matriptase, in lysates with abundant SP-domain in the supernatant. Interestingly, the HMW form of TMPRSS13 appears to be preferentially cleaved by both TMPRSS13 and matriptase, which indicates that this form is likely accessible on the cell surface to exogenously added protease. This is in agreement with the biotinylation assay using HA-S506A-TMPRSS13 which demonstrates that the HMW species is the primary species observed at the cell surface (Fig. 5E).

3.3.4 TMPRSS13 is phosphorylated

To characterize the HMW form of TMPRSS13, we first performed deglycosylation of lysates from cells expressing untagged S506A- or R320Q-TMPRSS13, which resulted in the HMW species to migrate at ~73 kDa, which is ~13 kDa greater than the full-length deglycosylated TMPRSS13 (Fig. 7A). This confirms that the HMW form is subject to additional post-translational modification(s). Initial tests were conducted to determine whether the HMW form represents a ubiquitinated species of TMPRSS13, since mono-ubiquitination is a common covalent post-translational modification of cell surface proteins that results in the attachment of the ~8.5 kDa ubiquitin protein (138). Deubiquitination of whole cell lysates using the recombinant catalytic domain of deubiquitinase USP2 (139-141) did not result in a mobility shift of the HMW species (Fig.8A). Only two lysine residues exist in the intracellular domain of

Figure 7: TMPRSS13 is a phosphorylated TTSP family member

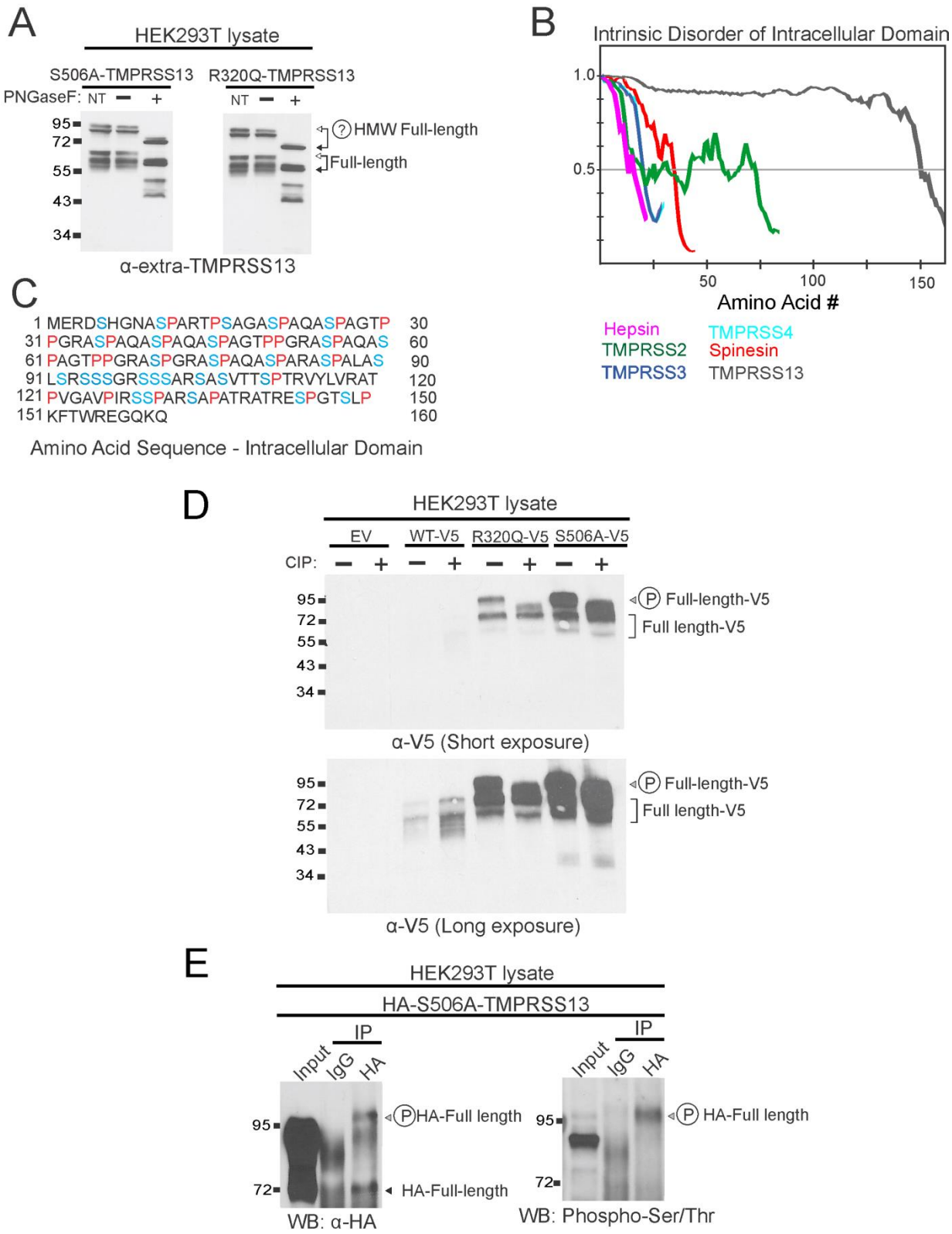

Figure 7. (**A**) Protein lysates from cells expressing S506A- or R320Q-TMPRSS13 were either untreated (NT) or treated with PNGaseF (+) or without (-) (incubated in deglycosylation buffer minus PNGaseF) for 60 min at 37°C prior to reducing SDS-PAGE and Western blotting using α-extra-TMPRSS13. The white arrowheads connected to black arrowheads indicate the reduction in apparent molecular weight of the glycosylated forms of TMPRSS13. (**B)** Graph representing the intrinsic disorder of Hepsin/TMPRSS family member's intracellular domains. Full-length FASTA sequences of hepsin, TMPRSS2, TMPRSS3, TMPRSS4, spinesin, and TMPRSS13 were analyzed using PONDR-FIT (142) and the intracellular domains were plotted on a single graph for comparison. The blue line represents TMPRSS3 overlaying TMPRSS4 (turquoise line) since the profiles of the two are virtually identical. The final X-axis data point for each protein indicates the last amino acid of the intracellular domain. **(C)** Amino acid sequence of the 160 amino acid proline (26 residues, red) and serine rich (30 residues, blue) intracellular domain of TMPRSS13. **(D)** Two different exposures of Western blot analysis of lysates from cells expressing WT-TMPRSS13, S506A-TMPRSS13-V5, or R320Q-TMPRSS13-V5 that were treated with or without CIP and incubated at 37ºC for 60 minutes. (**E**) Lysates from HEK293T cells expressing HA-S506A-TMPRSS13 were immunoprecipitated using an α-HA or an α-IgG control antibody. Samples were separated in parallel and analyzed by Western by probing with α-phospho-serine/threonine or α-HA antibodies.

Figure 8: TMPRSS13 is not ubiquitinated

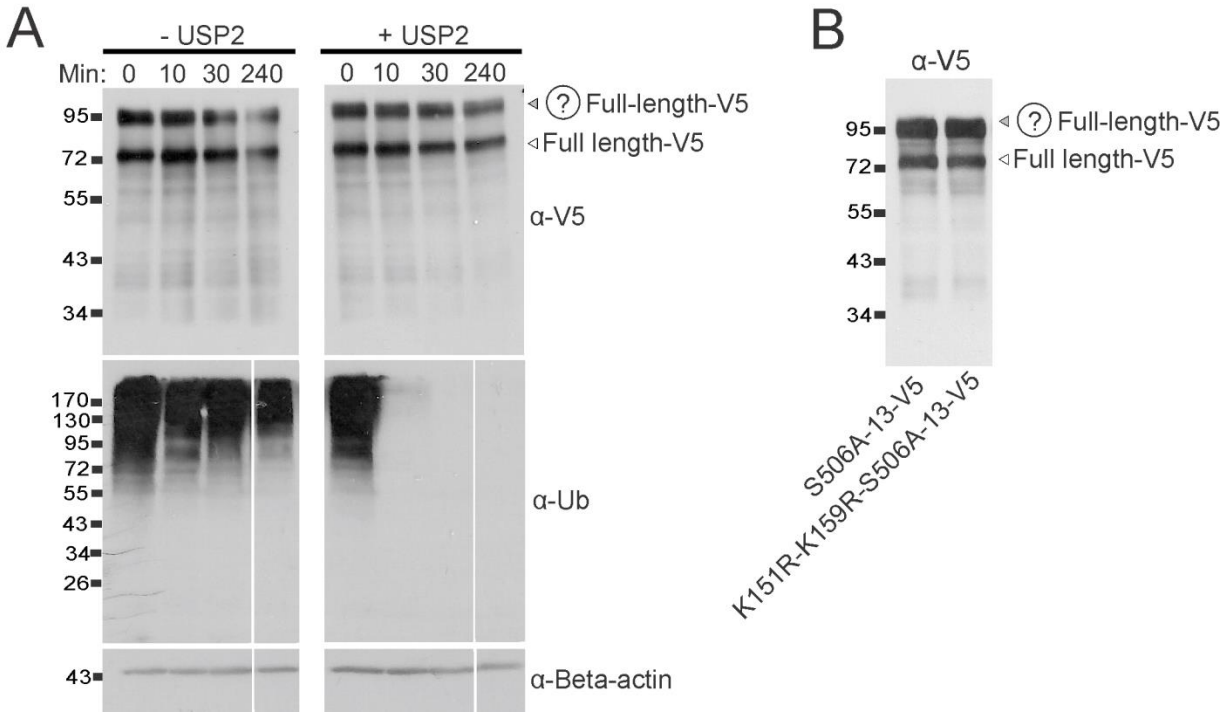

Figure 8. (**A**) Lysates from cells expressing S506A-TMPRSS13-V5 were treated (+) with the deubiquitinase USP2 or vehicle (-) for 0, 10, 30, or 240 minutes. At each time point the samples were boiled in Laemmli sample buffer with 5% 2-Mercaptoethanol for 5 minutes prior to Western blot analysis. A parallel Western blot was probed using anti-ubiquitin to ensure USP2 activity. Efficient deubiquitination is observed after 10 min (lower right panel) but no shift of the ~95 kDa is observed. (**B**) The two lysine residues within the intracellular domain of TMPRSS13 were mutated in S506A-TMPRSS13-V5 to arginine (K151R-K159R-S506A-13-V5) to prevent potential ubiquitination of TMPRSS13. Mutant constructs were expressed in HEK293T cells and protein lysates were analyzed by Western blotting. No change in the migration or expression level of the ~95 kDa species is observed.

TMPRSS13 and upon mutation to prevent ubiquitin modification ($K^{151}R$ and $K^{159}R$) no effect on the abundance or size of the HMW species was observed (Fig. 8B). Taken together, these observations strongly indicate that ubiquitination does not contribute to the HMW form of TMPRSS13.

Currently, the only reported post-translational modifications of other Hepsin/TMPRSS family members are glycosylation and proteolytic cleavage (3). Other types of post-translational modifications, including phosphorylation, are often found in transmembrane proteins that contain IDRs (143,144). Intrinsic disorder occurs in ~50% of transmembrane proteins and proteins with IDRs are more likely to be phosphorylated than proteins that lack them (143). Therefore, we conducted computational prediction of IDRs within the intracellular domain of TMPRSS13 and four additional TMPRSS/Hepsin family members using PONDR-FIT (142) to determine whether there is a higher degree of disorder in the intracellular domain of TMPRSS13 compared to the other family members (Fig. 7B). The comparative analysis revealed that a large segment of TMPRSS13, the first 125 amino acids, displays a high degree of disorder followed by a sharp decline to a lower disorder disposition before the beginning of the transmembrane domain (Fig. 7B). In comparison, the intracellular domain of TMPRSS2, which contains the second longest intracellular domain of the Hepsin/TMPRSS family, contains a short segment of only 10 amino acids with a high degree of disorder before a sharp decline (Fig. 7B). IDRs are also often enriched in disorder promoting amino acid residues such as proline (P), and serine (S) (24); the intracellular domain of TMPRSS13 contains 15% proline and 19% serine residues (Fig. 7C). In sum, TMPRSS13 contains the largest intracellular domain with a higher degree of intrinsic disorder compared to other Hepsin/TMPRSS family members. Based on this observation and on the fact that transmembrane proteins that contain IDRs are frequently phosphorylated (3,143,144), we investigated whether the HMW species represents a phosphorylated form of full-length TMPRSS13.

Phosphorylation of proteins occasionally causes mobility shifts in Western blot analysis due to the negative charge of the covalently attached phosphate group, thereby reducing negatively charged SDS from interacting with the phosphorylated protein (145). Whole lysates from cells expressing WT, - R320Q, - or S506A-TMPRSS13-V5 were dephosphorylated by treatment with calf intestinal alkaline phosphatase (CIP) and separated by SDS-PAGE. Western blot analysis of the CIP-treated samples revealed a mobility shift of the HMW form (Fig. 7D) indicating that the higher molecular weight product is a full-length phosphorylated and glycosylated TMPRSS13 species. Of note, dephosphorylation did not reduce the HMW species to the identical molecular weight of the non-phosphorylated V5-tagged full-length species of ~75 kDa. A possible reason for this may be that the phosphorylated species is differentially glycosylated compared to the non-phosphorylated full-length, or that dephosphorylation of lysates results in incomplete removal of total phosphorylated residues of the intracellular domain.

The intracellular domain of TMPRSS13 contains a total of 30 serine, 12 threonine, and 1 tyrosine residue(s). Previous reports indicate that transmembrane proteins that contain IDRs, like TMPRSS13, are more likely to have greater than 10 phosphorylation sites than proteins that lack IDRs (143). Since it is likely that one or more serine or threonine residues are phosphorylated, and to confirm the phosphorylation of the HMW TMPRSS13 species, immunoprecipitation of lysates from cells expressing HA-S506A-TMPRSS13 was performed. Affinity pull-downs of HA-S506A-TMPRSS13 with α-HA followed by immunoblotting with an α-HA antibody, and an antibody specifically recognizing phospho-serine/threonine residues, confirmed that the HMW species is phosphorylated. (Fig. 7E). As expected, probing with α-HA reveals both full-length TMPRSS13 and phosphorylated TMPRSS13 (Fig. 7E, left panel). When α-Phospho-Ser/Thr was used for detection, a single band corresponding to HMW TMPRSS13 was detected (Fig. 7E, right panel). Together, these data show that HMW TMPRSS13 represents a phosphorylated form of the protease.

3.3.5 Endogenous TMPRSS13 is phosphorylated and glycosylated

To determine whether endogenous TMPRSS13 is present in a phosphorylated form, the human breast cancer cell lines HCC1937, MCF-7, and BT-20, as well as the colorectal adenocarcinoma cell line DLD1 were screened for expression of TMPRSS13 by Western blotting. Lysates were analyzed side-by-side with untagged WT- or S506A-TMPRSS13 for comparison and detected with the α-intra-TMPRSS13 (Fig. 9A and Supplementary 1) We observed bands corresponding in size to the glycosylated full-length (~70 kDa), a non-glycosylated full-length (~60 kDa), as well as a HMW TMPRSS13 (~90 kDa) in all four cell lines, with varying amounts of HMW TMPRSS13 relative to total TMPRSS13 among the different cell lines (Fig. 5A).We also analyzed the expression of the endogenous Kunitz-type serine protease inhibitors, HAI-1 and HAI-2 in these cell lines, which are critical regulators of proteolytic activity of several TTSP family members (3,36,126). Lysates of cell lines were analyzed by Western blotting and probed for TMPRSS13, HAI-1, and HAI-2. Both inhibitors were detected in all four cell lines (Fig. 9B). To ensure α-intra-TMPRSS13 antibody specificity, TMPRSS13 was knocked down in the MCF-7 (Fig. 9C, left) and DLD1 cells lines (Fig. 9C, right) using two different non-overlapping siRNAs targeting the TMPRSS13 transcript. At 72 hours after siRNA transfection, cells lysates were analyzed by Western blotting. Levels of endogenous, full-length TMPRSS13 and the HMW species of ~90kDa TMPRSS13 were significantly reduced upon TMPRSS13 silencing, confirming that the antibody is suitable to study endogenous TMPRSS13 (Fig. 9C).

To determine whether the ~90kDa product of the endogenous form of TMPRSS13 is a phosphorylated species in MCF-7 and DLD1 cells, whole cell lysates were dephosphorylated with Lambda Protein Phosphatase (lambda PP) (Fig. 9D). Dephosphorylation of lysates resulted in a mobility shift of the ~90kDa band, indicating that the HMW species is a phosphorylated endogenous TMPRSS13 species. To additionally validate that endogenous HMW TMPRSS13 represents the phosphorylated form of the protease, immunoprecipitation of whole lysates from DLD1 cells using the α-intra-TMPRSS13 was performed. Isolated proteins

Figure 9: Endogenous TMPRSS13 is phosphorylated

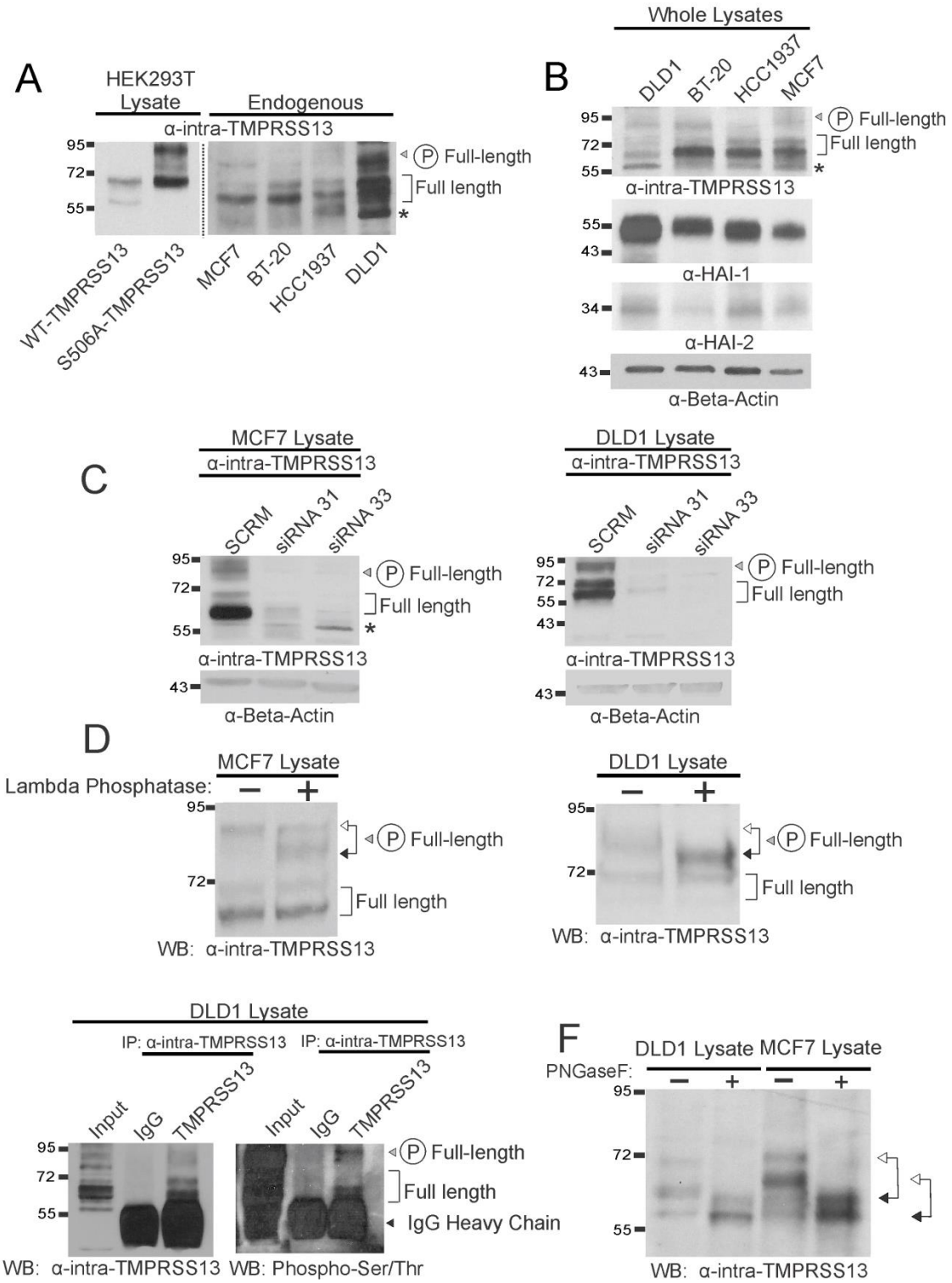

Figure 9. (**A**) Lysates from HEK293T cells expressing untagged WT-TMPRSS13 or S506A-TMPRSS13 were analyzed side by side with lysates from the breast cancer cell lines

MCF7, BT20, and HCC1937, and the colorectal carcinoma cell lines DLD1. The figure shows a short exposure (left) for the exogenously expressed TMPRSS13, and a long exposure (right) for the endogenously expressed TMPRSS13 to compare sizes. Original Western blot exposures can be found in supplementary Fig. *21A*. Asterisk indicates non-specific bands (**B**) Lysates from the indicated cell lines were analyzed for expression of TMPRSS13, HAI-1, and HAI-2. Asterisk indicates non-specific bands. (**C**) MCF-7 and DLD-1 cells were treated with two non-overlapping RNA duplexes (siRNA 31 and 33) targeting the TMPRSS13 transcript or a scrambled GC-matched control (SCRM). After 72 hours post-treatment, cells were lysed and analyzed by Western blotting to analyze decreased expression of TMPRSS13. Asterisk indicates non-specific bands. (**D)** MCF-7 and DLD-1 cell lysates treated with (+) or without (-) lambda phosphatase and analyzed by Western blotting to detect endogenous TMPRSS13 using the α-intra-TMPRSS13 antibody under reducing conditions. (**E**) DLD-1 cell lysates were immunoprecipitated with either α-intra-TMPRSS13 or α-IgG control. Precipitated samples were separated in parallel and analyzed by Western by probing for either α-phospho-serine/threonine or α-intra-TMPRSS13. Input lane contains samples from lysates prior to immunoprecipitation. (**F**) Lysates from DLD1 or MCF-7 cells were treated with (+) or without (-) PNGaseF and analyzed by Western under reducing conditions

were analyzed by Western blotting and upon probing with anti-Phospho-Ser/Thr, a band corresponding to HMW TMPRSS13 was detected (Fig. 9E, right panel). Taken together these data indicate that the ~90 kDa species is representative of an endogenous phosphorylated TMPRSS13 species.

To assess the glycosylation status of endogenous TMPRSS13, lysates from MCF and DLD1 cells were deglycosylated with PNGaseF for 60 minutes (Fig. 9F). In the control lane (-) two bands of ~70 kDa and ~60 kDa are observed; upon deglycosylation (+ lane) two bands of ~60 kDa and 58 kDa are observed. It is likely that the ~70 kDa band is reduced to the ~60 kDa species since similar observations are seen upon deglycosylation of TMPRSS13 in HEK293T cells (Fig. 2D). Notable, upon deglycosylation is the presence of two bands, which may represent two different TMPRSS13 isoforms rather than two different glycosylated full-length species. Currently there are two known TMPRSS13 isoforms that have been identified in lung, placenta, pancreas, prostate and testis (5). Deglycosylation of lysates that expressed high levels of detectable endogenous phosphorylated TMPRSS13 revealed that the phosphorylated species shifts from ~90 kDa to ~73 kDa (Supplementary Fig. 21B) which is similar to what we observed upon deglycosylation of S506A-TMPRSS13 (Fig. 7A). Collectively, these results demonstrate that endogenous TMPRSS13 is post-translationally modified by glycosylation and phosphorylation.

3.3.6 HAI-1 and HAI-2 mediate TMPRSS13 cell-surface localization and phosphorylation

The data above indicate that loss of TMPRSS13 proteolytic activity, either directly by mutation of a residue within the catalytic triad, or indirectly, by mutation of the activation site, results in a detectable, phosphorylated, full-length form of TMPRSS13 and its cell surface localization. The Kunitz-type serine protease inhibitors, HAI-1 and HAI-2, are critical regulators of proteolytic activity of several TTSP family members (3,36,126) and play a role in proper cell-surface localization (124,146,147). As shown in Fig. 9B, the cancer cell lines DLD1, BT20, HCC1937, and MCF7 all express endogenous HAI-1 and HAI-2. Therefore, we reasoned that

HAI-1 and/or HAI-2 could facilitate TMPRSS13 phosphorylation and cell surface localization. To test the inhibitory activity of HAI-1 and HAI-2 towards TMPRSS13, we performed a peptidolytic assay using active recombinant TMPRSS13 SP-domain, generated in *Pichia Pastoris*, with known inhibitors of TTSP family members including HAI-1, HAI-2, aprotinin, leupeptin, and benzamidine. The test was performed in parallel with active matriptase SP-domain, generated in the same expression system, for comparison with a well-characterized reference protease and to ensure inhibitor activity (132) (Fig. 10A). Active TMPRSS13 or matriptase were incubated with the chromogenic peptide Suc-Ala-Ala-Pro-Arg-pNA in the absence or presence of the indicated serine protease inhibitors (inhibitor and substrate added concomitantly) and changes in absorbance were analyzed. Similar to previous reports, recombinant HAI-1 and HAI-2 both inhibit matriptase activity (132,148,149). HAI-1 appeared to be a poor inhibitor of TMPRSS13 activity in this *in vitro* setting, whereas incubation with HAI-2 resulted in nearly complete loss of measurable proteolytic activity. This is similar to previous reports where HAI-1, containing both Kunitz inhibitory domains, displayed weak inhibitory activity towards recombinant TMPRSS13 compared to HAI-2 in a cell-free assay (66). We also observed TMPRSS13 inhibition with the globular polypeptide, Kunitz-type serine protease inhibitor, aprotinin (bovine pancreatic trypsin inhibitor) and leupeptin, whereas benzamidine was a poor inhibitor of TMPRSS13 in this assay.

To validate the HAI-1/HAI-2 inhibitor observations in a cellular setting, we conducted peptidolytic activity assays utilizing whole cell extracts of cells expressing untagged TMPRSS13 either alone or together with HAI-1 or HAI-2 (Fig. 10B). No significant inhibition of activity, as measured by decreased absorbance compared to lysates of cells expressing WT-TMPRSS13 alone, was observed upon TMPRSS13/HAI-1 co-expression, whereas significant TMPRSS13 inhibition was seen when co-expressed with HAI-2. As expected, no substrate conversion above mock background levels was observed when HAI-1 or HAI-2 was expressed without TMPRSS13, or when catalytically inactive S506A-TMPRSS13 was expressed. Taken together,

Figure 10: HAI-1 and HAI-2 mediate TMPRSS13 phosphorylation.

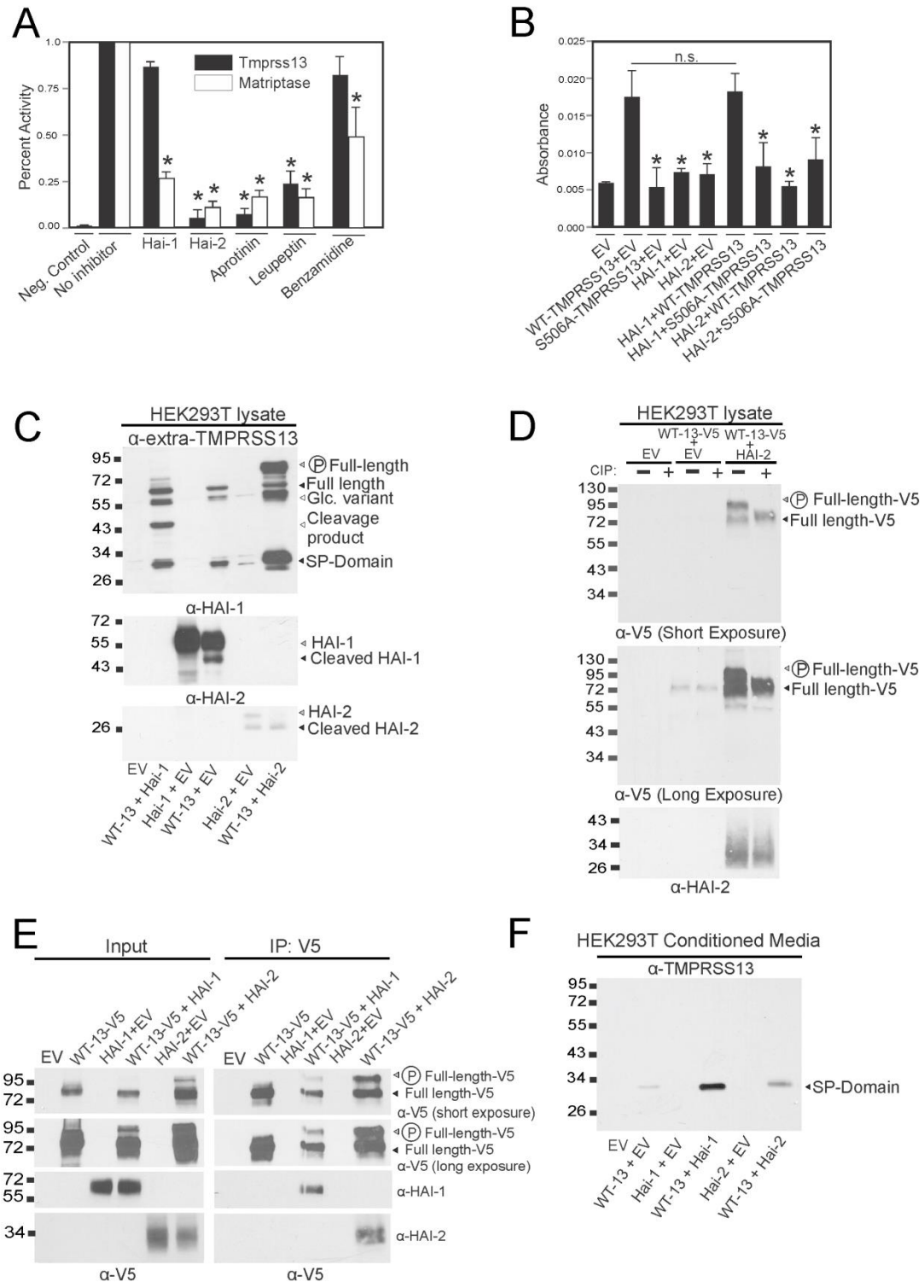

Figure 10. (**A**) Recombinant protease (5 nM) from *Pichia pastoris* clones transfected with either TMPRSS13 (black bars) or matriptase (white bars) was incubated at 37 °C for 60 min with the synthetic chromogenic peptide Suc-Ala-Ala-Pro-Arg-pNA (100 μm) in the absence or presence of the inhibitor indicated (inhibitor and substrate added concomitantly). The absorbance at 405 nm was recorded and enzyme activities for each enzyme are depicted relative to activity when no inhibitor was added. Asterisks indicate significant inhibition (ANOVA multiple comparisons: $p < 0.0001$) compared to "no inhibitor" measurements. (**B**) 200 μg of whole cell protein lysates from HEK293T cells transfected with the plasmids indicated were incubated with the chromogenic peptide Suc-Ala-Ala-Pro-Arg-pNA (100 μm) at 37 °C for 60 min and absorbance at 405 nm was recorded. Asterisks indicate significant decrease in proteolytic activity compared to WT-TMPRSS13+EV measurement (ANOVA multiple comparisons ($p < 0.01$)). n.s. = no significance. (**C**) Lysates from HEK293T cells that were transiently transfected with full-length human HAI-1 alone, HAI-2 alone, or together with WT-TMPRSS13 or either empty vector (EV), were separated by SDS-PAGE and analyzed by Western blotting. (**D**) Protein lysates (5 μg) from cells expressing WT-TMPRSS13-V5 with HAI-2 were treated with CIP for 60 minutes at 37ºC and analyzed by Western blotting under reducing conditions. WT-13-V5 = WT-TMPRSS13-V5. (**E**) Cells expressing empty vector (EV), WT-TMPRSS13-V5/EV, HAI-1/EV, HAI-2/EV or WT-TMPRSS13-V5 with either HAI-1 or HAI-2 were immunoprecipitated with α-V5 antibody and analyzed by Western blotting (right panels). Whole cell lysates were analyzed by Western to verify expression before precipitation (input) (left panels). (**F**) Conditioned media from HEK293T cells expressing the indicated proteins were collected 24 hours after addition of serum free media and analyzed by Western blotting under reducing conditions.

these data are in concordance with the results from cell-free assays above (Fig. 10A) and further indicate that HAI-2 is a more efficient inhibitor of TMPRSS13 proteolytic activity than HAI-1.

To determine whether there is a functional link between TMPRSS13 activation, phosphorylation, and HAI, lysates from HEK293T cells co-expressing either HAI-1 or HAI-2, and WT-TMPRSS13 were analyzed by Western blotting (Fig. 10C). Co-expression of HAI-2 and WT-TMPRSS13 resulted in the appearance of a HMW species that corresponds in size to the phosphorylated form of TMPRSS13. This species was verified to be phosphorylated TMPRSS13 by CIP treatment, which led to the expected shift in mobility (Fig. 10D). Co-expression of WT-TMPRSS13 with HAI-1 resulted in no or weak signal of the phosphorylated TMPRSS13 species in whole cell lysates by Western blotting (Fig. 10C). We suspected this could, at least in part, be due to limited detection capability of the α-extra-TMPRSS13 antibody, since a signal was detected in whole cell lysates of cells expressing WT-TMPRSS13-V5 and HAI-1 at longer exposure (Fig. 10E, input, and Fig. 12A, whole lysate). When WT-TMPRSS13-V5 was immunoprecipitated from lysates of cells co-expressing either HAI-1 or HAI-2, phosphorylated TMPRSS13-V5 was detected in both samples, albeit at lower relative levels for HAI-1 (Fig. 10E, IP:V5), indicating that both HAI-1 and HAI-2 lead to increased TMPRSS13 phosphorylation. Additionally, the co-immunoprecipitation of TMPRSS13-V5 with HAI-1 and HAI-2, respectively, indicates association between each of the inhibitors and TMPRSS13 (Fig. 10E). Taken together, these data indicate that co-expression of HAI-1 or HAI-2 with TMPRSS13 promotes TMPRSS13 phosphorylation.

We consistently observed lower levels of both total and phosphorylated TMPRSS13 when expressed with HAI-1 compared to HAI-2 (Fig. 10C and 10E), which could be due to enhanced activation and shedding of TMPRSS13 from the cell surface when co-expressed with HAI-1. Conditioned media analyzed from cells co-expressing untagged WT-TMPRSS13 with either HAI-1 or HAI-2 revealed that co-expression of TMPRSS13 with either inhibitor results in

increased shedding of the TMPRSS13 active SP-domain into the media compared to WT-TMPRSS13 without HAI expression (Fig. 10F). A greater relative amount of the shed SP-domain is observed upon HAI-1 co-expression compared to HAI-2 co-expression alongside TMPRSS13. Similar observations were previously described for the TTSP family member, matriptase. When matriptase was co-expressed with either HAI-1 or HAI-2, more shed matriptase was detected in the presence of HAI-1 in MDCK cells (124). These data suggest that the lower levels of the phosphorylated TMPRSS13 observed in cells co-expressing HAI-1 compared with HAI-2 may have resulted from increased activation and shedding of TMPRSS13 due to lower inhibitory potential of HAI-1 towards TMPRSS13 compared to HAI-2 (Figs. 10A-B, F).

To further study the role of HAI-1 and HAI-2 in regulating cell surface localization of TMPRSS13, HEK293T cells were co-transfected with WT-TMPRSS13-V5 and either empty vector, HAI-1, or HAI-2, followed by immunocytochemical analysis (Fig. 11). Visualization of HAI-1 was accomplished using the M19 antibody (125) and HAI-2 was visualized using a vector expressing a HAI-2-EYFP fusion protein (124). As expected, transfection with WT-TMPRSS13-V5 alone resulted in intracellular, perinuclear accumulation of the protease (Fig. 11A). In contrast, co-expression with HAI-1, which itself mainly localizes to the cell surface, led to cell-surface localization of TMPRSS13 as well as some intracellular staining (Fig.11B). In cells co-expressing HAI-2-EYFP and WT-TMPRSS13-V5, HAI-2 localizes mostly intracellularly (Fig. 11C), in accordance with previous observations in MDCK cells (124). TMPRSS13 appears to co-localize with HAI-2 intracellularly as well as at the cell surface (also refer to the surface biotinylation data below). It is plausible that interactions between TMPRSS13 and HAI-2 take place along the secretory pathway since co-localization of HAI-2 with endoplasmic reticulum and cis-Golgi markers has been previously reported (124,150).

To verify that TMPRSS13 is localizing to the cell surface, and to identify which form(s) of TMPRSS13 is(are) surface-associated, we performed biotin-labeling of cell surface proteins on

Figure 11: HAI-1 and HAI-2 mediate TMPRSS13 cell-surface localization

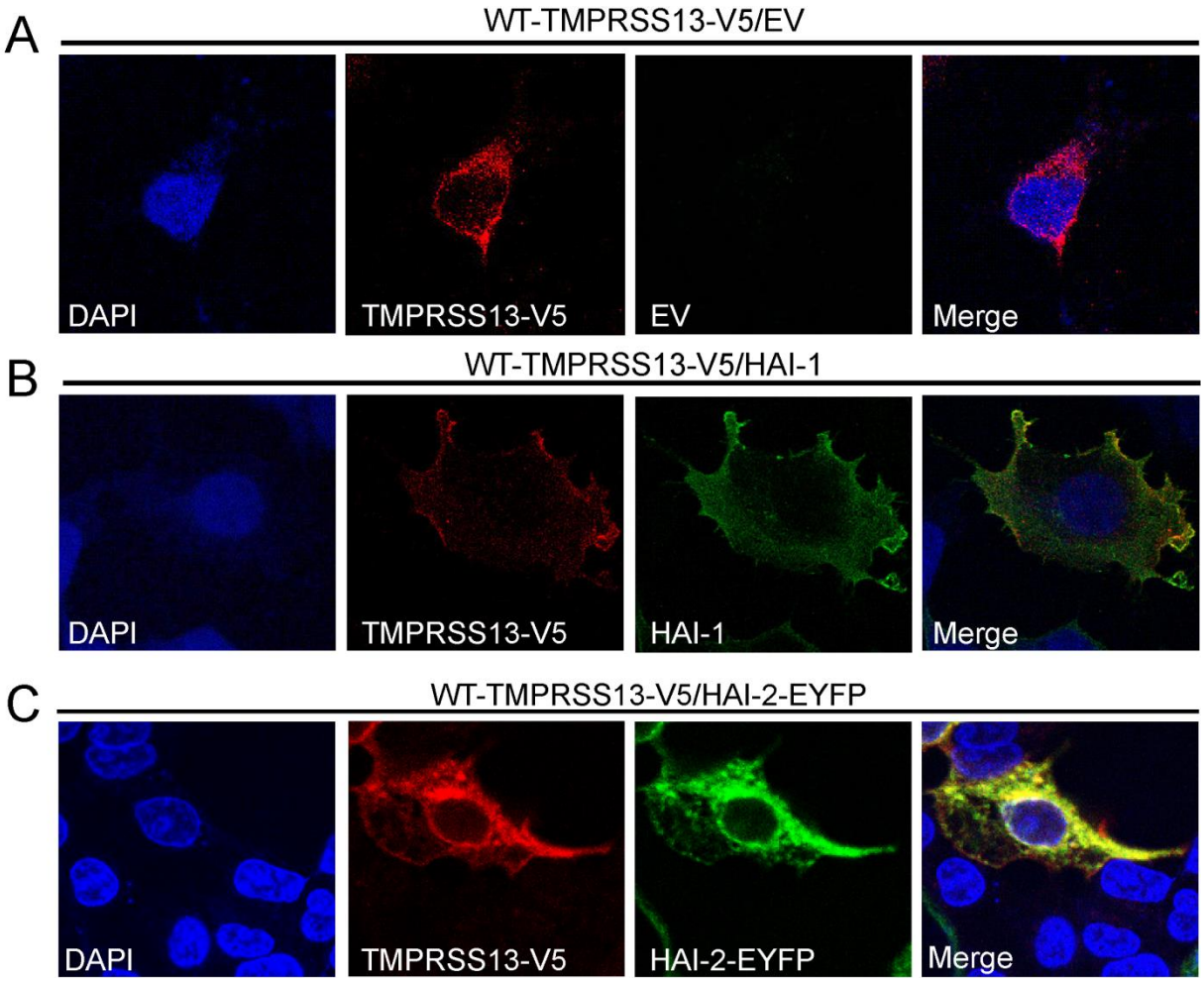

Figure 11. Permeabilized cells transfected with WT-TMPRSS13-V5 alone (**A**) or co-transfected with HAI-1 (**B**), or HAI-2-EYFP (**C**) were stained with anti-V5 (**A and C**), or anti-V5 and the anti-HAI-1 M19 antibody **(B)**. The cells were visualized by confocal fluorescence microscopy. Nuclei (DAPI) (blue, **A, B, C**), WT-TMPRSS13-V5 (red, **A, B, C**), HAI-1 (green, **B**), and HAI-2-EYFP (green, **C**). Merged images are shown in panels on the right.

Figure 12: Localization of phosphorylated TMPRSS13 on the cell surface

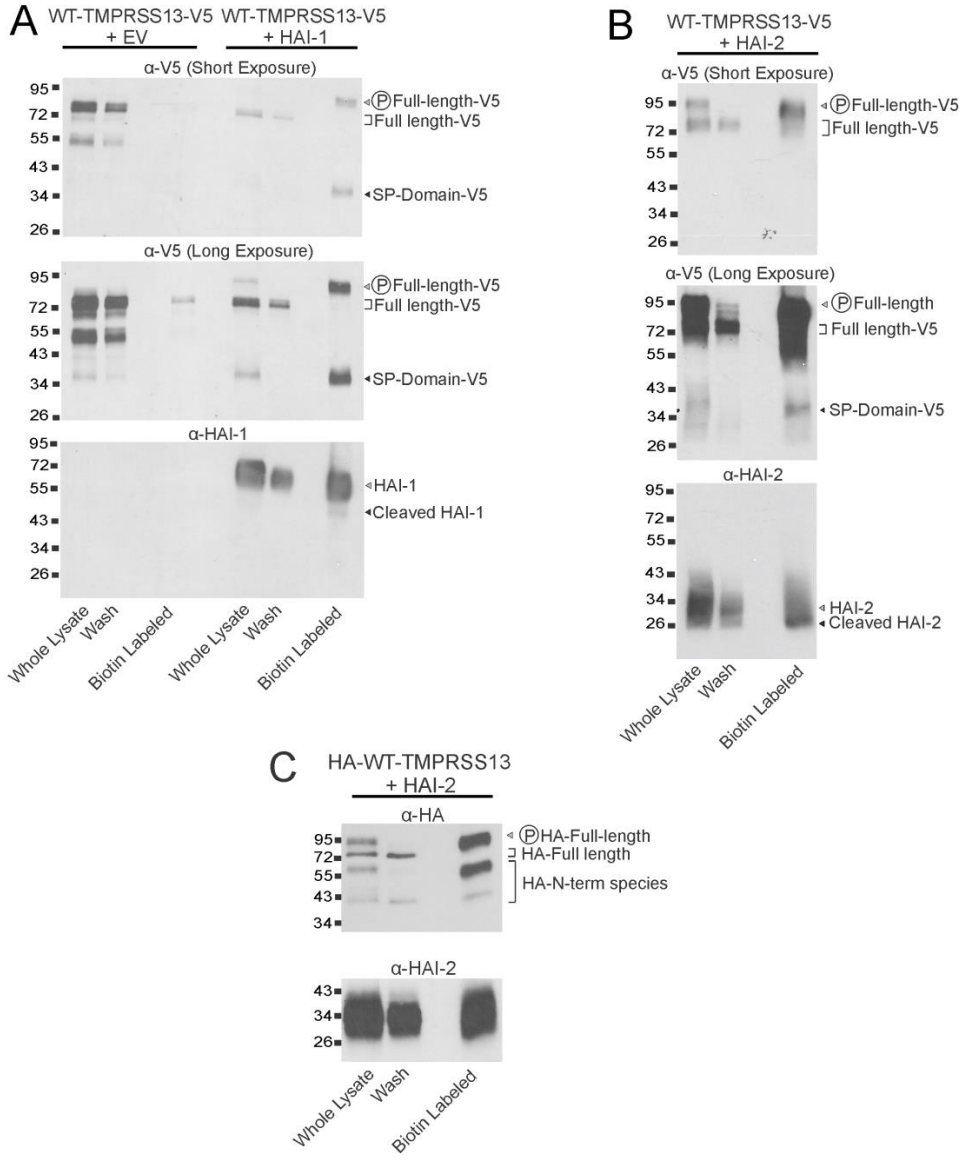

Figure 12. Cell surface proteins of HEK293T cells expressing WT-TMPRSS13-V5 or HA-WT-TMPRSS13 **(C)** with either empty vector (EV) (**A**, left), HAI-1 (**A**, right), or HAI-2 (**B**) were biotin labeled at room temperature for 30 minutes. Biotin-labeled proteins were precipitated with streptavidin agarose for 60 minutes at 4ºC. Streptavidin-agarose beads were then pelleted and the supernatant containing proteins that were not precipitated with streptavidin agarose were collected (wash). Biotin-labeled proteins were eluted from beads by treatment with Laemmli sample buffer with 5% 2-Mercaptoethanol and run side-by-side with non-labeled proteins and whole lysates prior to streptavidin treatment. Different exposures for V5 Western blot membranes are displayed.

intact HEK293T cells expressing WT-TMPRSS13-V5 with either empty vector, HAI-1, or HAI-2 (Fig. 12A and 12B). As expected, when WT-TMPRSS13-V5 was expressed without HAI-1 or HAI-2, no or very low levels of cell-surface biotin-labeled protease were detected by Western blotting (Fig. 8A, left) in accordance with the immunocytochemistry data in figures 5A and 11A. In contrast, co-expression with HAI-1 or HAI-2 resulted in surface-associated TMPRSS13 (Figs. 12A, right and 12B). Interestingly, the V5-tagged phosphorylated, full-length inactive (~95 kDa) and active protease (~38 kDa) SP-domain species appeared to be predominantly localized at the cell surface, since those TMPRSS13 species were readily detected in the biotin labeled samples, and little to no phosphorylated or active TMPRSS13 was observed in the corresponding, non-biotinylated fractions (wash lanes). Correspondingly, the non-phosphorylated, full-length inactive TMPRSS13 species (~75 kDa) was detected in the wash lanes (Fig. 12A and 12B). This experiment was repeated with co-transfection of N-terminal HA-tagged (HA-WT-TMPRSS13) and HAI-2 with similar results (Fig. 12C). According to these data, the non-phosphorylated, inactive full-length species localizes primarily intracellularly. Notably, cells expressing TMPRSS13 with HAI-1 display the highest active SP-domain to total TMPRSS13 ratio comparatively to TMPRSS13 with HAI-2 on the cell surface. It is possible that this could, at least in part, be attributed to the poor inhibitory capability of HAI-1 towards TMPRSS13, which may lead to increased auto-activation of TMPRSS13. Importantly, both HAI-1 and HAI-2 are detected in the biotinylated samples indicating that they both localize to the cell surface. Collectively, these data indicate that HAI-1 and HAI-2 promote TMPRSS13 phosphorylation and cell surface localization of the protease, and that phosphorylated TMPRSS13 is the predominant form present at the cell surface.

3.3 Biochemical Characterization Discussion

As an effort to characterize the hepsin/TMPRSS subfamily member, TMPRSS13, we performed biochemical and cell biological analyses. Expression of human, full-length TMPRSS13 cDNA in mammalian cells led to the production of a recombinant glycoprotein that

could be detected in both cell lysates and as a shed form in conditioned media. Full-length TMPRSS13 displayed proteolytic activity both in whole cell extracts and in conditioned media. Like various other TTSPs, including matriptase, matriptase-2, hepsin, TMPRSS2, TMPRSS3, and TMPRSS4 that are capable of auto-activation (36), the proteolytic activity of TMPRSS13 also appears to be involved in its own activation. Mutation of the active site serine residue led to decreased levels of detectable active SP-domain by Western blotting. Addition of active, recombinant TMPRSS13 to cell surface catalytically deficient TMPRSS13 (S506A-TMPRSS13-V5) also led to TMPRSS13 two-chain conversion. Intriguingly, the well-studied TTSP family member, matriptase, is also capable of cleaving TMPRSS13 at its activation site. Therefore, matriptase may function as an activator of TMPRSS13 in certain conditions; however the physiological relevance of this phenomenon awaits further study.

Cell imaging studies revealed that catalytic inactivation of TMPRSS13 by either mutation of the catalytic serine, or of the arginine residue in the zymogen activation site, results in efficient cell surface localization of TMPRSS13. WT-TMPRSS13 failed to localize at the cell surface and was largely detected intracellularly. However, when TMPRSS13 is expressed with either HAI-1 or HAI-2, efficient cell surface localization is observed using both immunocytochemistry and cell surface protein biotinylation assays. Therefore, the cognate inhibitors HAI-1 and HAI-2 may facilitate TMPRSS13 localization by preventing aberrant intracellular activation. In this regard, it is interesting to note that HAI-1 displays weak inhibitory activity towards TMPRSS13. Previous reports examining the transport of the TTSP family member matriptase to the cell surface have proposed that HAI-1 interacts with the zymogen form of matriptase, thus preventing intracellular activation and to aid in its transport to the cell surface (124,146,147,151). Therefore HAI-1 may function in a similar manner by interacting with the zymogen form of TMPRSS13 to prevent artificial intracellular activation of TMPRSS13.

One of the most intriguing findings of our studies is the presence of a phosphorylated form of TMPRSS13. To our knowledge, this is the first time a TTSP, or any other membrane

serine protease, has been demonstrated to be modified by phosphorylation. Biotinylation studies revealed that the phosphorylated species primarily localizes at the cell surface, presenting the possibility that phosphorylation of TMPRSS13 promotes its translocation to the cell surface. Additionally, in the experiments designed to determine whether TMPRSS13 is capable of auto-activation, the full-length phosphorylated species is the predominate species to be converted into the two-chain form. The mechanism of TTSP auto-activation is not known, however it is thought to involve oligomerization (36). Therefore, one possibility is that phosphorylation of TMPRSS13 promotes oligomerization and cleavage into the two-chain species, thus linking phosphorylation events to zymogen conversion of TMPRSS13. Indeed, previous reports on proteins that contain IDR's have demonstrated that phosphorylation of disordered regions allows for tight control over protein-protein interactions (152,153). Additional studies are needed to gain a better understanding of the consequences of TMPRSS13 phosphorylation.

Previous studies of protease phosphorylation mainly focused on intracellular proteases including caspases and deubiquitinating enzymes (DUBs) (154). ADAM (A Disintegrin And Metalloproteinase) proteases have also been shown to be phosphorylated (155). The C-terminal domain of the transmembrane ADAM17 undergoes phosphorylation at different sites including Thr^{735} and Ser^{819} and phosphorylation at Thr^{735} was found to be necessary for ADAM17-catalysed shedding of TGF-alpha. With ADAM15, phosphorylation of the cytoplasmic domain resulted in interaction with several potential signaling proteins, including the Src kinases, Hck and Lek (156). It is plausible that phosphorylation of TMPRSS13 regulates similar and/or additional processes including localization, protein-protein interactions, and activation.

Currently, the kinases responsible for TMPRSSS13 phosphorylation are unknown. Phosphorylation software tools predict potential candidates for multiple serine residues within the intracellular domain, including the stress activated kinases JNK and p38MAPK, the cyclin dependent kinases (CDK) 2 and 5, and ERK1. Other candidates have been suggested including

CaM kinase II and protein kinase C (128,129). Future studies to identify the kinase(s) responsible for TMPRSS13 phosphorylation may reveal novel insights into the cellular pathways in which TMPRSS13 is involved.

TMPRSS13, HAI-1, and HAI-2 are co-expressed in many developing and adult mammalian epithelia including simple, transitional, and multi-layered squamous epithelia (65,149,157). The current study provides novel information about the regulation of TMPRSS13 activity, HAI-mediated cell surface localization, and phosphorylation, and may represent a new post-translational mechanism critical for cellular regulation and function of TMPRSS13 and other, similar proteases.

CHAPTER 4: TMPRSS13 IN BREAST CANCER

4.1 Materials and methods

4.1.1 Animals

All procedures involving live animals were performed in an Association for Assessment and Accreditation of Laboratory Animal Care International-accredited vivarium following institutional guidelines and standard operating procedures. Tmprss13 deficient mice (Tmprss13^{tm1Dgen}) were generated by Deltagen Inc. and acquired from Jackson Laboratories (Bar Harbor, ME). The mice were generated by homologous gene recombination using a gene targeting vector containing a promoterless LacZ-Neo fusion gene (β-galactosidase reporter) in 129P2 OlaHsd-derived E14 embryonic stem cells. Recombination resulted in an in-frame insertion and deletion of exon 10 and 92 bp of exon 9 encoding the Asp residue of the catalytic triad. Expression results in a fusion protein consisting of the first 377 amino acids of TMPRSS13 fused to β-galactosidase (65). Genotyping was performed using the following primer sets for Tmprss13: moIMR0012 (5'-GGGTGGGATTAGATAAATGCCTGCTCT-3'), oIMR6316 (5'-AAATGACCCACCTAATTAGCTGTAG-3'), and oIMR6318 (5'-GCCTCAATGAGACCTGTTGGATCAC-3').

Mice transgenic for the MMTV-Polyoma virus middle T oncogene (PyVT) in the FVB/N background (strain: FVB/N-Tg (MMTV-PyVT)634Mul) were obtained from The Jackson Laboratory and crossed with Tmprss13$^{-/-}$ mice to generate F1 PyVT/Tmprss13$^{+/-}$ mice. Male F1 PyVT/Tmprss13$^{+/-}$ mice were then crossed with Tmprss13$^{-/-}$ mice to generate F2 study cohorts of PyVT/Tmprss13$^{+/-}$ (hereafter referred as PymT/Tmprss13-control mice) and PyVT/Tmprss13$^{-/-}$ (hereafter referred as PymT/Tmprss13$^{-/-}$ mice) female littermates. Genotyping for the PymT allele was performed with the following primer sets: PymT up: (5'-CGGCGGAGCGAGGAACTGAGGAGAG-3'), and PymT down: (5'-TCAGAAGACTCGGCAGTCTTAGGCG-3')

4.1.2 Western blotting

Cultured human cells were lysed using RIPA buffer: 50 mM, Tris, 150 mM, NaCl, 0.1% SDS, 0.5% deoxycholic-acid, 1% NP-40, pH 7.4 supplemented with protease inhibitor cocktail (Sigma-Aldrich, St. Louis, MO) and cleared by centrifugation at 12,000 x g at 4ºC. Protein concentrations were determined using a Pierce BCA Protein Assay Kit (Thermo Scientific, Waltham, MA). Lysates were separated under reducing conditions on 10% SDS-page gels and blotted onto PVDF membranes. Breast cancer lysates for cell line expression panel were a kind gift from Dr. Julie Boerner (Karmanos Cancer Institute, Detroit M). Antibodies used in western blot detection were: rabbit anti-TMPRSS13 (ab59862 – Abcam, Cambridge, MA), rabbit anti-PARP (9532S – Cell Signaling Technologies, Danvers, MA), rabbit anti-Bcl-xL (2764 – Cell Signaling Technologies, Danvers, MA), and mouse anti-beta-actin (Sigma St. Louis, MO). Secondary antibodies were goat anti-rabbit or goat anti-mouse HRP-linked (Millipore, Billerica, MA). For detection, secondary antibodies conjugated with horseradish peroxidase (Chemicon, Temecula, CA) in combination with Super-SignalWest Femto or ECL Chemiluminescent Substrate (Pierce, Rockford, IL) were used.

4.1.3 Cell culture of human breast cancer cell lines

MCF7 cells were cultured in Dulbecco's modified Eagle's media (DMEM) (Gibco, Life Technologies, Grand Island, NY) supplemented with 10% fetal bovine serum (Atlanta Biologicals, Lawrenceville, GA). BT-20 cells were grown in Eagles + NEAA media (Eagle's MEM with 2 mM L-glutamine and Earle's BSS adjusted to contain 1.5g/L sodium bicarbonate, 0.1 mM non-essential amino acids, 1mM sodium pyruvate, and 10% FBS). HCC1937 cells were grown in RPMI + L-GLUT media (RPMI-1640 media with 2 mM L-glutamine adjusted to contain 1.5 g/L sodium bicarbonate, 4.5 g/L glucose, 10 mM HEPES, 1 mM sodium pyruvate, and 10% FBS). Transient knockdown of TMPRSS13 expression was performed using Lipofectamine® RNAiMAX according to the manufacturer's instructions (Invitrogen, Life Technologies, Grand Island, NY). Stealth siRNA^{TM} constructs were obtained from Invitrogen life

technologies (HSS130532 [corresponding to siRNA-32], and HSS130531 [corresponding to siRNA-31]).

4.1.4 X-gal staining of mouse tissue

Resected mouse tissue was stained with BetaBlue reaction Millipore Burlington, MA) buffer overnight at 37ºC. Tissues were then fixed for 24 hours in 10% neutral-buffered zinc formalin (Z-fix, Anatech, Battle Creek, MI), processed and embedded into paraffin and sectioned.

4.1.5 Immunohistochemistry analyses of mouse tissue

Tissues were fixed for 24 hours in 10% neutral-buffered zinc formalin (Z-fix, Anatech, Battle Creek, MI), processed into paraffin and sectioned. Antigens were retrieved by heating in epitope retrieval buffer-reduced pH (Bethyl Laboratories, Montgomery, TX). The sections were blocked for 1 hour at room temperature with 2.5% normal horse serum in PBS prior to incubation overnight at 4°C with primary antibody. Primary antibodies used were rabbit anti-matriptase (1:100) and goat anti-c-Met (1:100)(R&D Systems, Minneapolis, MN). Cell proliferation was visualized by intraperitoneal injection of 100 µg/g bromodeoxyuridine (BrdU) (Sigma Chemical Co, St. Louis, MO) 2 h before euthanasia. BrdU incorporation was detected with a rat anti-BrdU antibody (Accurate Chemical and Scientific Corporation, Westbury, NY, 1:10). Macrophages were detected by a rat anti-F4/80 antibody (1:50) (Invitrogen, Life Technologies, Grand Island, NY). As negative controls for macrophage staining, IHC samples were treated with biotinylated anti-rat IgG (Vector Laboratories Burlingame, CA) and labeled with vectastain ABC Kit (Vector laboratories Burlingame, CA). Apoptotic cells were detected with rat anti-cleaved caspase-3 (Cell Signaling Technologies, Danvers, MA). Negative controls were treated with non-immune rabbit IgG(adjusted to same final concentration as specific primary antibodies). Primary antibody labeling was then performed using ImmPRESS Reagent Kit anti-rabbit Ig kit (Vector laboratories Burlingame, CA). All staining was performed with SIGMAFAST™ 3,3′-Diaminobenzidine tablets (Sigma-Aldrich St. Louis, MO).

4.1.6 Breast cancer tissue array

The use of human tissue paraffin embedded samples was approved according to the Institutional Review Board Administration. The “BR723 and T088A” breast cancer tissue arrays with pathology grading were obtained from US Biomax, Inc. (Rockville, MD). Tissue arrays were deparaffinized with xylene and hydrated with graded ethanol solutions. Antigen retrieval was performed using heated citrate buffer, reduced pH (Bethyl Laboratories, Montgomery, TX). The arrays were blocked with 2 % bovine serum albumin in PBS, and immunostained overnight at 4°C5. Primary antibodies were rabbit anti-TMPRSS13 (PA5-30935 1:250) (Thermo Scientific, Waltham, MA). As negative control rabbit IgG was used (Sigma, St. Louis, MO) (adjusted to same final concentration as specific primary antibodies). Primary antibody labeling was then performed using ImmPRESS Reagent Kit anti-rabbit Ig kit (Vector laboratories Burlingame, CA). All staining was performed with SIGMAFAST™ 3,3′-Diaminobenzidine tablets (Sigma-Aldrich St. Louis, MO).

4.1.7 Proliferation assays in human breast cancer cell lines

Breast cancer cell lines were seeded in 12-well plates at 50,000 cells/well. Simultaneous reverse transfection with siRNA targeting TMPRSS13, or GC-matched control, was performed upon seeding using RNAiMAX according to the manufacturer’s instructions (Invitrogen, Life Technologies, Grand Island, NY). Cells were counted using a hemocytometer at the indicated days post knockdown and adjusted to number of cells originally seeded. Necrotic cells were labeled with 0.4% trypan blue stain (Life Techonologies (Grand Island, NY) prior to counting.

4.1.8 Invasion assays

Cells were first seeded in 6-well plates while performing simultaneous reverse transfection with either siRNA targeting TMPRSS13 or GC-matched control using RNAiMAX according to the manufacturer’s instructions (Invitrogen, Life Technologies, Grand Island, NY). Fourty-eight hours post silencing, cells were seeded in 8.0uM pore size chambers (Corning Corning, NY) pre-treated with Matrigel™ matrix at 1mG/mL concentration in reduced serum

media. Full-serum media was placed underneath chambers to act as chemoattractant. Cells were allowed to invade overnight and the number of cells that had invaded were stained with Diff-Quik Stain Set (Siemens Newark, DE) per manufacturer's protocol and counted using ImageJ software.

4.1.9 Cell viability assays

Cells were first seeded in 6-well plates while performing simultaneous reverse transfection with either siRNA targeting TMPRSS13 or GC-matched control using RNAiMAX according to the manufacturer's instructions (Invitrogen, Life Technologies, Grand Island, NY). Forty-eight hours post silencing cells were counted and 12,000 cells/well were added to 96-well black, clear bottom plates (Corning Corning, NY). Twenty-four hours post seeding cells were treated with vehicle control or Paclitaxel (T7402 - Sigma-Aldrich St. Louis, MO). Forty-eight hours after treatment cell viability was analyzed Calcein AM Cell Viability Assay per manufacturers protocol (Trevigen Gaithersburg, MD)

4.2 TMPRSS13 in breast cancer - Introduction

Breast cancer progression is accompanied by increased expression of extracellular and cell-surface proteases that are capable of degrading the extracellular matrix as well as cleaving and activating downstream targets. Traditionally, proteolytic processes were thought to exclusively be involved in modifying the tissue microenvironment within the breast to allow for cancer cell invasion and dissemination to other organs. However, more recently, proteases have gained attention for also playing a role in the promotion of cancer progression via the regulation of pro-oncogenic signaling pathways. These proteolytic pathways have been shown to be significantly involved in the relationship between the proliferating tumor and its surrounding stroma to mediate various aspects of tumor progression including proliferation, angiogenesis, inflammation, and survival (2,158,159).

The vast majority of studied proteases involved in cancer progression are secreted proteases expressed in the stroma of breast tumors by fibroblasts or inflammatory cells.

However, a new protease family of 17 structurally unique multi-domain serine proteases that are anchored directly to the plasma membrane, termed the type II transmembrane serine proteases (TTSPs), was discovered at the turn of the millennium (36). Since their discovery, this family of proteases has been shown to play critical and essential roles in normal development, tissue homeostasis, and disease, including cancer (126,160). The expression of TTSP's in cancer is often dysregulated, and various TTSP's, cancer including matriptase, hepsin, TMPRSS2, and TMPRSS4, have been shown to play important tumor promoting roles (159).

To identify novel TTSP family members that may play a role in breast cancer progression, we performed a systematic screening of the expression profiles of TTSP family members in both normal and invasive ductal carcinoma (IDC) patient samples. A candidate family member known as Transmembrane Protease, Serine 13 (TMPRSS13) showed significantly increased mRNA expression in IDC compared to normal breast tissue. Currently, no published study has examined the expression or function of TMPRSS13 in cancer. Several studies have been published indicating a role for TMPRSS13 in influenza infection due to its ability to proteolytically modify the viral protein hemagglutinin, thereby mediating membrane fusion of the pathogenic avian influenza viruses (130,131). Additionally, a physiological role has been implicated for TMPRSS13 through characterization of TMRPSS13-deficient mice, which display a defect in skin development with impaired epidermal barrier acquisition (65). Several biochemical studies have also been published on TMPRSS13, one of which demonstrated that the serine protease domain of TMPRSS13 is capable of activating the pro-oncogenic signaling molecule hepatocyte growth factor (HGF) *in vitro (66)*, and it is currently the only known TTSP family member to be phosphorylated, which may play a role in its cell surface localization (40).

In the current study, *in vivo* "loss-of-function" strategies using novel genetic mouse models along with complementary human cell culture models were performed to determine whether TMPRSS13 plays a role in breast cancer. We demonstrate here that TMPRSS13 expression is increased in both human and murine breast cancer, and that genetic ablation of

TMPRSS13 impairs mammary cancer progression resulting from decreased proliferation and increased apoptosis *in vivo*. Additionally, we demonstrate that loss of TMPRSS13 in human triple negative breast cancer (TNBC) cell lines increases chemosensitivity to paclitaxel treatment, suggesting a pro-survival role of TMPRSS13 in breast cancer.

4.3 TMPRSS13 in breast cancer - Results

4.3.1 Increased expression of TMPRSS13 in breast cancer

As part of ongoing efforts to determine the expression and function of the type-II transmembrane serine protease (TTSP) family members in breast cancer, a systematic expression analysis using the Oncomine^{TM} database was performed. The *in sillico* analysis revealed that TMPRSS13 transcript levels are significantly increased in invasive ductal carcinoma (IDC) patient samples compared to normal breast tissue using The Cancer Genome Atlas (TCGA) dataset (Fig. 13A). To verify the increased expression at the protein level a panel of breast epithelial cell lines were screened for expression by Western blotting, and patient tumor samples were stained for TMPRSS13 expression by immunohistochemistry (IHC). Western blotting results demonstrate that TMPRSS13 has increased expression in several breast cancer cell lines of a diverse origin compared to the non-malignant breast epithelial cell lines, MCF10a and hTERT-HME1, which show little to no expression of TMPRSS13 (Fig. 13B). IHC analysis of TMPRSS13 expression from 24 patient samples displayed an increase in TMPRSS13 protein expression in the IDC samples compared to the normal and benign breast lesions (Fig.13D). Additionally, TMPRSS13 expression is specifically localized to the malignant epithelial cells and not the surrounding stroma, whereas little to no detection of TMPRSS13 is observed in the non-malignant samples (Fig. 13C). Taken together these data indicate that TMPRSS13 expression is increased in breast cancer at both the transcript and protein levels.

4.3.2 Increased TMPRSS13 expression in the MMTV-PymT model of breast cancer

To examine the effects of TMPRSS13 on breast cancer progression *in vivo*, the mouse mammary tumor virus (MMTV) Polyoma middle T (PymT) transgenic mammary tumor model

Figure 13: TMPRSS13 expression in breast cancer

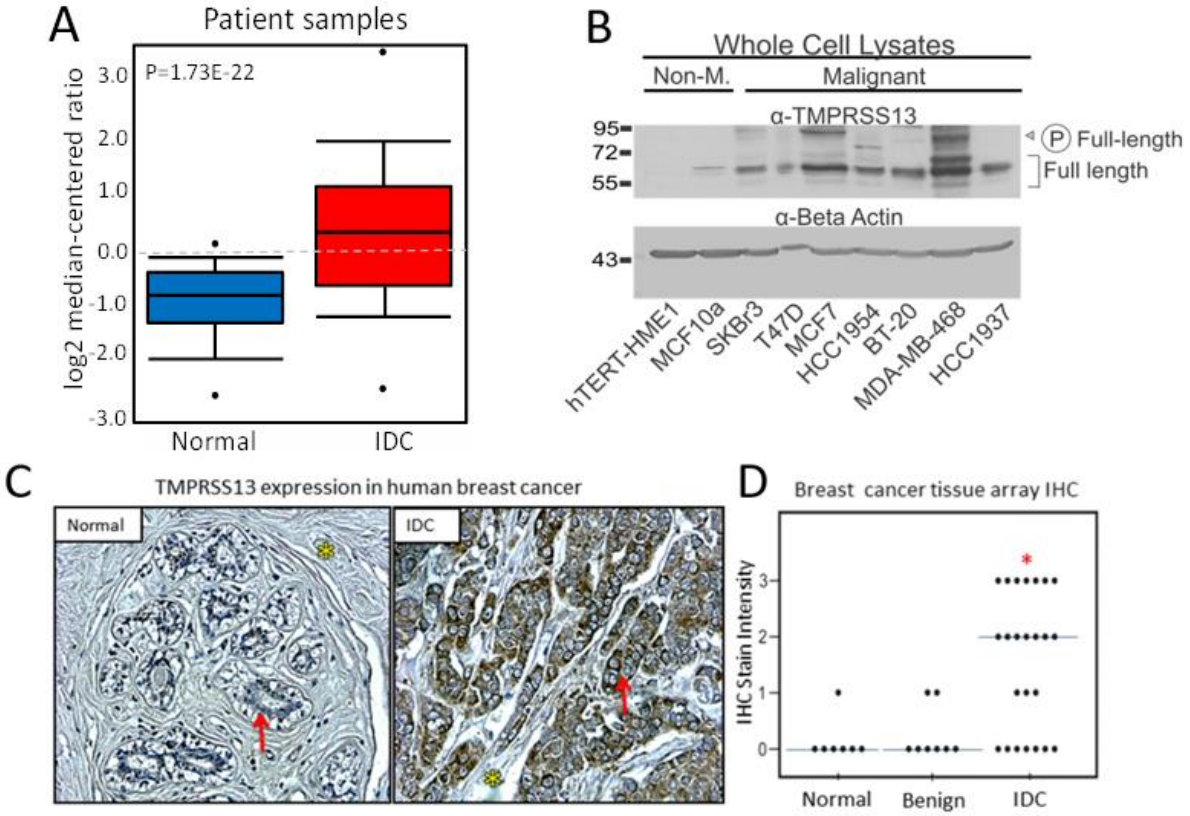

Fig. 13. (A) Box and whisker plot representing TMPRSS13 mRNA expression data for normal breast (N=60, median= -0.8) and IDC (N=468, median= 0.3) from the Oncomine^{TM} microarray database (TCGA data). Boxes show interquartile range, and medians are indicated by horizontal lines **(B)** Elevated TMPRSS13 expression in seven breast cancer lines compared to two non-malignant breast epithelial lines assessed by Western blotting. **(C)** IHC analysis of human patient samples reveals very low to no detectable TMPRSS13 in normal mammary glands (duct indicated with arrow) and pronounced TMPRSS13 staining in carcinoma cells (brown) with no detectable expression in the stroma (yellow asterisk). **(D)** Staining intensity was assessed using defined scoring criteria by two different investigators unaware of sample identity. Dots represent samples from individual patients. Significant differences are observed between normal versus IDC ($P<0.05$) and benign (adenosis and fibroadenoma) versus IDC ($P<0.05$). Blue horizontal line=median.

was utilized. These transgenic mice express the Polyoma middle-T antigen under the transcriptional control of the mouse mammary tumor virus promoter, thus resulting in the expression of the PymT oncoprotein in mammary epithelial cells. Due to the expression of the PymT oncoprotein in mammary epithelial cells, mice develop mammary tumors approximately 1 to 6 months after birth (50). Furthermore, the MMTV-PymT model of breast cancer is further characterized by having a 100 percent penetrance of primary tumors, with a high occurrence of lung metastasis, and closely resembles the progression of human breast cancer. (161-163)

In order to ensure that the MMTV-PymT mouse mammary cancer model mimics the observations described above in human breast cancer and the normal breast, we assessed the expression and localization of murine TMPRSS13 protein. We took advantage of the promoterless β-galactosidase reporter gene cassette being under the transcriptional control of the endogenous *Tmprss13* promoter in TMPRSS13$^{+/-}$ mice. Therefore, X-gal staining of tissue followed by whole mount or histological examination allows for precise detection of TMPRSS13 expression in mouse tissue. Glands from heterozygous TMPRSS13$^{+/-}$ mice with or without the MMTV-PymT transgene were examined and revealed that TMPRSS13 expression is not detected in the normal mammary gland (Fig. 14C), whereas it is readily detected in mammary carcinomas (Figs. 14A and D). Additionally, the expression of TMPRSS13 is specifically expressed in the malignant epithelial cells and not the surrounding stroma, corresponding to the expression pattern observed in human patient samples (Figs. 13C and 14D). Furthermore, whole mount staining of resected lungs from 170-day old mice reveals that TMPRSS13 is also expressed at the metastatic lung lesions (Fig. 14B).

4.3.3 TMPRSS13 deficiency delays tumor development and decreases tumor burden, growth rate, and metastasis *in vivo*

To test the effects of genetic ablation of TMPRSS13 *in vivo* on breast cancer progression, comparative analyses were performed on TMPRSS13-deficient and control mice harboring the MMTV-PymT transgene. Prospective littermate cohorts were established by

Figure 14: TMPRSS13 is expressed in cancer cells of murine mammary carcinomas

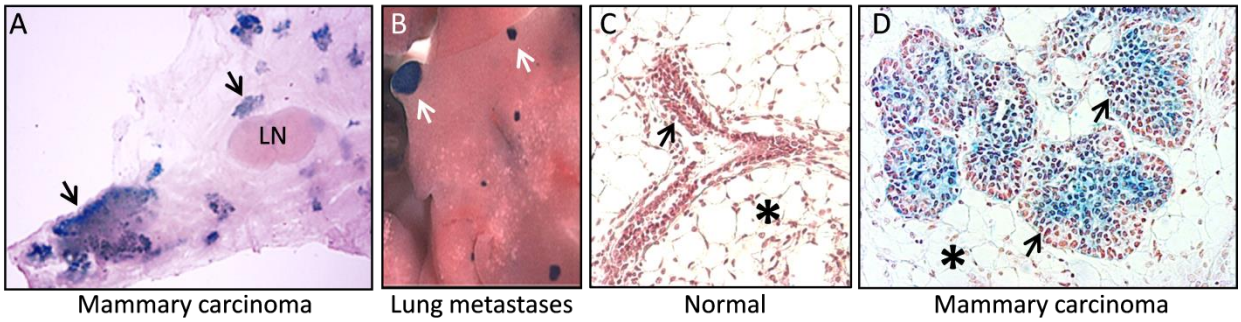

Fig. 14. Endogenous TMPRSS13 visualized by X-gal staining (blue). **(A)** TMPRSS13 is expressed in MMTV-PymT mammary carcinomas (arrows) and **(B)** in lung lesions (arrows) in whole mounts. **(C-D)** Histological analysis: no detectable TMPRSS13 in normal mammary ducts (arrow in C) **(C)** whereas TMPRSS13 is readily detected (blue, arrows in D) in carcinoma cells in tumors from MMTV-PymT transgenic mice **(D)**. No detectable expression of TMPRSS13 in the stroma (asterisk). LN=lymph node. You probably need to include tumor WT without blue too as E.

crossing TMPRSS13$^{+/-}$/MMTV-PymT with TMPRSS13$^{-/-}$ mice to generate TMPRSS13-deficient/MMTV-PymT and control mice (TMPRSS13$^{-/-}$/MMTV-PymT and TMPRSS13$^{+/-}$/MMTV-PymT respectively). Established littermate-controlled cohorts were monitored weekly for detection of the first palpable mammary mass (tumor latency). A 129-day end-point was established where total mammary tumor burden was assessed and calculated by the total weight of the postmortem excised mammary glands of each individual mouse, and total tumor area was calculated by caliper measurements. In addition, the presence of lung metastasis was determined at the termination of the cohort experiment (day 129). TMPRSS13 deficiency affected all tumorigenic parameters measured (Fig. 15). Thus genetic ablation of TMPRSS13 resulted in a significant delay in the formation of palpable mammary tumors in TMPRSS13-deficient mice (Fig. 15A). Additionally, a significant decrease in the overall final tumor burden was observed in TMPRSS13-deficient mice compared to control, with a 62% overall reduction in the final tumor burden in TMPRSS13$^{-/-}$/MMTV-PymT mice (median tumor burden of TMPRSS13$^{+/-}$/MMTV-PymT, 3.03 g, TMPRSS13$^{-/-}$/MMTV-PymT, 1.16 g) (Fig. 15B). The growth rate was also significantly reduced in TMPRSS13-deficient mice with a median growth rate of 1.53 mm^2/day in TMPRSS13-deficient mice, compared to TMPRSS13 control mice that displayed a growth rate of 2.67mm^2/day (Fig. 15C). Furthermore, TMPRSS13-deficient mice had a decreased incidence of lung metastasis (Fig. 15D) (P=0.052, Chi-square test). Taken together these data indicate that TMPRSS13 deficiency impairs mammary cancer progression.

4.3.4 TMPRSS13 deficiency decreases tumor cell proliferation and increases apoptotic cell death *in vivo*

TMPRSS13 deficiency results in a decreased final tumor burden and tumor growth rate *in vivo* (Fig. 15B and C). To determine whether the decreased tumor growth in TMPRSS13$^{-/-}$ mice were due to either decreased proliferative abilities and/or increased programmed cell death rates in TMPRSS13$^{-/-}$/PymT tumors, tumor tissues were stained for either BrdU or the cleaved form of caspase-3 as a marker for cells undergoing apoptosis. Adult 129-day old cohort

Figure 15: Delayed tumor development, smaller tumors, decreased growth rate and metastasis in TMPRSS13$^{-/-}$ mice

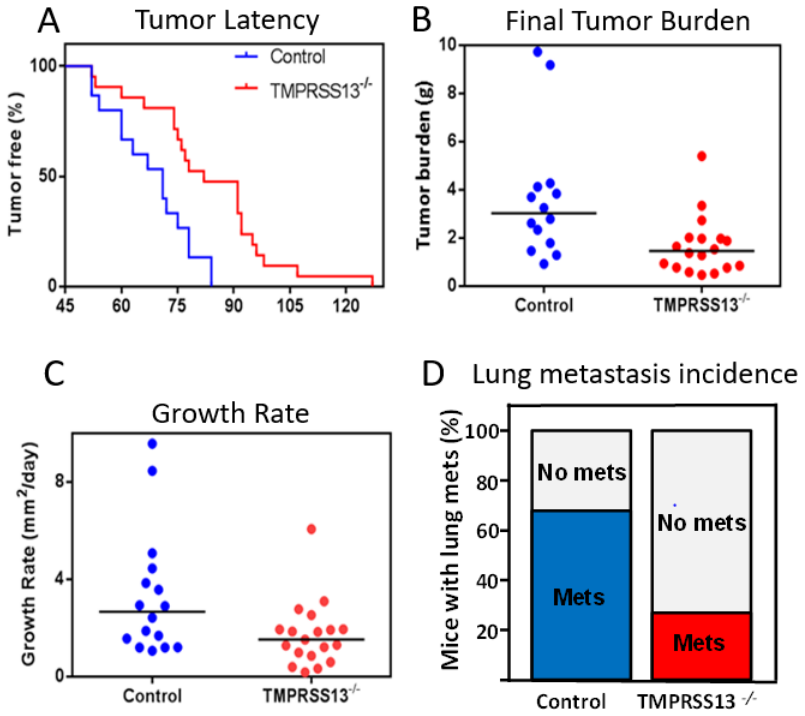

Fig. 15. (A) Kaplan-Meier plot of prospective cohort of littermate TMPRSS13^{+}/MMTV-PymT (N=15) and TMPRSS13$^{-/-}$/MMTV-PymT mice (N=21). Mice were palpated weekly to detect time of tumor formation. All control mice had palpable tumors at 84 days and TMPRSS13$^{-/-}$ mice at 127 days (P<0.001). **(B)** Tumor burden at 129 days. Mice were euthanized, mammary tumors were resected and the total tumor weight was recorded. Median values; 3.03 g (control, N=14) and 1.16 g (-/-, N=18) P<0.004. **(C)** Growth rate of mammary tumors in TMPRSS13^{+} (blue circles) and TMPRSS13$^{-/-}$ (red circles) mice, P<0.05. **(D)** Presence of lung metastasis was determined at the termination of the cohort experiment (day 129). Lung lesions were detected using a dissection microscope and in H&E slides; Control mice 8/12 (67%) and TMPRSS$^{-/-}$ mice 4/14 (29%) P=0.052.

mice were injected with the BrdU nucleotide analog 2 hours prior to sacrifice. Tumors were then removed, fixed and paraffin embedded, and histological staining was performed for BrdU positive cells. TMPRSS13$^{-/-}$ mice displayed a decrease in proliferation with a 47% reduction in the number of proliferating cells compared to control mice (Fig. 16A and B). TMPRSS13$^{-/-}$ mice also displayed a marked increase in apoptotic cell death compared to the control littermate mice, with a six-fold increase in the number of apoptotic cells in TMPRSS13$^{-/-}$ mice. (Fig. 16C and D)

4.3.5 Silencing TMPRSS13 expression in human breast cancer cells decreases proliferation and induces apoptosis

To test whether loss of TMPRSS13 effects cancer cell proliferation in human mammary epithelial cells, TMPRSS13 expression was silenced in three separate breast cancer cell lines. The BT20, HCC1937, and MCF-7 cell lines were chosen for these analyses because they, in addition to expressing endogenous TMPRSS13, represent different breast cancer subtypes; the highly invasive, TNBC, basal-like subtype (HCC1937 and BT20) and the *poorly invasive,* ER+, PR+ Luminal A subtype (MCF-7). TMPRSS13 was silenced using two non-overlapping synthetic RNA duplexes and scrambled GC-matched duplexes were used as controls. Cells were plated in serum containing media, trypsinized, and counted on the days indicated (Fig. 17A). MCF-7 cells displayed a loss of cells at day 3 after TMPRSS13 silencing, indicative of cell death. In HCC1937 and BT-20 significantly lower cell numbers were detected in TMPRSS13 silenced cells (decrease in the slopes, siRNA vs. control). This indicates decreased proliferation and/or cell survival. Taken together these data indicate that loss of TMPRSS13 expression reduces the proliferation potential in breast cancer.

Loss of TMPRSS13 expression in the luminal like MCF7 breast cancer cell line results in an overall decrease in cell numbers. To test whether the decrease in cell numbers is due to increased apoptosis, lysates were collected at the indicated days for all three cell lines. The levels of cleaved Poly (ADP-ribose) polymerase (PARP), a marker for apoptosis, in breast

Figure 16: Decreased proliferation and increased apoptosis in TMPRSS13$^{-/-}$ mice

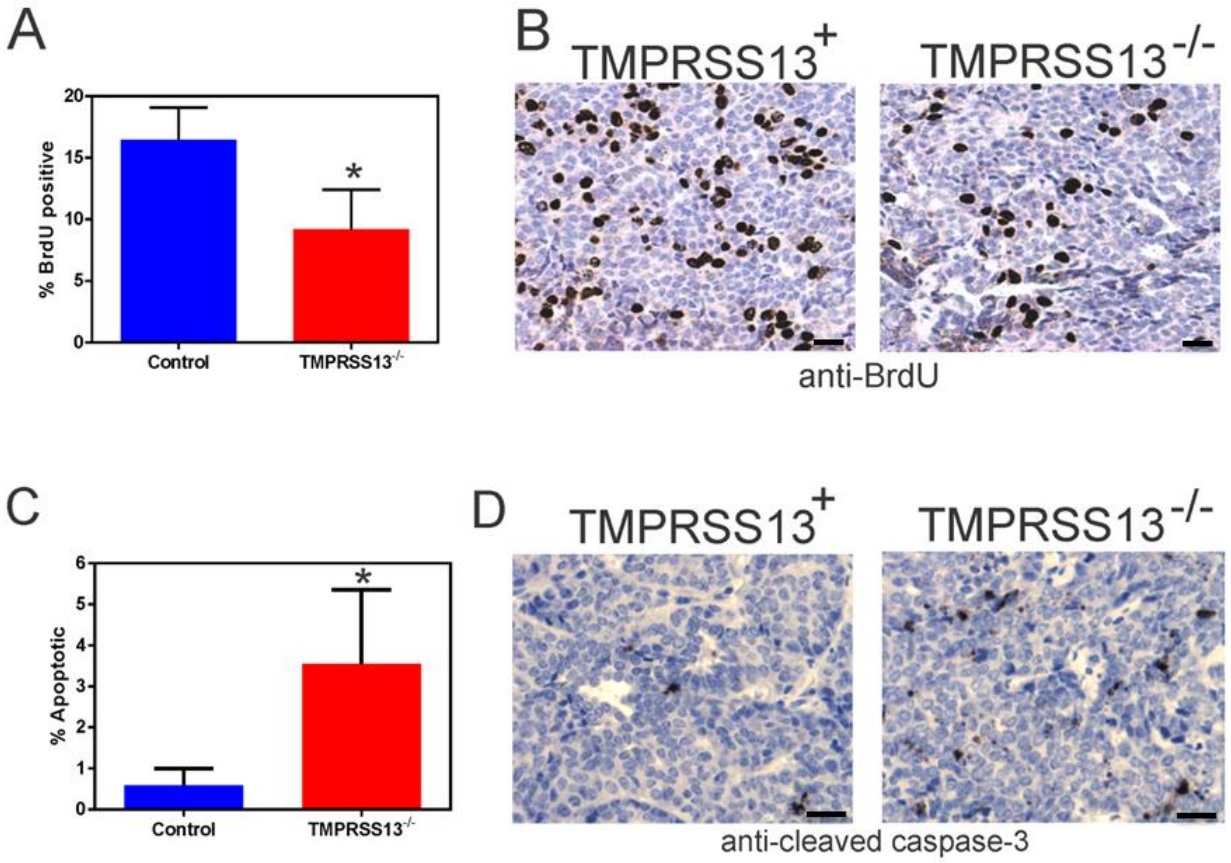

Fig. 16 (A) Quantification of the number of BrdU positive proliferating cells in mammary tumors from 129 day old TMPRSS13^{+}/PymT (N=3) and TMPRSS13$^{-/-}$/PymT (N=3) mice. Means: TMPRSS13^{+} = 16.5% TMPRSS13$^{-/-}$ = 9.2% $p<0.05$ **(B)** Representative staining for the number of BrdU positive cells in TMPRSS13^{+}/PymT (left) and TMPRSS13$^{-/-}$/PymT (right) mice. **(C)** Quantification of the number of apoptotic cells in 129 day old TMPRSS13^{+}/PymT (N=4) and TMPRSS13$^{-/-}$/PymT (N=4) mouse tumors. Means: TMPRSS13^{+} = 0.59% TMPRSS13$^{-/-}$ = 3.55% $p<0.05$. Positive cells were counted by an investigator who was unaware of genotypes.

Figure 17: TMPRSS13 silencing decreases human TNBC cell proliferation and induces apoptosis

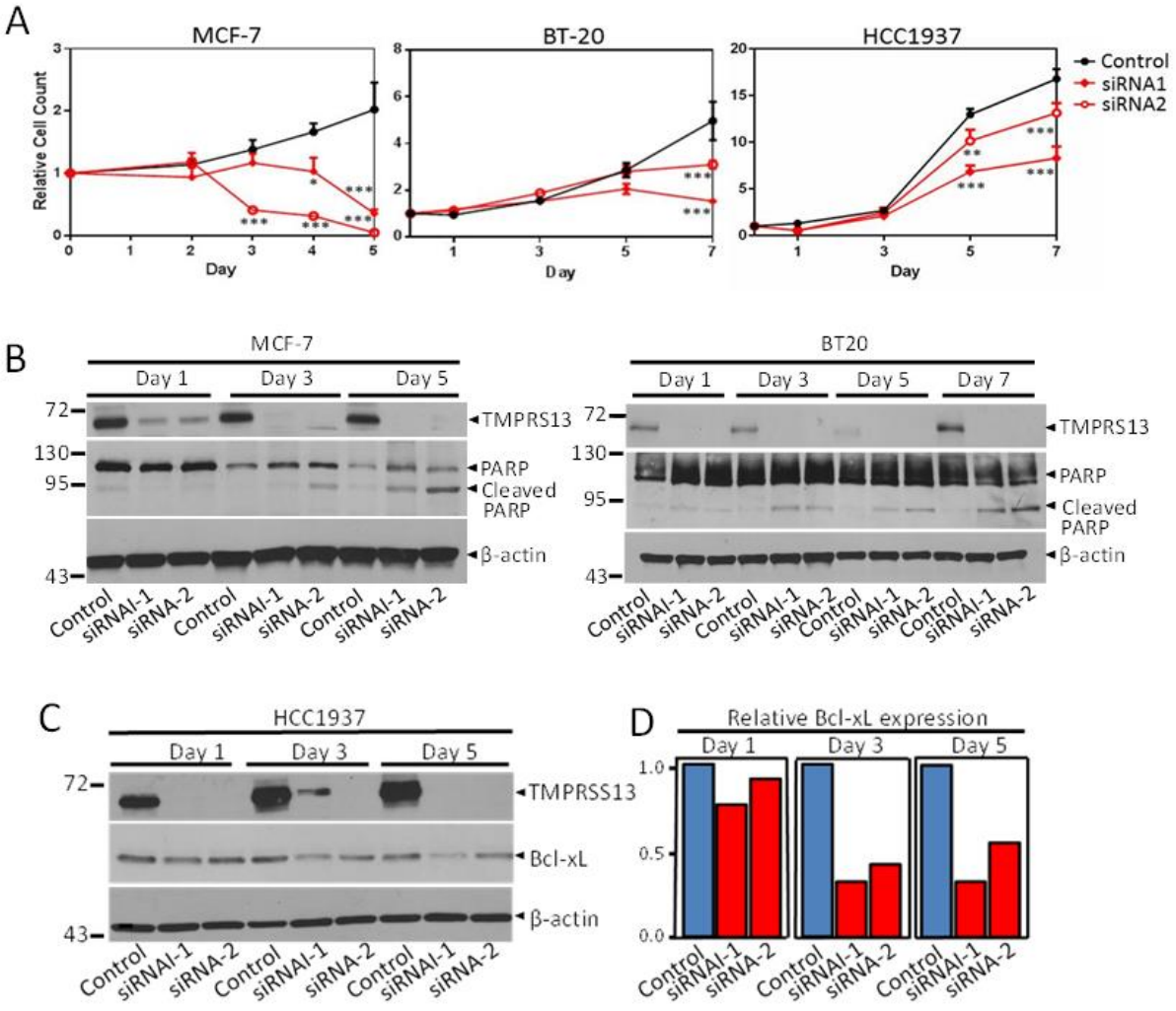

Fig. 17 (A) Relative mean cell numbers by hemocytometer counting following siRNA-mediated knockdown of TMPRSS13 were assessed over time in serum containing media in three breast cancer cell lines (MCF-7, BT20, and HCC1937). Each experimental condition was done in triplicate. Error bars represent SD. Graphs are representative of three independent experiments. Asterisks indicate significant difference from scrambled GC-matched control, *p <0.01. **p<0.001,***p<0.0001. Black lines=control, red lines=TMPRSS13 knockdown. **(B)** Western blot analysis of TMPRSS13, PARP and β-actin upon silencing with two different RNA duplexes targeting TMPRSS13. **(C)** Western blot analysis of TMPRSS13, Bcl-xL, and β-actin upon silencing with two different RNA duplexes targeting TMPRSS13 in HCC1937 cells **(D)** Quantification of Bcl-xL protein normalized to β-actin.

cancer cell lysates were detected by Western blot analysis. Loss of TMPRSS13 expression led to increased PARP cleavage, in both the luminal like MCF7 and the TNBC cancer cell lines BT20 and HCC1937 (Figs. 17B and 19D, right panel), indicative of enhanced apoptosis. Additionally, Western blot analysis for the pro-survival marker BCL-xL in HCC1937 cells revealed a decrease in expression (Fig. 17C and D), suggesting that loss of TMPRSS13 results in decreased expression of pro-survival proteins.

4.3.6 TMPRSS13 deficiency reduces tumor cell invasive potential

TMPRSS13$^{-/-}$ mice display decreased incidence of metastatic lesions compared to control mice. Therefore, we next analyzed whether TMPRSS13 may directly affect tumor cell invasion potential – an important determinant for metastatic ability. The invasion potential of breast cancer cells was studied using a transwell Matrigel® assay in which cells were seeded on top of the matrix in serum free media and allowed to invade overnight towards serum containing media in the bottom chamber (Fig. 18). Upon silencing of TMPRSS13 using two non-overlapping synthetic RNA duplexes, a significant decrease in invasive potential was observed in BT20 cells. Importantly, the experiment was carried out at day 2 after siRNA transfection when no difference in cell number is observed between control and TMPRSS13 silenced cells (Fig. 17A). This eliminates interference from differences in cell proliferation/survival with the invasion assay results. Taken together, these data suggest that TMPRSS13 is critical for breast cancer cell survival and invasion.

4.3.7 Loss of TMPRSS13 enhances chemosensitivity in triple negative breast cancer cell lines

Silencing TMPRSS13 expression results in apoptotic cell death in human cell culture models as well as reduced expression of the pro-survival marker Bcl-xL. Additionally, increased spontaneous apoptotic cell death is observed *in vivo*. Taken together these data suggest that TMPRSS13 may play a role in mediating tumor cell survival. TNBC is typically treated with a combination of radiation therapy and chemotherapy; yet, patients with TNBC have a significantly

Figure 18: TMPRSS13 silencing decreases human TNBC cell proliferation and induces apoptosis

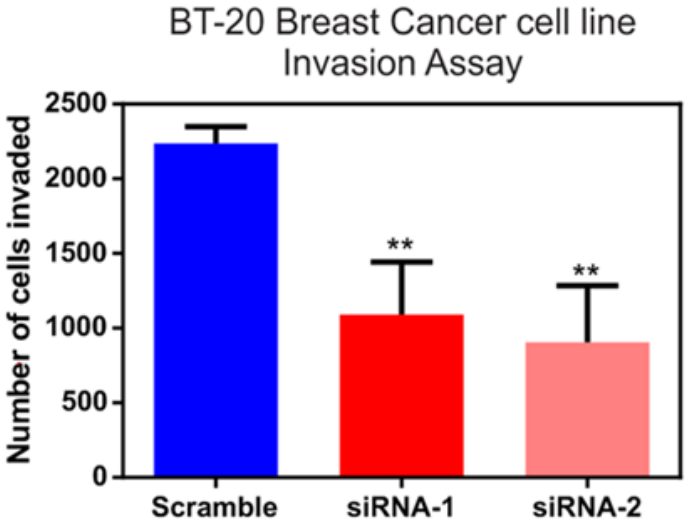

Fig. 18 Forty-eight hours post silencing, BT20 cells were serum starved in Transwell chambers with polycarbonate filters coated with Matrigel®. Using serum containing media in the lower chambers as chemoattractant, cells were allowed to invade through the matrix for 12 hours. Cells that had invaded were stained with crystal violet and counted. Error bars=SD ,** P<0.01.

lower 5-year survival than patients with other breast cancer subtypes. The major reason for low response rates in TNBC patients is chemoresistance and there is an urgent need to identify new targets that can be used as monotherapy or in combination therapy with established drugs. To specifically explore expression of this protease in TNBC, we analyzed IDC data sets stratified into TNBC versus non-TNBC (other hormone receptor status/hormone receptor positive). Two representative data sets reveal significantly higher levels of TMPRSS13 in TNBC (red) compared to receptor positive breast cancers (blue) (Fig. 19A). Thus, our data presented above point to TMPRSS13 as a promising target in TNBC treatment.

To test whether TMPRSS13 promotes tumor survival under chemotherapeutic stress conditions, preliminary experiments were performed to determine TMPRSS13-dependent sensitivity to the chemotherapeutic agent paclitaxel. The two TNBC cancer cell lines BT20 (WT PTEN and BRCA1 (164,165)) and HCC1937 (mutated PTEN and BRCA1 (164,165)) were chosen to perform these experiments. Currently, taxanes (e.g. paclitaxel) are commonly used as adjuvant and neoadjuvant therapies in TNBC patients (166). Taxanes are microtubule targeting agents that prevent microtubule formation, resulting in cell cycle arrest. Additionally, HCC1937 cells have been shown to be the most resistant to taxane and anthracycline treatment since BRCA1 mutations are critical for chemotherapeutic sensitivity, and reconstitution of WT-BRCA1 restores chemosensitivity to both taxanes and anthracycline resistance in HCC1937 cells (167).

The effects of silencing TMPRSS13 alone, drug treatment alone, or combination were analyzed by both Western blot analysis of lysates from treated cells, and cell viability was measured by Calcein AM treatment. Combination therapy results in a significant decrease in cell viability compared to either treatment alone for both cell types (Fig. 19 B and C). Additionally, analysis of lysates reveals increased amounts of PARP cleavage in combination treatment compared to either treatment alone, indicative of increased apoptotic cell death (Fig. 19D).

Figure 19: Increased chemosensitivity upon TMPRSS13 silencing in TNBC cell lines

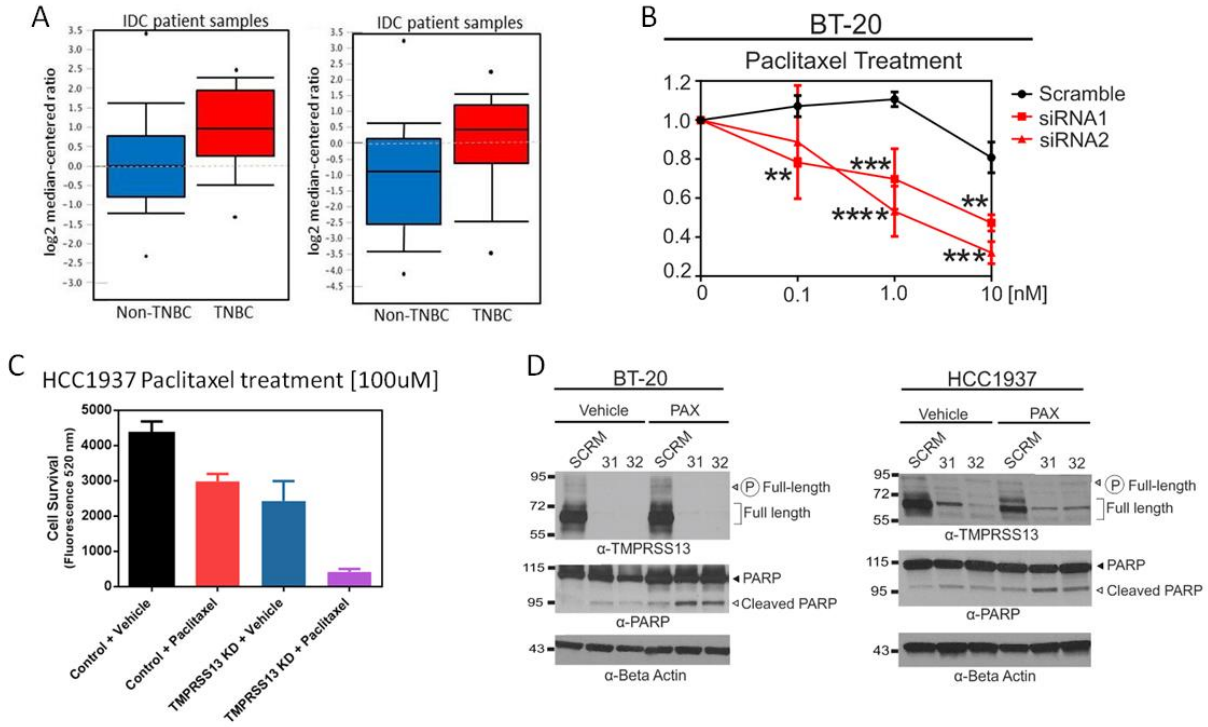

Fig. 19 (A) Box and whisker plots representing TMPRSS13 mRNA expression data for (A) Non-TNBC (N=250, median= -0.01) and TNBC (N=46, median= 0.9) (TCGA) and (B) Non-TNBC (N=129, median= -0.9) and TNBC (N=39, median= 0.4)(Bittner) from the OncomineTM microarray database. Boxes show interquartile range and medians are indicated by horizontal lines. p<0.0001 for both A and B.. **(B)** BT-20 cells were treated with increasing concentrations of paclitaxel in TMPRSS13 silenced cells or control cells treated with GC matched siRNA. Percent decrease in viability was compared to no treatment control group for each cell type (GC-matched control, siRNA1, siRNA2) **(C)** RNAi Knock-down (KD) cells or control cells were treated with vehicle or 1 µM paclitaxel for 48h. Cell survival was measured using Calcein AM. The combination treatment (purple bar) reduced cell survival by 91% compared to 31% with paclitaxel alone (red bar). Negative control=no cells. Error bars=SD. **p<0.001. ***p<0.0001 compared to control/vehicle, ***p<0.0001, combination treatment compared to each mono-treatment. (D) Corresponding lysates of BT-20 (treated with [100nM] paclitaxel or vehicle control] or HCC1937 (treated with [100µM] paclitaxel or vehicle control) cells probed for TMPRSS13, PARP, and beta-actin

Taken together, these experiments indicate that loss of TMPRSS13 expression increases chemosensitivity in breast cancer.

4.4 Discussion

In the current study, we report for the first time that TMPRSS13 expression is increased in breast cancer, and that TMPRSS13 deficiency impairs breast cancer progression *in vivo*. Additionally, loss of TMPRSS13 decreased proliferation and increased apoptotic cell death both in human cell culture models and in tumors from the genetic MMTV-PymT model of breast cancer. Furthermore, reduced number of lung metastasis is observed in TMPRSS13$^{-/-}$ mice compared to control mice, and decreased invasion potential is observed upon TMPRSS13 silencing in the TNBC BT20 cell line. Together the data provides a comprehensive analysis of the promotional role of TMPRSS13 in breast cancer.

To the best of our knowledge, this is the first study examining the biological role of TMPRSS13 in cancer. A few other TTSP family members have been studied in breast cancer, including both matriptase and hepsin, and both have been shown to promote tumor progression. Matriptase was shown to be essential for the proteolytic conversion of pro-HGF into active HGF to induce c-Met signaling and proliferation (81,168). Using both human cell culture models and genetic *in vivo* models, it was demonstrated that reduced matriptase expression prevents conversion of pro-HGF into active HGF, identifying pro-HGF as a physiological substrate for matriptase in breast cancer and that matriptase is the primary pro-HGF activator in the models used (which included the cells lines HCC1937 and BT20). Even though, TMPRSS13 has been reported to cleave and activate pro-HGF in vitro, it is therefore unlikely that loss of TMPRSS13-mediated activation critically impairs of pro-HGF activation and subsequent c-Met activation. However, it cannot not be formally excluded that TMPRSS13 could contribute to pro-HGF activation under conditions not tested in the previous (81,168) or present study. Additionally, hepsin was shown to have increased expression levels in breast cancer, and that hepsin overexpression in the non-transformed basal-like MCF10a cell line results in reduced

expression of the desmosomal protein desmoglein 2, along with disruption of apical polarity and cellular cohesion (98). The TTSP family member matriptase-2 has also been studied in breast cancer, where lost expression of matriptase-2 expression occurs, and its re-expression results in suppressed tumorigenic properties of breast cancer cells, suggesting tumor suppressive functions of matriptase-2 in breast cancer (169). A previous study examining the TTSP family member TMPRSS4 found that TMPRSS4 expression regulates the EMT transcription factor slug in prostate cancer.

Interestingly, this study reports for the first time that loss of a TTSP family member results in increased spontaneous apoptosis in cancer *in vivo*, as well as increased breast cancer chemosensitivity. Therefore, this suggests that TMPRSS13 plays a pro-survival role in breast cancer progression by promoting tumor cell survival and proliferation. The mechanism by which TMPRSS13 exerts pro-survival effects is currently unknown and future studies examining potential proteolytic substrates of TMPRSS13 may provide key insights. Additionally, TMPRS13 is currently the only TTSP family member known to be modified by phosphorylation, and that its phosphorylation may result in its translocation to the cell surface (170). Kinase software prediction tools have predicted that the c-jun n-terminal kinases, JNK1 and JNK2, may be responsible for TMPRSS13 phosphorylation (170). During times of cellular stress various signaling pathways are activated, and it is currently unknown whether TMPRSS13 is phosphorylated during certain stress conditions. Therefore identifying the kinase(s) responsible for TMPRSS13 phosphorylation, as well as the signaling pathways involved in TMPRSS13 phosphorylation may yield interesting insights into TMPRSS13 pro-survival mechanisms.

In conclusion, this study demonstrates that TMPRSS13 plays a promotional role in breast cancer, and that loss of TMPRSS13 expression impairs breast cancer progression *in vivo*. Additionally, we indicate that TMPRSS13 deficiency results in increased chemosensitivity, suggesting that TMPRSS13 functions in a pro-survival manner during breast cancer progression to support tumor growth.

CHAPTER 5: FUTURE DIRECTIONS

The data above indicate that TMPRSS13 plays a pro-survival role in breast cancer, however the mechanism by which it promotes cell survival remains unknown. During times of cellular stress various signaling pathways are activated to either promote cell survival, or induce cell death, depending on the duration and strength of the stress signaling (171,172). Therefore, it is interesting to note that while characterizing TMPRSS13 it was revealed that TMPRSS13 is phosphorylated, and that the stress activated protein kinases, Jun N-terminal kinase-1, -2 (JNK1 and JNK2), were predicted to be responsible for phosphorylation of TMPRSS13. JNK1 and JNK2 are activated under various stress conditions, including oxidative stress (173). Therefore, in preliminary experiments to test whether TMPRSS13 is phosphorylated under oxidative stress conditions, MCF7 cells were treated with H_2O_2 or vehicle control and lysates were collected and analyzed by Western blotting. Interestingly, TMPRSS13 appears to be phosphorylated in a time dependent manner under H_2O_2 treatment (Fig. 20). The kinases directly responsible for phosphorylating TMPRSS13 after H_2O_2 treatment remains unknown, and it is important to note that other kinases, including JNK1 and JNK2, are activated under oxidative stress (173,174). Therefore, future studies using RNAi, or inhibitors targeting specific kinases, will provide novel insights into the kinases directly responsible for TMPRSS13 phosphorylation.

To further identify TMPRSS13 specific kinases, and to examine whether other types of stimulation may induce TMPRSS13 phosphorylation, MCF7 cells were treated with the PKC activator Phorbol 12-myristate 13-acetate (PMA). PMA and vehicle control treated cells were lysed and protein extracts were collected at 15 minutes, 4 hours, or 16 hours after treatment. Interestingly, no increase in TMPRSS13 phosphorylation was observed at any timepoint compared to vehicle control group (data not shown). Therefore, this suggests that TMPRSS13 phosphorylation is not mediated by PKC, and that phosphorylation may be specific to increases in reactive oxygen species (ROS) levels. Various stressors have been shown to increase ROS

Figure 20: Oxidative stress induced phosphorylation of TMPRSS13

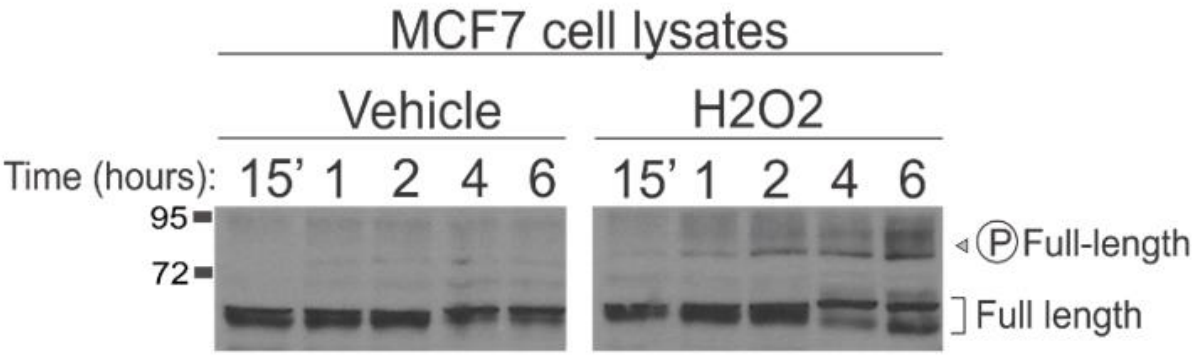

Fig. 20 (A) MCF7 cells were treated with H_2O_2 (2mM) or vehicle control for the indicated times and analyzed by Western blotting for the detection of the phosphorylated species. Western analysis reveals that TMPRSS13 is increasingly phosphorylated under hydrogen peroxide treatment over time.

levels, including UV irradiation and chemotherapeutic stress (175,176), and future studies examining the role of ROS levels in mediating TMPRSS13 phosphorylation may provide further insights into TMPRSS13's function in breast cancer. Additionally, the effect of phosphorylation on TMPRSS13 is currently unknown, but it is speculated that it promotes its localization to the cell surface (170). Therefore, it is interesting to speculate that under cellular stress, TMPRSS13 is phosphorylated resulting in TMPRSS13 translocation to the cell surface, however future studies are needed to confirm this.

Future studies examining candidate proteolytic substrates of TMPRSS13 will provide further key insights into the role of TMPRSS13 in breast cancer. Ongoing investigations into identifying physiologically relevant substrates for TTSP family members is currently underway, and only a handful of known substrates for a select few TTSP family members are known (159). It has previously been reported that the TTSP family member matriptase is responsible for the conversion of the oncogenic signaling molecule pro-HGF into active HGF to induce c-MET signaling in breast cancer (168). However, currently no physiological substrates have been validated for TMPRSS13. Therefore, future studies using both biased *(in vitro* co-incubation studies), and unbiased proteomics approaches are being developed. Candidate substrates will then be validated using both *in vivo* and cell culture models to assess whether decreased proteolytic processing of candidate substrates is observed of upon loss of TMPRSS13 expression.

Additionally, the findings outlined above indicate that targeting TMPRSS13 in TNBC cancer cell lines impairs cell survival/proliferation and invasion. Additionally, targeting TMPRSS13 increases the sensitivity of breast cancer cells to chemotherapy. Based on these findings, future studies to validate TMPRSS13 as a viable, druggable target in breast cancer have been initiated. It is important to note that in characterizing TMPRSS13$^{-/-}$ mice, TMPRSS13 deficiency has no discernible consequences on adult mouse health (65), thereby indicating limited adverse side effects would be observed with therapeutic TMPRSS13 inhibition. In early

investigations into the development of TMPRSS13 specific small molecule inhibitors a collaboration has been established with Drs. Leduc, Marsault and Richter at the Universitè De Sherbrooke in Québec, Canada. After development of TMPRSS13 specific inhibitors, future studies examining the effects of TMPRSS13 inhibition both alone, or in combination therapy with established chemotherapeutics, will be performed.

Of the 17 TTSP family members, TMPRSS13 has been relatively uncharacterized in both normal physiological development and disease. Characterization of TMPRSS13 deficient mice yielded insights into a physiological role in epidermal barrier acquisition, however the mechanism through which it mediates that effect remains unknown. Through biochemical characterization, and investigations into a role of TMPRSS13 in breast cancer, thoughtful insights into the functional role of TMPRSS13 in cancer progression have been elucidated. Future studies in developing TMPRSS13 specific inhibitors, identification of TMPRSS13 specific substrates, and identifying signaling pathways involved in TMPRSS13 phosphorylation will yield fruitful answers to understanding the functional role of TMPRSS13 in both normal development and disease.

APPENDIX: SUPPLEMENTARY FIGURE

Supplementary Figure 21: Endogenous TMPRSS13 species size and glycosylation status

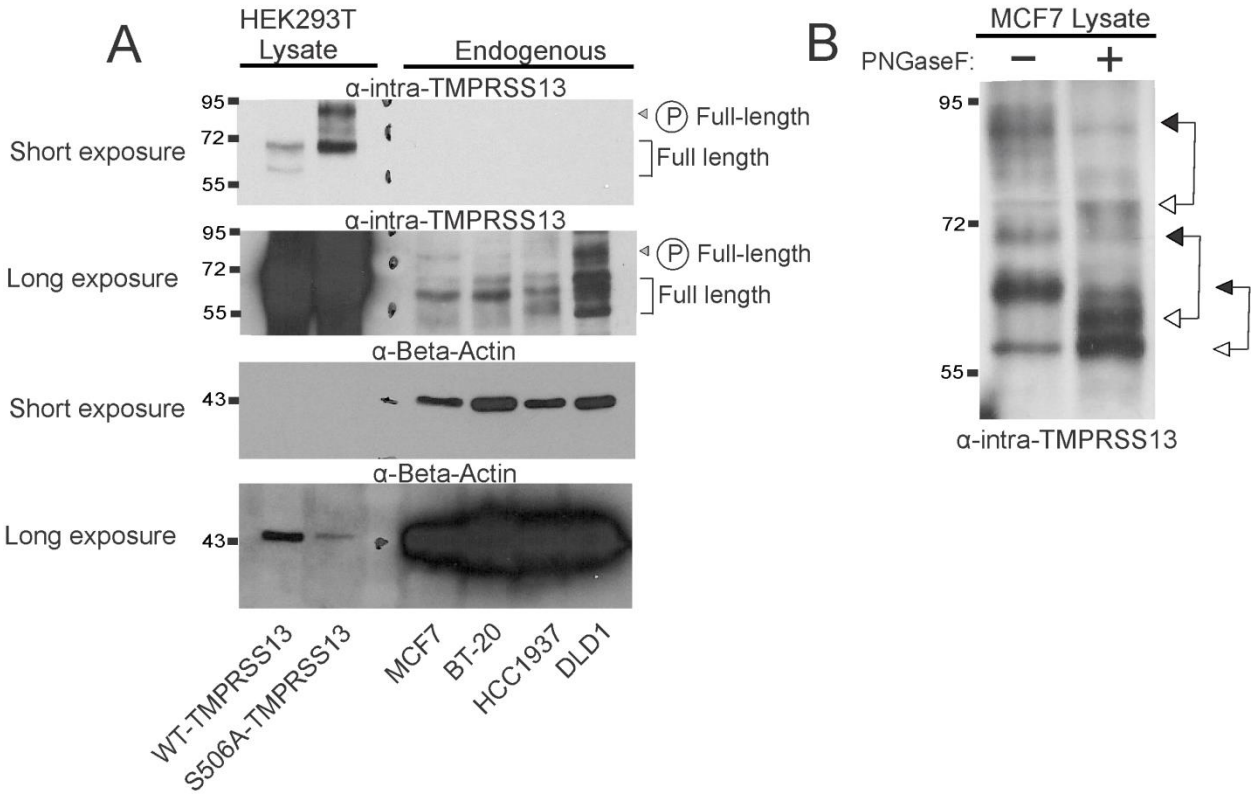

Figure 21. **(A)** Lysates from HEK293T cells expressing WT-TMPRSS13 or S506A-TMPRSS13 were separated side-by-side with lysates from the indicated cell lines. Samples of lysates expressing exogenous TMPRSS13 and lysates from samples containing endogenous TMPRSS13 were separated by a ladder. (**B**) DLD1 cell lysates were treated with or without PNGaseF and analyzed by Western blotting under reducing conditions using the α-intra-TMPRSS13 antibody. The white arrowheads connected to black arrowheads indicate the reduction in apparent molecular weight of the glycosylated forms of TMPRSS13.

REFERENCES

1. Howlader, N., Altekruse, S. F., Li, C. I., Chen, V. W., Clarke, C. A., Ries, L. A. G., and Cronin, K. A. (2014) US Incidence of Breast Cancer Subtypes Defined by Joint Hormone Receptor and HER2 Status. *JNCI: Journal of the National Cancer Institute* **106**, dju055-dju055
2. Sevenich, L., and Joyce, J. A. (2014) Pericellular proteolysis in cancer. *Genes & development* **28**, 2331-2347
3. Antalis, T. M., Buzza, M. S., Hodge, K. M., Hooper, J. D., and Netzel-Arnett, S. (2010) The cutting edge: membrane-anchored serine protease activities in the pericellular microenvironment. *Biochem J* **428**, 325-346
4. Lopez-Otin, C., and Bond, J. S. (2008) Proteases: multifunctional enzymes in life and disease. *The Journal of biological chemistry* **283**, 30433-30437
5. Gomis-Rüth, F. X. (2003) Structural aspects of the metzincin clan of metalloendopeptidases. *Molecular Biotechnology* **24**, 157-202
6. Khokha, R., Murthy, A., and Weiss, A. (2013) Metalloproteinases and their natural inhibitors in inflammation and immunity. **13**, 649
7. Sterchi, E. E., Stocker, W., and Bond, J. S. (2008) Meprins, membrane-bound and secreted astacin metalloproteinases. *Molecular aspects of medicine* **29**, 309-328
8. Turk, B. (2006) Targeting proteases: successes, failures and future prospects. *Nat Rev Drug Discov* **5**, 785-799
9. Coussens, L. M., Fingleton, B., and Matrisian, L. M. (2002) Matrix metalloproteinase inhibitors and cancer: trials and tribulations. *Science (New York, N.Y.)* **295**, 2387-2392
10. Overall, C. M., and Lopez-Otin, C. (2002) Strategies for MMP inhibition in cancer: innovations for the post-trial era. *Nature reviews. Cancer* **2**, 657-672

11. Grzonka, Z., Jankowska, E., Kasprzykowski, F., Kasprzykowska, R., Lankiewicz, L., Wiczk, W., Wieczerzak, E., Ciarkowski, J., Drabik, P., Janowski, R., Kozak, M., Jaskolski, M., and Grubb, A. (2001) Structural studies of cysteine proteases and their inhibitors. *Acta biochimica Polonica* **48**, 1-20

12. Alnemri, E. S., Livingston, D. J., Nicholson, D. W., Salvesen, G., Thornberry, N. A., Wong, W. W., and Yuan, J. Human ICE/CED-3 Protease Nomenclature. *Cell* **87**, 171

13. Riedl, S. J., and Salvesen, G. S. (2007) The apoptosome: signalling platform of cell death. *Nature reviews. Molecular cell biology* **8**, 405-413

14. Ashkenazi, A., and Salvesen, G. (2014) Regulated cell death: signaling and mechanisms. *Annual review of cell and developmental biology* **30**, 337-356

15. Elmore, S. (2007) Apoptosis: A Review of Programmed Cell Death. *Toxicologic pathology* **35**, 495-516

16. Turk, B., and Stoka, V. (2007) Protease signalling in cell death: caspases versus cysteine cathepsins. *FEBS letters* **581**, 2761-2767

17. Turk, V., Stoka, V., Vasiljeva, O., Renko, M., Sun, T., Turk, B., and Turk, D. (2012) Cysteine cathepsins: from structure, function and regulation to new frontiers. *Biochimica et biophysica acta* **1824**, 68-88

18. Mohamed, M. M., and Sloane, B. F. (2006) Cysteine cathepsins: multifunctional enzymes in cancer. *Nature reviews. Cancer* **6**, 764-775

19. Storr, S. J., Carragher, N. O., Frame, M. C., Parr, T., and Martin, S. G. (2011) The calpain system and cancer. *Nature reviews. Cancer* **11**, 364-374

20. Di Cera, E. (2009) Serine Proteases. *IUBMB life* **61**, 510-515

21. Buen, E. P.-d., Orozco-Mosqueda, A., Leal-Cortés, C., Vázquez-Camacho, G., Fuentes-Orozco, C., Alvarez-Villaseñor, A. S., Macías-Amezcua, M. D., and González-Ojeda, A. (2014) Fibrinogen and thrombin concentrations are critical for fibrin glue adherence in rat high-risk colon anastomoses. *Clinics* **69**, 259-264

22. Palta, S., Saroa, R., and Palta, A. (2014) Overview of the coagulation system. *Indian Journal of Anaesthesia* **58**, 515-523

23. Pipe, S. W. (2017) Gene therapy for hemophilia. *Pediatric blood & cancer*

24. Bugge, T. H., Flick, M. J., Daugherty, C. C., and Degen, J. L. (1995) Plasminogen deficiency causes severe thrombosis but is compatible with development and reproduction. *Genes & development* **9**, 794-807

25. Netzel-Arnett, S., Hooper, J. D., Szabo, R., Madison, E. L., Quigley, J. P., Bugge, T. H., and Antalis, T. M. (2003) Membrane anchored serine proteases: a rapidly expanding group of cell surface proteolytic enzymes with potential roles in cancer. *Cancer metastasis reviews* **22**, 237-258

26. Antalis, T. M., Bugge, T., and Wu, Q. (2011) Membrane-anchored serine proteases in health and disease. *Progress in molecular biology and translational science* **99**, 1-50

27. Wong, G. W., Tang, Y., Feyfant, E., Sali, A., Li, L., Li, Y., Huang, C., Friend, D. S., Krilis, S. A., and Stevens, R. L. (1999) Identification of a new member of the tryptase family of mouse and human mast cell proteases which possesses a novel COOH-terminal hydrophobic extension. *J Biol Chem* **274**, 30784-30793

28. Wong, G. W., Foster, P. S., Yasuda, S., Qi, J. C., Mahalingam, S., Mellor, E. A., Katsoulotos, G., Li, L., Boyce, J. A., Krilis, S. A., and Stevens, R. L. (2002) Biochemical and Functional Characterization of Human Transmembrane Tryptase (TMT)/Tryptase γ: TMT IS AN EXOCYTOSED MAST CELL PROTEASE THAT INDUCES AIRWAY HYPERRESPONSIVENESS IN VIVO VIA AN INTERLEUKIN-13/INTERLEUKIN-4 RECEPTOR α/SIGNAL TRANSDUCER AND ACTIVATOR OF TRANSCRIPTION (STAT) 6-DEPENDENT PATHWAY. *Journal of Biological Chemistry* **277**, 41906-41915

29. Wernersson, S., and Pejler, G. (2014) Mast cell secretory granules: armed for battle. *Nature reviews. Immunology* **14**, 478-494

30. Hansbro, P. M., Hamilton, M. J., Fricker, M., Gellatly, S. L., Jarnicki, A. G., Zheng, D., Frei, S. M., Wong, G. W., Hamadi, S., Zhou, S., Foster, P. S., Krilis, S. A., and Stevens, R. L. (2014) Importance of Mast Cell Prss31/Transmembrane Tryptase/Tryptase-γ in Lung Function and Experimental Chronic Obstructive Pulmonary Disease and Colitis. *The Journal of Biological Chemistry* **289**, 18214-18227

31. Hummler, E., Dousse, A., Rieder, A., Stehle, J. C., Rubera, I., Osterheld, M. C., Beermann, F., Frateschi, S., and Charles, R. P. (2013) The channel-activating protease CAP1/Prss8 is required for placental labyrinth maturation. *PLoS One* **8**, e55796

32. Leyvraz, C., Charles, R. P., Rubera, I., Guitard, M., Rotman, S., Breiden, B., Sandhoff, K., and Hummler, E. (2005) The epidermal barrier function is dependent on the serine protease CAP1/Prss8. *The Journal of cell biology* **170**, 487-496

33. Hooper, J. D., Nicol, D. L., Dickinson, J. L., Eyre, H. J., Scarman, A. L., Normyle, J. F., Stuttgen, M. A., Douglas, M. L., Loveland, K. A., Sutherland, G. R., and Antalis, T. M. (1999) Testisin, a new human serine proteinase expressed by premeiotic testicular germ cells and lost in testicular germ cell tumors. *Cancer Res* **59**, 3199-3205

34. Netzel-Arnett, S., Bugge, T. H., Hess, R. A., Carnes, K., Stringer, B. W., Scarman, A. L., Hooper, J. D., Tonks, I. D., Kay, G. F., and Antalis, T. M. (2009) The Glycosylphosphatidylinositol-Anchored Serine Protease PRSS21 (Testisin) Imparts Murine Epididymal Sperm Cell Maturation and Fertilizing Ability. *Biology of Reproduction* **81**, 921-932

35. Szabo, R., and Bugge, T. H. (2011) Membrane-anchored serine proteases in vertebrate cell and developmental biology. *Annual review of cell and developmental biology* **27**, 213-235

36. Bugge, T. H., Antalis, T. M., and Wu, Q. (2009) Type II transmembrane serine proteases. *J Biol Chem* **284**, 23177-23181

37. Jiang, J., Yang, J., Feng, P., Zuo, B., Dong, N., Wu, Q., and He, Y. (2014) N-glycosylation is required for matriptase-2 autoactivation and ectodomain shedding. *The Journal of biological chemistry* **289**, 19500-19507

38. Wang, H., Zhou, T., Peng, J., Xu, P., Dong, N., Chen, S., and Wu, Q. (2015) Distinct Roles of N-Glycosylation at Different Sites of Corin in Cell Membrane Targeting and Ectodomain Shedding. *Journal of Biological Chemistry* **290**, 1654-1663

39. Oberst, M. D., Williams, C. A., Dickson, R. B., Johnson, M. D., and Lin, C.-Y. (2003) The Activation of Matriptase Requires Its Noncatalytic Domains, Serine Protease Domain, and Its Cognate Inhibitor. *Journal of Biological Chemistry* **278**, 26773-26779

40. Murray, A. S., Varela, F. A., Hyland, T. E., Schoenbeck, A. J., White, J. M., Tanabe, L. M., Todi, S. V., and List, K. (2017) Phosphorylation of the type II transmembrane serine protease, TMPRSS13 in Hepatocyte Growth Factor Activator Inhibitor-1 and 2-mediated cell surface localization. *The Journal of biological chemistry*

41. Nonboe, A. W., Krigslund, O., Soendergaard, C., Skovbjerg, S., Friis, S., Andersen, M. N., Ellis, V., Kawaguchi, M., Kataoka, H., Bugge, T. H., and Vogel, L. K. (2017) HAI-2 stabilizes, inhibits and regulates SEA-cleavage-dependent secretory transport of matriptase. *Traffic (Copenhagen, Denmark)* **18**, 378-391

42. Antalis, T. M., Buzza, M. S., Hodge, K. M., Hooper, J. D., and Netzel-Arnett, S. (2010) The Cutting Edge: Membrane Anchored Serine Protease Activities in the Pericellular Microenvironment. *The Biochemical journal* **428**, 325-346

43. Kojima, K., Tsuzuki, S., Fushiki, T., and Inouye, K. (2008) Roles of functional and structural domains of hepatocyte growth factor activator inhibitor type 1 in the inhibition of matriptase. *The Journal of biological chemistry* **283**, 2478-2487

44. Szabo, R., Hobson, J. P., Christoph, K., Kosa, P., List, K., and Bugge, T. H. (2009) Regulation of cell surface protease matriptase by HAI2 is essential for placental

development, neural tube closure and embryonic survival in mice. *Development (Cambridge, England)* **136**, 2653-2663

45. Tanaka, H., Nagaike, K., Takeda, N., Itoh, H., Kohama, K., Fukushima, T., Miyata, S., Uchiyama, S., Uchinokura, S., Shimomura, T., Miyazawa, K., Kitamura, N., Yamada, G., and Kataoka, H. (2005) Hepatocyte growth factor activator inhibitor type 1 (HAI-1) is required for branching morphogenesis in the chorioallantoic placenta. *Mol Cell Biol* **25**, 5687-5698

46. Szabo, R., Molinolo, A., List, K., and Bugge, T. H. (2007) Matriptase inhibition by hepatocyte growth factor activator inhibitor-1 is essential for placental development. *Oncogene* **26**, 1546-1556

47. Szabo, R., Uzzun Sales, K., Kosa, P., Shylo, N. A., Godiksen, S., Hansen, K. K., Friis, S., Gutkind, J. S., Vogel, L. K., and Hummler, E. (2012) Reduced prostasin (CAP1/PRSS8) activity eliminates HAI-1 and HAI-2 deficiency-associated developmental defects by preventing matriptase activation. *PLoS Genet* **8**

48. Muller, T., Wijmenga, C., Phillips, A. D., Janecke, A., Houwen, R. H., Fischer, H., Ellemunter, H., Fruhwirth, M., Offner, F., Hofer, S., Muller, W., Booth, I. W., and Heinz-Erian, P. (2000) Congenital sodium diarrhea is an autosomal recessive disorder of sodium/proton exchange but unrelated to known candidate genes. *Gastroenterology* **119**, 1506-1513

49. Heinz-Erian, P., Muller, T., Krabichler, B., Schranz, M., Becker, C., Ruschendorf, F., Nurnberg, P., Rossier, B., Vujic, M., Booth, I. W., Holmberg, C., Wijmenga, C., Grigelioniene, G., Kneepkens, C. M., Rosipal, S., Mistrik, M., Kappler, M., Michaud, L., Doczy, L. C., Siu, V. M., Krantz, M., Zoller, H., Utermann, G., and Janecke, A. R. (2009) Mutations in SPINT2 cause a syndromic form of congenital sodium diarrhea. *Am J Hum Genet* **84**, 188-196

50. Janecke, A. R., Heinz-Erian, P., and Muller, T. (2016) Congenital Sodium Diarrhea: A Form of Intractable Diarrhea, With a Link to Inflammatory Bowel Disease. *Journal of pediatric gastroenterology and nutrition* **63**, 170-176

51. Wu, C.-J., Feng, X., Lu, M., Morimura, S., and Udey, M. C. (2017) Matriptase-mediated cleavage of EpCAM destabilizes claudins and dysregulates intestinal epithelial homeostasis. *The Journal of Clinical Investigation* **127**, 623-634

52. Faller, N., Gautschi, I., and Schild, L. (2014) Functional analysis of a missense mutation in the serine protease inhibitor SPINT2 associated with congenital sodium diarrhea. *PloS one* **9**, e94267

53. List, K., Bugge, T. H., and Szabo, R. (2006) Matriptase: potent proteolysis on the cell surface. *Mol Med* **12**, 1-7

54. List, K., Szabo, R., Molinolo, A., Sriuranpong, V., Redeye, V., Murdock, T., Burke, B., Nielsen, B. S., Gutkind, J. S., and Bugge, T. H. (2005) Deregulated matriptase causes ras-independent multistage carcinogenesis and promotes ras-mediated malignant transformation. *Genes & development* **19**, 1934-1950

55. Kirchhofer, D., Peek, M., Lipari, M. T., Billeci, K., Fan, B., and Moran, P. (2005) Hepsin activates pro-hepatocyte growth factor and is inhibited by hepatocyte growth factor activator inhibitor-1B (HAI-1B) and HAI-2. *FEBS Lett* **579**, 1945-1950

56. List, K., Haudenschild, C. C., Szabo, R., Chen, W., Wahl, S. M., Swaim, W., Engelholm, L. H., Behrendt, N., and Bugge, T. H. (2002) Matriptase/MT-SP1 is required for postnatal survival, epidermal barrier function, hair follicle development, and thymic homeostasis. *Oncogene* **21**, 3765-3779

57. Netzel-Arnett, S., Currie, B. M., Szabo, R., Lin, C. Y., Chen, L. M., Chai, K. X., Antalis, T. M., Bugge, T. H., and List, K. (2006) Evidence for a matriptase-prostasin proteolytic cascade regulating terminal epidermal differentiation. *The Journal of biological chemistry* **281**, 32941-32945

58. Basel-Vanagaite, L., Attia, R., Ishida-Yamamoto, A., Rainshtein, L., Ben Amitai, D., Lurie, R., Pasmanik-Chor, M., Indelman, M., Zvulunov, A., Saban, S., Magal, N., Sprecher, E., and Shohat, M. (2007) Autosomal recessive ichthyosis with hypotrichosis caused by a mutation in ST14, encoding type II transmembrane serine protease matriptase. *Am J Hum Genet* **80**, 467-477

59. Alef, T., Torres, S., Hausser, I., Metze, D., Tursen, U., Lestringant, G. G., and Hennies, H. C. (2009) Ichthyosis, follicular atrophoderma, and hypotrichosis caused by mutations in ST14 is associated with impaired profilaggrin processing. *J Invest Dermatol* **129**, 862-869

60. Guipponi, M., Tan, J., Cannon, P. Z., Donley, L., Crewther, P., Clarke, M., Wu, Q., Shepherd, R. K., and Scott, H. S. (2007) Mice deficient for the type II transmembrane serine protease, TMPRSS1/hepsin, exhibit profound hearing loss. *The American journal of pathology* **171**, 608-616

61. Hsu, Y. C., Huang, H. P., Yu, I. S., Su, K. Y., Lin, S. R., Lin, W. C., Wu, H. L., Shi, G. Y., Tao, M. H., Kao, C. H., Wu, Y. M., Martin, P. E., Lin, S. Y., Yang, P. C., and Lin, S. W. (2012) Serine protease hepsin regulates hepatocyte size and hemodynamic retention of tumor cells by hepatocyte growth factor signaling in mice. *Hepatology* **56**, 1913-1923

62. Folgueras, A. R., de Lara, F. M., Pendas, A. M., Garabaya, C., Rodriguez, F., Astudillo, A., Bernal, T., Cabanillas, R., Lopez-Otin, C., and Velasco, G. (2008) Membrane-bound serine protease matriptase-2 (Tmprss6) is an essential regulator of iron homeostasis. *Blood* **112**, 2539-2545

63. Finberg, K. E., Heeney, M. M., Campagna, D. R., Aydinok, Y., Pearson, H. A., Hartman, K. R., Mayo, M. M., Samuel, S. M., Strouse, J. J., Markianos, K., Andrews, N. C., and Fleming, M. D. (2008) Mutations in TMPRSS6 cause iron-refractory iron deficiency anemia (IRIDA). *Nat Genet* **40**, 569-571

64. Silvestri, L., Pagani, A., Nai, A., De Domenico, I., Kaplan, J., and Camaschella, C. (2008) The serine protease matriptase-2 (TMPRSS6) inhibits hepcidin activation by cleaving membrane hemojuvelin. *Cell metabolism* **8**, 502-511

65. Madsen, D. H., Szabo, R., Molinolo, A. A., and Bugge, T. H. (2014) TMPRSS13 deficiency impairs stratum corneum formation and epidermal barrier acquisition. *The Biochemical journal* **461**, 487-495

66. Hashimoto, T., Kato, M., Shimomura, T., and Kitamura, N. (2010) TMPRSS13, a type II transmembrane serine protease, is inhibited by hepatocyte growth factor activator inhibitor type 1 and activates pro-hepatocyte growth factor. *The FEBS journal* **277**, 4888-4900

67. Cheng, M. F., Tzao, C., Tsai, W. C., Lee, W. H., Chen, A., Chiang, H., Sheu, L. F., and Jin, J. S. (2006) Expression of EMMPRIN and matriptase in esophageal squamous cell carcinoma: correlation with clinicopathological parameters. *Dis Esophagus* **19**, 482-486

68. Bugge, T. H., List, K., and Szabo, R. (2007) Matriptase-dependent cell surface proteolysis in epithelial development and pathogenesis. *Front Biosci* **12**, 5060-5070

69. List, K., Kosa, P., Szabo, R., Bey, A. L., Wang, C. B., Molinolo, A., and Bugge, T. H. (2009) Epithelial integrity is maintained by a matriptase-dependent proteolytic pathway. *The American journal of pathology* **175**, 1453-1463

70. Webb, S. L., Sanders, A. J., Mason, M. D., and Jiang, W. G. (2011) Type II transmembrane serine protease (TTSP) deregulation in cancer. *Front Biosci (Landmark Ed)* **16**, 539-552

71. Tanimoto, H., Underwood, L. J., Wang, Y., Shigemasa, K., Parmley, T. H., and O'Brien, T. J. (2001) Ovarian tumor cells express a transmembrane serine protease: a potential candidate for early diagnosis and therapeutic intervention. *Tumour Biol* **22**, 104-114

72. Tanimoto, H., Shigemasa, K., Tian, X., Gu, L., Beard, J. B., Sawasaki, T., and O'Brien, T. J. (2005) Transmembrane serine protease TADG-15 (ST14/Matriptase/MT-SP1): expression and prognostic value in ovarian cancer. *British journal of cancer* **92**, 278-283

73. Lee, J. W., Yong Song, S., Choi, J. J., Lee, S. J., Kim, B. G., Park, C. S., Lee, J. H., Lin, C. Y., Dickson, R. B., and Bae, D. S. (2005) Increased expression of matriptase is associated with histopathologic grades of cervical neoplasia. *Hum Pathol* **36**, 626-633

74. Szabo, R., and Bugge, T. H. (2008) Type II transmembrane serine proteases in development and disease. *Int J Biochem Cell Biol* **40**, 1297-1316

75. Szabo, R., Kosa, P., List, K., and Bugge, T. H. (2009) Loss of matriptase suppression underlies spint1 mutation-associated ichthyosis and postnatal lethality. *The American journal of pathology* **174**, 2015-2022

76. Oberst, M. D., Johnson, M. D., Dickson, R. B., Lin, C. Y., Singh, B., Stewart, M., Williams, A., al-Nafussi, A., Smyth, J. F., Gabra, H., and Sellar, G. C. (2002) Expression of the serine protease matriptase and its inhibitor HAI-1 in epithelial ovarian cancer: correlation with clinical outcome and tumor clinicopathological parameters. *Clinical cancer research : an official journal of the American Association for Cancer Research* **8**, 1101-1107

77. Saleem, M., Adhami, V. M., Zhong, W., Longley, B. J., Lin, C. Y., Dickson, R. B., Reagan-Shaw, S., Jarrard, D. F., and Mukhtar, H. (2006) A novel biomarker for staging human prostate adenocarcinoma: overexpression of matriptase with concomitant loss of its inhibitor, hepatocyte growth factor activator inhibitor-1. *Cancer Epidemiol Biomarkers Prev* **15**, 217-227

78. Vogel, L. K., Saebo, M., Skjelbred, C. F., Abell, K., Pedersen, E. D., Vogel, U., and Kure, E. H. (2006) The ratio of Matriptase/HAI-1 mRNA is higher in colorectal cancer adenomas and carcinomas than corresponding tissue from control individuals. *BMC Cancer* **6**, 176

79. Bergum, C., Zoratti, G., Boerner, J., and List, K. (2012) Strong expression association between matriptase and its substrate prostasin in breast cancer. *Journal of cellular physiology* **227**, 1604-1609

80. Nakamura, K., Hongo, A., Kodama, J., and Hiramatsu, Y. (2011) The role of hepatocyte growth factor activator inhibitor (HAI)-1 and HAI-2 in endometrial cancer. *International journal of cancer* **128**, 2613-2624

81. Zoratti, G. L., Tanabe, L. M., Varela, F. A., Murray, A. S., Bergum, C., Colombo, E., Lang, J. E., Molinolo, A. A., Leduc, R., Marsault, E., Boerner, J., and List, K. (2015) Targeting matriptase in breast cancer abrogates tumour progression via impairment of stromal-epithelial growth factor signalling. *Nat Commun* **6**, 6776

82. Colombo, E., Desilets, A., Duchene, D., Chagnon, F., Najmanovich, R., Leduc, R., and Marsault, E. (2012) Design and synthesis of potent, selective inhibitors of matriptase. *ACS Med Chem Lett* **3**, 530-534

83. Gray, K., Elghadban, S., Thongyoo, P., Owen, K. A., Szabo, R., Bugge, T. H., Tate, E. W., Leatherbarrow, R. J., and Ellis, V. (2014) Potent and specific inhibition of the biological activity of the type-II transmembrane serine protease matriptase by the cyclic microprotein MCoTI-II. *Thromb Haemost* **112**, 402-411

84. Galkin, A. V., Mullen, L., Fox, W. D., Brown, J., Duncan, D., Moreno, O., Madison, E. L., and Agus, D. B. (2004) CVS-3983, a selective matriptase inhibitor, suppresses the growth of androgen independent prostate tumor xenografts. *The Prostate* **61**, 228-235

85. Steinmetzer, T., Schweinitz, A., Sturzebecher, A., Donnecke, D., Uhland, K., Schuster, O., Steinmetzer, P., Muller, F., Friedrich, R., Than, M. E., Bode, W., and Sturzebecher, J. (2006) Secondary amides of sulfonylated 3-amidinophenylalanine. New potent and selective inhibitors of matriptase. *Journal of medicinal chemistry* **49**, 4116-4126

86. Leytus, S. P., Loeb, K. R., Hagen, F. S., Kurachi, K., and Davie, E. W. (1988) A novel trypsin-like serine protease (hepsin) with a putative transmembrane domain expressed by human liver and hepatoma cells. *Biochemistry* **27**, 1067-1074

87. Tsuji, A., Torres-Rosado, A., Arai, T., Chou, S. H., and Kurachi, K. (1991) Characterization of hepsin, a membrane bound protease. *Biomedica biochimica acta* **50**, 791-793

88. Tsuji, A., Torres-Rosado, A., Arai, T., Le Beau, M. M., Lemons, R. S., Chou, S. H., and Kurachi, K. (1991) Hepsin, a cell membrane-associated protease. Characterization, tissue distribution, and gene localization. *The Journal of biological chemistry* **266**, 16948-16953

89. Hanifa, S., Scott, H. S., Crewther, P., Guipponi, M., and Tan, J. (2010) Thyroxine treatments do not correct inner ear defects in tmprss1 mutant mice. *Neuroreport* **21**, 897-901

90. Xing, P., Li, J. G., Jin, F., Zhao, T. T., Liu, Q., Dong, H. T., and Wei, X. L. (2011) Clinical and biological significance of hepsin overexpression in breast cancer. *J Investig Med* **59**, 803-810

91. Tanimoto, H., Yan, Y., Clarke, J., Korourian, S., Shigemasa, K., Parmley, T. H., Parham, G. P., and O'Brien, T. J. (1997) Hepsin, a cell surface serine protease identified in hepatoma cells, is overexpressed in ovarian cancer. *Cancer research* **57**, 2884-2887

92. Betsunoh, H., Mukai, S., Akiyama, Y., Fukushima, T., Minamiguchi, N., Hasui, Y., Osada, Y., and Kataoka, H. (2007) Clinical relevance of hepsin and hepatocyte growth factor activator inhibitor type 2 expression in renal cell carcinoma. *Cancer science* **98**, 491-498

93. Matsuo, T., Nakamura, K., Takamoto, N., Kodama, J., Hongo, A., Abrzua, F., Nasu, Y., Kumon, H., and Hiramatsu, Y. (2008) Expression of the serine protease hepsin and clinical outcome of human endometrial cancer. *Anticancer research* **28**, 159-164

94. Klezovitch, O., Chevillet, J., Mirosevich, J., Roberts, R. L., Matusik, R. J., and Vasioukhin, V. (2004) Hepsin promotes prostate cancer progression and metastasis. *Cancer Cell* **6**, 185-195

95. Valkenburg, K. C., Yu, X., De Marzo, A. M., Spiering, T. J., Matusik, R. J., and Williams, B. O. (2014) Activation of Wnt/beta-catenin signaling in a subpopulation of murine prostate luminal epithelial cells induces high grade prostate intraepithelial neoplasia. *The Prostate* **74**, 1506-1520

96. Bruxvoort, K. J., Charbonneau, H. M., Giambernardi, T. A., Goolsby, J. C., Qian, C. N., Zylstra, C. R., Robinson, D. R., Roy-Burman, P., Shaw, A. K., Buckner-Berghuis, B. D., Sigler, R. E., Resau, J. H., Sullivan, R., Bushman, W., and Williams, B. O. (2007) Inactivation of Apc in the mouse prostate causes prostate carcinoma. *Cancer research* **67**, 2490-2496

97. Li, W., Wang, B. E., Moran, P., Lipari, T., Ganesan, R., Corpuz, R., Ludlam, M. J., Gogineni, A., Koeppen, H., Bunting, S., Gao, W. Q., and Kirchhofer, D. (2009) Pegylated kunitz domain inhibitor suppresses hepsin-mediated invasive tumor growth and metastasis. *Cancer research* **69**, 8395-8402

98. Tervonen, T. A., Belitskin, D., Pant, S. M., Englund, J. I., Marques, E., Ala-Hongisto, H., Nevalaita, L., Sihto, H., Heikkila, P., Leidenius, M., Hewitson, K., Ramachandra, M., Moilanen, A., Joensuu, H., Kovanen, P. E., Poso, A., and Klefstrom, J. (2016) Deregulated hepsin protease activity confers oncogenicity by concomitantly augmenting HGF/MET signalling and disrupting epithelial cohesion. *Oncogene* **35**, 1832-1846

99. Jacquinet, E., Rao, N. V., Rao, G. V., Zhengming, W., Albertine, K. H., and Hoidal, J. R. (2001) Cloning and characterization of the cDNA and gene for human epitheliasin. *Eur J Biochem* **268**, 2687-2699

100. Clark, J. P., and Cooper, C. S. (2009) ETS gene fusions in prostate cancer. *Nature reviews. Urology* **6**, 429-439

101. Shah, S., and Small, E. (2010) Emerging biological observations in prostate cancer. *Expert review of anticancer therapy* **10**, 89-101

102. Lucas, J. M., True, L., Hawley, S., Matsumura, M., Morrissey, C., Vessella, R., and Nelson, P. S. (2008) The androgen-regulated type II serine protease TMPRSS2 is differentially expressed and mislocalized in prostate adenocarcinoma. *The Journal of pathology* **215**, 118-125

103. Ko, C. J., Huang, C. C., Lin, H. Y., Juan, C. P., Lan, S. W., Shyu, H. Y., Wu, S. R., Hsiao, P. W., Huang, H. P., Shun, C. T., and Lee, M. S. (2015) Androgen-Induced TMPRSS2 Activates Matriptase and Promotes Extracellular Matrix Degradation, Prostate Cancer Cell Invasion, Tumor Growth, and Metastasis. *Cancer research* **75**, 2949-2960

104. Lucas, J. M., Heinlein, C., Kim, T., Hernandez, S. A., Malik, M. S., True, L. D., Morrissey, C., Corey, E., Montgomery, B., Mostaghel, E., Clegg, N., Coleman, I., Brown, C. M., Schneider, E. L., Craik, C., Simon, J. A., Bedalov, A., and Nelson, P. S. (2014) The androgen-regulated protease TMPRSS2 activates a proteolytic cascade involving components of the tumor microenvironment and promotes prostate cancer metastasis. *Cancer Discov* **4**, 1310-1325

105. Kim, T. S., Heinlein, C., Hackman, R. C., and Nelson, P. S. (2006) Phenotypic analysis of mice lacking the Tmprss2-encoded protease. *Mol Cell Biol* **26**, 965-975

106. Wilson, S., Greer, B., Hooper, J., Zijlstra, A., Walker, B., Quigley, J., and Hawthorne, S. (2005) The membrane-anchored serine protease, TMPRSS2, activates PAR-2 in prostate cancer cells. *The Biochemical journal* **388**, 967-972

107. Wilson, S. R., Gallagher, S., Warpeha, K., and Hawthorne, S. J. (2004) Amplification of MMP-2 and MMP-9 production by prostate cancer cell lines via activation of protease-activated receptors. *The Prostate* **60**, 168-174

108. Meyer, D., Sielaff, F., Hammami, M., Bottcher-Friebertshauser, E., Garten, W., and Steinmetzer, T. (2013) Identification of the first synthetic inhibitors of the type II transmembrane serine protease TMPRSS2 suitable for inhibition of influenza virus activation. *The Biochemical journal* **452**, 331-343

109. Garten, W., Braden, C., Arendt, A., Peitsch, C., Baron, J., Lu, Y., Pawletko, K., Hardes, K., Steinmetzer, T., and Bottcher-Friebertshauser, E. (2015) Influenza virus activating host proteases: Identification, localization and inhibitors as potential therapeutics. *Eur J Cell Biol* **94**, 375-383

110. Lahiry, P., Racacho, L., Wang, J., Robinson, J. F., Gloor, G. B., Rupar, C. A., Siu, V. M., Bulman, D. E., and Hegele, R. A. (2013) A mutation in the serine protease TMPRSS4 in a novel pediatric neurodegenerative disorder. *Orphanet journal of rare diseases* **8**, 126

111. Wallrapp, C., Hahnel, S., Muller-Pillasch, F., Burghardt, B., Iwamura, T., Ruthenburger, M., Lerch, M. M., Adler, G., and Gress, T. M. (2000) A novel transmembrane serine protease (TMPRSS3) overexpressed in pancreatic cancer. *Cancer research* **60**, 2602-2606

112. Kebebew, E., Peng, M., Reiff, E., Duh, Q. Y., Clark, O. H., and McMillan, A. (2005) ECM1 and TMPRSS4 are diagnostic markers of malignant thyroid neoplasms and improve the accuracy of fine needle aspiration biopsy. *Annals of surgery* **242**, 353-361; discussion 361-353

113. Kim, S., Kang, H. Y., Nam, E. H., Choi, M. S., Zhao, X. F., Hong, C. S., Lee, J. W., Lee, J. H., and Park, Y. K. (2010) TMPRSS4 induces invasion and epithelial-mesenchymal transition through upregulation of integrin alpha5 and its signaling pathways. *Carcinogenesis* **31**, 597-606

114. Larzabal, L., Nguewa, P. A., Pio, R., Blanco, D., Sanchez, B., Rodriguez, M. J., Pajares, M. J., Catena, R., Montuenga, L. M., and Calvo, A. (2011) Overexpression of TMPRSS4

in non-small cell lung cancer is associated with poor prognosis in patients with squamous histology. *British journal of cancer* **105**, 1608-1614

115. Guan, H., Liang, W., Liu, J., Wei, G., Li, H., Xiu, L., Xiao, H., and Li, Y. (2015) Transmembrane protease serine 4 promotes thyroid cancer proliferation via CREB phosphorylation. *Thyroid* **25**, 85-94

116. Hamamoto, J., Soejima, K., Naoki, K., Yasuda, H., Hayashi, Y., Yoda, S., Nakayama, S., Satomi, R., Terai, H., Ikemura, S., Sato, T., Arai, D., Ishioka, K., Ohgino, K., and Betsuyaku, T. (2015) Methylation-induced downregulation of TFPI-2 causes TMPRSS4 overexpression and contributes to oncogenesis in a subset of non-small-cell lung carcinoma. *Cancer science* **106**, 34-42

117. de Aberasturi, A. L., and Calvo, A. (2015) TMPRSS4: an emerging potential therapeutic target in cancer. *British journal of cancer* **112**, 4-8

118. de Aberasturi, A. L., Redrado, M., Villalba, M., Larzabal, L., Pajares, M. J., Garcia, J., Evans, S. R., Garcia-Ros, D., Bodegas, M. E., Lopez, L., Montuenga, L., and Calvo, A. (2016) TMPRSS4 induces cancer stem cell-like properties in lung cancer cells and correlates with ALDH expression in NSCLC patients. *Cancer letters* **370**, 165-176

119. Cheng, D., Kong, H., and Li, Y. (2013) TMPRSS4 as a poor prognostic factor for triple-negative breast cancer. *International journal of molecular sciences* **14**, 14659-14668

120. Cheng, D., Liang, B., and Li, Y. (2013) High TMPRSS4 expression is a predictor of poor prognosis in cervical squamous cell carcinoma. *Cancer epidemiology* **37**, 993-997

121. Wu, X. Y., Zhang, L., Zhang, K. M., Zhang, M. H., Ruan, T. Y., Liu, C. Y., and Xu, J. Y. (2014) Clinical implication of TMPRSS4 expression in human gallbladder cancer. *Tumour Biol* **35**, 5481-5486

122. Wang, C. H., Guo, Z. Y., Chen, Z. T., Zhi, X. T., Li, D. K., Dong, Z. R., Chen, Z. Q., Hu, S. Y., and Li, T. (2015) TMPRSS4 facilitates epithelial-mesenchymal transition of

hepatocellular carcinoma and is a predictive marker for poor prognosis of patients after curative resection. *Scientific reports* **5**, 12366

123. Kang, S., Min, H. J., Kang, M. S., Jung, M. G., and Kim, S. (2013) Discovery of novel 2-hydroxydiarylamide derivatives as TMPRSS4 inhibitors. *Bioorg Med Chem Lett* **23**, 1748-1751

124. Larsen, B. R., Steffensen, S. D., Nielsen, N. V., Friis, S., Godiksen, S., Bornholdt, J., Soendergaard, C., Nonboe, A. W., Andersen, M. N., Poulsen, S. S., Szabo, R., Bugge, T. H., Lin, C. Y., Skovbjerg, H., Jensen, J. K., and Vogel, L. K. (2013) Hepatocyte growth factor activator inhibitor-2 prevents shedding of matriptase. *Exp Cell Res* **319**, 918-929

125. Lin, C. Y., Anders, J., Johnson, M., and Dickson, R. B. (1999) Purification and characterization of a complex containing matriptase and a Kunitz-type serine protease inhibitor from human milk. *The Journal of biological chemistry* **274**, 18237-18242

126. Antalis, T. M., Bugge, T. H., and Wu, Q. (2011) Membrane-anchored serine proteases in health and disease. *Progress in molecular biology and translational science* **99**, 1-50

127. Kim, D. R., Sharmin, S., Inoue, M., and Kido, H. (2001) Cloning and expression of novel mosaic serine proteases with and without a transmembrane domain from human lung. *Biochim Biophys Acta* **1518**, 204-209

128. Kido, H., and Okumura, Y. (2008) Mspl/Tmprss13. *Front Biosci* **13**, 754-758

129. Kido, H., Okumura, Y., Takahashi, E., Pan, H. Y., Wang, S., Chida, J., Le, T. Q., and Yano, M. (2008) Host envelope glycoprotein processing proteases are indispensable for entry into human cells by seasonal and highly pathogenic avian influenza viruses. *J Mol Genet Med* **3**, 167-175

130. Okumura, Y., Takahashi, E., Yano, M., Ohuchi, M., Daidoji, T., Nakaya, T., Bottcher, E., Garten, W., Klenk, H. D., and Kido, H. (2010) Novel type II transmembrane serine proteases, MSPL and TMPRSS13, Proteolytically activate membrane fusion activity of

the hemagglutinin of highly pathogenic avian influenza viruses and induce their multicycle replication. *Journal of virology* **84**, 5089-5096

131. Zmora, P., Blazejewska, P., Moldenhauer, A. S., Welsch, K., Nehlmeier, I., Wu, Q., Schneider, H., Pohlmann, S., and Bertram, S. (2014) DESC1 and MSPL activate influenza A viruses and emerging coronaviruses for host cell entry. *Journal of virology* **88**, 12087-12097

132. Miller, G. S., Zoratti, G. L., Murray, A. S., Bergum, C., Tanabe, L. M., and List, K. (2014) HATL5: a cell surface serine protease differentially expressed in epithelial cancers. *PloS one* **9**, e87675

133. Kato, M., Hashimoto, T., Shimomura, T., Kataoka, H., Ohi, H., and Kitamura, N. (2012) Hepatocyte growth factor activator inhibitor type 1 inhibits protease activity and proteolytic activation of human airway trypsin-like protease. *J Biochem* **151**, 179-187

134. Maurer, E., Gutschow, M., and Stirnberg, M. (2013) Hepatocyte growth factor activator inhibitor type 2 (HAI-2) modulates hepcidin expression by inhibiting the cell surface protease matriptase-2. *Biochem J* **450**, 583-593

135. van der Lee, R., Buljan, M., Lang, B., Weatheritt, R. J., Daughdrill, G. W., Dunker, A. K., Fuxreiter, M., Gough, J., Gsponer, J., Jones, D. T., Kim, P. M., Kriwacki, R. W., Oldfield, C. J., Pappu, R. V., Tompa, P., Uversky, V. N., Wright, P. E., and Babu, M. M. (2014) Classification of intrinsically disordered regions and proteins. *Chem Rev* **114**, 6589-6631

136. van der Lee, R., Lang, B., Kruse, K., Gsponer, J., Sanchez de Groot, N., Huynen, M. A., Matouschek, A., Fuxreiter, M., and Babu, M. M. (2014) Intrinsically disordered segments affect protein half-life in the cell and during evolution. *Cell Rep* **8**, 1832-1844

137. Jiang, J., Wu, S., Wang, W., Chen, S., Peng, J., Zhang, X., and Wu, Q. (2011) Ectodomain shedding and autocleavage of the cardiac membrane protease corin. *J Biol Chem* **286**, 10066-10072

138. Hicke, L., and Dunn, R. (2003) Regulation of membrane protein transport by ubiquitin and ubiquitin-binding proteins. *Annu Rev Cell Dev Biol* **19**, 141-172

139. Komander, D., Clague, M. J., and Urbe, S. (2009) Breaking the chains: structure and function of the deubiquitinases. *Nat Rev Mol Cell Biol* **10**, 550-563

140. Clague, M. J., Barsukov, I., Coulson, J. M., Liu, H., Rigden, D. J., and Urbe, S. (2013) Deubiquitylases from genes to organism. *Physiol Rev* **93**, 1289-1315

141. Singh, S. K., Sahu, I., Mali, S. M., Hemantha, H. P., Kleifeld, O., Glickman, M. H., and Brik, A. (2016) Synthetic Uncleavable Ubiquitinated Proteins Dissect Proteasome Deubiquitination and Degradation, and Highlight Distinctive Fate of Tetraubiquitin. *J Am Chem Soc* **138**, 16004-16015

142. Xue, B., Dunbrack, R. L., Williams, R. W., Dunker, A. K., and Uversky, V. N. (2010) PONDR-FIT: a meta-predictor of intrinsically disordered amino acids. *Biochimica et biophysica acta* **1804**, 996-1010

143. Burgi, J., Xue, B., Uversky, V. N., and van der Goot, F. G. (2016) Intrinsic Disorder in Transmembrane Proteins: Roles in Signaling and Topology Prediction. *PLoS One* **11**, e0158594

144. Dunker, A. K., Brown, C. J., Lawson, J. D., Iakoucheva, L. M., and Obradovic, Z. (2002) Intrinsic disorder and protein function. *Biochemistry* **41**, 6573-6582

145. Wegener, A. D., and Jones, L. R. (1984) Phosphorylation-induced mobility shift in phospholamban in sodium dodecyl sulfate-polyacrylamide gels. Evidence for a protein structure consisting of multiple identical phosphorylatable subunits. *J Biol Chem* **259**, 1834-1841

146. Friis, S., Sales, K. U., Schafer, J. M., Vogel, L. K., Kataoka, H., and Bugge, T. H. (2014) The protease inhibitor HAI-2, but not HAI-1, regulates matriptase activation and shedding through prostasin. *J Biol Chem* **289**, 22319-22332

147. Oberst, M. D., Chen, L. Y., Kiyomiya, K., Williams, C. A., Lee, M. S., Johnson, M. D., Dickson, R. B., and Lin, C. Y. (2005) HAI-1 regulates activation and expression of matriptase, a membrane-bound serine protease. *Am J Physiol Cell Physiol* **289**, C462-470

148. Benaud, C., Dickson, R. B., and Lin, C. Y. (2001) Regulation of the activity of matriptase on epithelial cell surfaces by a blood-derived factor. *Eur J Biochem* **268**, 1439-1447

149. Szabo, R., Hobson, J. P., List, K., Molinolo, A., Lin, C. Y., and Bugge, T. H. (2008) Potent inhibition and global co-localization implicate the transmembrane Kunitz-type serine protease inhibitor hepatocyte growth factor activator inhibitor-2 in the regulation of epithelial matriptase activity. *The Journal of biological chemistry* **283**, 29495-29504

150. Lai, Y. J., Chang, H. H., Lai, H., Xu, Y., Shiao, F., Huang, N., Li, L., Lee, M. S., Johnson, M. D., Wang, J. K., and Lin, C. Y. (2015) N-Glycan Branching Affects the Subcellular Distribution of and Inhibition of Matriptase by HAI-2/Placental Bikunin. *PLoS One* **10**, e0132163

151. Miyake, Y., Yasumoto, M., Tsuzuki, S., Fushiki, T., and Inouye, K. (2009) Activation of a membrane-bound serine protease matriptase on the cell surface. *Journal of biochemistry* **146**, 273-282

152. Bah, A., Vernon, R. M., Siddiqui, Z., Krzeminski, M., Muhandiram, R., Zhao, C., Sonenberg, N., Kay, L. E., and Forman-Kay, J. D. (2015) Folding of an intrinsically disordered protein by phosphorylation as a regulatory switch. *Nature* **519**, 106-109

153. Wright, P. E., and Dyson, H. J. (2015) Intrinsically disordered proteins in cellular signalling and regulation. *Nature reviews. Molecular cell biology* **16**, 18-29

154. Lopez-Otin, C., and Hunter, T. (2010) The regulatory crosstalk between kinases and proteases in cancer. *Nature reviews. Cancer* **10**, 278-292

155. Duffy, M. J., Mullooly, M., O'Donovan, N., Sukor, S., Crown, J., Pierce, A., and McGowan, P. M. (2011) The ADAMs family of proteases: new biomarkers and therapeutic targets for cancer? *Clin Proteomics* **8**, 9

156. Poghosyan, Z., Robbins, S. M., Houslay, M. D., Webster, A., Murphy, G., and Edwards, D. R. (2002) Phosphorylation-dependent interactions between ADAM15 cytoplasmic domain and Src family protein-tyrosine kinases. *J Biol Chem* **277**, 4999-5007

157. Oberst, M., Anders, J., Xie, B., Singh, B., Ossandon, M., Johnson, M., Dickson, R. B., and Lin, C. Y. (2001) Matriptase and HAI-1 are expressed by normal and malignant epithelial cells in vitro and in vivo. *The American journal of pathology* **158**, 1301-1311

158. Tanabe, L. M., and List, K. (2017) The role of type II transmembrane serine protease-mediated signaling in cancer. *The FEBS journal* **284**, 1421-1436

159. Murray, A. S., Varela, F. A., and List, K. (2016) Type II transmembrane serine proteases as potential targets for cancer therapy. *Biol Chem* **397**, 815-826

160. List, K. (2009) Matriptase: a culprit in cancer? *Future Oncol* **5**, 97-104

161. Lin, E. Y., Jones, J. G., Li, P., Zhu, L., Whitney, K. D., Muller, W. J., and Pollard, J. W. (2003) Progression to malignancy in the polyoma middle T oncoprotein mouse breast cancer model provides a reliable model for human diseases. *The American journal of pathology* **163**, 2113-2126

162. Fluck, M. M., and Schaffhausen, B. S. (2009) Lessons in signaling and tumorigenesis from polyomavirus middle T antigen. *Microbiology and molecular biology reviews : MMBR* **73**, 542-563, Table of Contents

163. Fantozzi, A., and Christofori, G. (2006) Mouse models of breast cancer metastasis. *Breast cancer research : BCR* **8**, 212

164. Elstrodt, F., Hollestelle, A., Nagel, J. H., Gorin, M., Wasielewski, M., van den Ouweland, A., Merajver, S. D., Ethier, S. P., and Schutte, M. (2006) BRCA1 mutation analysis of 41

human breast cancer cell lines reveals three new deleterious mutants. *Cancer Res* **66**, 41-45

165. Chavez, K. J., Garimella, S. V., and Lipkowitz, S. (2010) Triple negative breast cancer cell lines: one tool in the search for better treatment of triple negative breast cancer. *Breast disease* **32**, 35-48

166. Wahba, H. A., and El-Hadaad, H. A. (2015) Current approaches in treatment of triple-negative breast cancer. *Cancer Biol Med* **12**, 106-116

167. Tassone, P., Tagliaferri, P., Perricelli, A., Blotta, S., Quaresima, B., Martelli, M. L., Goel, A., Barbieri, V., Costanzo, F., Boland, C. R., and Venuta, S. (2003) BRCA1 expression modulates chemosensitivity of BRCA1-defective HCC1937 human breast cancer cells. *Br J Cancer* **88**, 1285-1291

168. Zoratti, G. L., Tanabe, L. M., Varela, F. A., Murray, A. S., Bergum, C., Colombo, E., Lang, J. E., Molinolo, A. A., Leduc, R., and Marsault, E. (2015) Targeting matriptase in breast cancer abrogates tumour progression via impairment of stromal-epithelial growth factor signalling. *Nat Commun.* **6**

169. Parr, C., Sanders, A. J., Davies, G., Martin, T., Lane, J., Mason, M. D., Mansel, R. E., and Jiang, W. G. (2007) Matriptase-2 inhibits breast tumor growth and invasion and correlates with favorable prognosis for breast cancer patients. *Clinical cancer research : an official journal of the American Association for Cancer Research* **13**, 3568-3576

170. Murray, A. S., Varela, F. A., Hyland, T. E., Schoenbeck, A. J., White, J. M., Tanabe, L. M., Todi, S. V., and List, K. (2017) Phosphorylation of the type II transmembrane serine protease, TMPRSS13 in Hepatocyte Growth Factor Activator Inhibitor-1 and 2-mediated cell surface localization. *Journal of Biological Chemistry*

171. Tiligada, E. (2006) Chemotherapy: induction of stress responses. *Endocrine-related cancer* **13 Suppl 1**, S115-124

172. Kultz, D. (2005) Molecular and evolutionary basis of the cellular stress response. *Annual review of physiology* **67**, 225-257

173. Liou, G.-Y., and Storz, P. (2010) Reactive oxygen species in cancer. *Free radical research* **44**, 10.3109/10715761003667554

174. Schieber, M., and Chandel, N. S. (2014) ROS Function in Redox Signaling and Oxidative Stress. *Current biology : CB* **24**, R453-R462

175. Conklin, K. A. (2004) Chemotherapy-associated oxidative stress: impact on chemotherapeutic effectiveness. *Integrative cancer therapies* **3**, 294-300

176. Kulms, D., and Schwarz, T. (2002) Mechanisms of UV-induced signal transduction. *The Journal of dermatology* **29**, 189-196

ABSTRACT

IDENTIFYING THE ROLE OF THE TYPE-II TRANSMEMBRANE SERINE PROTEASE TMPRSS13 IN BREAST CANCER

by

ANDREW STEVAN MURRAY

May 2018

Advisor: Dr. Karin List

Major: Cancer Biology

Degree: Doctor of Philosophy

Breast cancer is the most frequently diagnosed cancer and the second leading cause of cancer death in women in the United States. Breast cancer progression is accompanied by increased expression of extracellular and cell surface proteases that are capable of degrading the extracellular matrix as well as cleaving and activating downstream targets. These proteolytic processes are critically involved in modifying the tissue microenvironment of the breast, which is necessary for cancer cell invasion and eventual dissemination of cancer cells to other organs. Therefore, identifying novel proteases that promote tumor progression is critical to create new approaches for developing improved breast cancer therapeutics. Systematic in silico data analysis followed by experimental validation identified increased expression of the type-II transmembrane serine protease (TTSP) family member, TMPRSS13 (transmembrane protease, serine 13), in invasive ductal carcinoma (IDC) patient tissue samples compared to normal breast tissue. Immunohistochemical analysis revealed that the expression of TMPRSS13 is strictly confined to the malignant epithelial cells and not the surrounding tumor stroma. Currently, no studies have examined the role of TMPRSS13 in any cancer type. Additionally, the basic biochemical properties (i.e. activation, localization, and post translational modifications) have not yet been explored. Therefore to understand the potential role of TMPRSS13 in breast

cancer, biochemical studies as well as thorough and comprehensive *in vivo* “loss-of-function” studies complemented by human cell culture models were performed. Biochemical characterization of TMPRSS13 show that TMPRSS13 is a glycosylated, active protease and that its own proteolytic activity mediates zymogen cleavage. Full-length, active TMPRSS13 exhibits impaired cell-surface expression in the absence of the cognate Kunitz-type serine protease inhibitors, hepatocyte growth factor activator inhibitor (HAI)-1 or HAI-2. Concomitant presence of TMPRSS13 with either HAI-1 or -2 mediates phosphorylation of residues in the intracellular domain of the protease, and it coincides with efficient transport of the protease to the cell surface and its subsequent shedding. Cell-surface labeling experiments indicate that the dominant form of TMPRSS13 on the cell surface is phosphorylated, whereas intracellular TMPRSS13 is predominantly non-phosphorylated.

Additionally, results from the breast cancer study indicates that genetic deletion of TMPRSS13 results in a significant decrease in overall tumor burden, growth rate, and a delayed detection of palpable mammary tumors (tumor latency), thereby indicating that TMPRSS13 plays a promotional role in breast cancer progression. Complementary studies using human cell culture models revealed that silencing TMPRSS13 expression decreases proliferation and induces apoptosis. Furthermore, silencing of TMPRSS13 in the invasive human breast cancer cell line BT20 attenuates its invasive potential. These studies are important to our understanding of novel proteolytic events that occur within the tumor microenvironment, and in determining whether TMPRSS13 may translate into a novel therapeutic target.

AUTOBIOGRAPHICAL STATEMENT

Andrew Stevan Murray

EDUCATION

Wayne State University Detroit, MI 2018
Doctor of Philosophy: Cancer Biology

Michigan State University East Lansing, MI 2011
Bachelor of Science: Microbiology & Human Biology

PUBLICATIONS

Murray AS, Varela FA, Hyland TE, Schoenbeck AJ, White JM, Tanabe LM, Todi SV, List K. Phosphorylation of the type II transmembrane serine protease, TMPRSS13 in Hepatocyte Growth Factor Activator Inhibitor-1 and 2-mediated cell surface localization. J Biol Chem. 2017 Jul 14. pii: jbc.M117.775999. doi: 10.1074/jbc.M117.775999. [Epub ahead of print] PubMed PMID: 28710277.

Murray AS, Varela FA, List K. Type II transmembrane serine proteases as potential targets for cancer therapy. Biol Chem. 2016 Sep 1;397(9):815-26. doi: 10.1515/hsz-2016-0131. Review. PubMed PMID: 27078673

Duhaime MJ, Page KO, Varela FA, Murray AS, Silverman ME, Zoratti GL, List K. Cell Surface Human Airway Trypsin-Like Protease Is Lost During Squamous Cell Carcinogenesis. J Cell Physiol. 2016 Jul;231(7):1476-83. doi: 10.1002/jcp.25173. Epub 2016 Feb 4. PubMed PMID: 26297835

Zoratti GL, Tanabe LM, Varela FA, Murray AS, Bergum C, Colombo É, Lang JE, Molinolo AA, Leduc R, Marsault E, Boerner J, List K. Targeting matriptase in breast cancer abrogates tumour progression via impairment of stromal-epithelial growth factor signalling. Nat Commun. 2015 Apr 15;6:6776. doi: 10.1038/ncomms7776. PubMed PMID: 25873032

Miller GS, Zoratti GL, Murray AS, Bergum C, Tanabe LM, List K. HATL5: a cell surface serine protease differentially expressed in epithelial cancers. PLoS One. 2014 Feb 3;9(2):e87675. doi: 10.1371/journal.pone.0087675. eCollection 2014. PubMed PMID: 24498351